

## Large-scale atmospheric conditions associated with major avalanche cycles and cold season weather hazards in Iceland

Nikolai Nawri

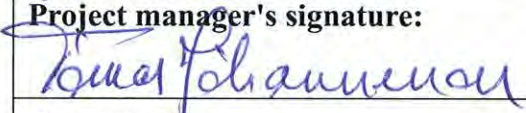


# Large-scale atmospheric conditions associated with major avalanche cycles and cold season weather hazards in Iceland

---

Nikolai Nawri, Icelandic Met Office



|  |                            |   |   |
|--|----------------------------|---|---|
| <b>Report no.:</b><br>VÍ 2013-004  | <b>Date.:</b><br>June 2013 | <b>ISSN:</b><br>1670-8261   | <b>Public</b> <input checked="" type="checkbox"/> <b>Restricted</b> <input type="checkbox"/><br><b>Provision:</b> |
| <b>Report title / including subtitle</b><br>Large-scale atmospheric conditions associated with major avalanche cycles and cold season weather hazards in Iceland   |                            | <b>No. of copies:</b> 5<br><b>Pages:</b> 95   |   |
| <b>Author(s):</b><br>Nikolai Nawri   |                            | <b>Managing director:</b><br>Jórunn Harðardóttir  |   |
|  |                            | <b>Project manager:</b><br>Tómas Jóhannesson  |   |
|  |                            | <b>Project number:</b><br>4351-0-0005   |   |
| <b>Project phase:</b>  |                            | <b>Case number:</b><br>n/a  |   |
| <b>Report contracted for:</b><br>Icelandic Avalanche and Landslide Fund  |                            |   |   |
| <b>Prepared in cooperation with:</b>   |                            |   |   |
| <b>Summary:</b><br>In this report, an analysis is presented of the regional and large-scale atmospheric conditions associated with all well-documented major avalanche cycles in those settled regions of Iceland, that are particularly affected by avalanches. The nature of these weather conditions is determined in comparison with a non-avalanche or “background” cold-season climatology, as well as with the atmospheric conditions associated with strong winds and heavy snowfall within corresponding regions of Iceland, that did not lead to the release of major avalanches at the locations considered here. The regions covered in this study are the northern part of the Westfjords, the area around Siglufjörður in Northern Iceland, and Seyðisfjörður and Neskaupstaður in the east. |                            |   |   |
| <b>Keywords:</b><br>Avalanche weather<br>Snowstorms<br>Winter weather hazards<br>Iceland<br>European reanalyses ERA-40, ERA-Interim  |                            | <b>Managing director's signature:</b><br> |   |
|  |                            | <b>Project manager's signature:</b><br>   |   |
|  |                            | <b>Reviewed by:</b><br>TóJ  |   |



# Contents

|          |  |    |
|----------|--|----|
| <b>1</b> | <b>Introduction</b> .....  | 9  |
| <b>2</b> | <b>Data and methodology</b> .....                                      | 12 |
| <b>3</b> | <b>Occurrence of severe snowstorms and major avalanches</b> .....      | 16 |
| <b>4</b> | <b>Weather conditions associated with major avalanche cycles</b> ..... | 18 |
| <b>5</b> | <b>Weather conditions for specific slope aspects</b> .....             | 20 |
| 5.1      | Skutulsfjörður .....   | 21 |
| 5.2      | Siglufjörður .....   | 21 |
| 5.3      | Eastern Iceland .....  | 22 |
| <b>6</b> | <b>Development of avalanche weather conditions</b> .....               | 22 |
| <b>7</b> | <b>Weather associated with individual avalanche cycles</b> .....       | 25 |
| <b>8</b> | <b>Summary</b> .....   | 28 |

## List of Figures

|    |  |    |
|----|--|----|
| 1  | Topographic map of the Westfjords .....  | 36 |
| 2  | Location of major avalanche slopes in the Westfjords.....  | 37 |
| 3  | Topographic map of Northern Iceland.....   | 38 |
| 4  | Location of major avalanche slopes in Northern Iceland .....   | 39 |
| 5  | Topographic map of Eastern Iceland.....  | 40 |
| 6  | Location of major avalanche slopes in Seyðisfjörður.....   | 41 |
| 7  | Annual averages of regional mean wind speed at 925 hPa .....   | 42 |
| 8  | Regional averages of annual snowfall based on ECMWF reanalyses .....   | 43 |
| 9  | Annual number of days with heavy snowfall and strong winds .....   | 44 |
| 10 | Annual number of days with severe snowstorm conditions .....   | 45 |
| 11 | Annual number of days with large or destructive avalanches.....  | 46 |
| 12 | Seasonal distribution of large or destructive avalanches .....   | 47 |
| 13 | Occurrence of avalanche cycles with a given duration .....   | 48 |
| 14 | Occurrence of avalanche cycles with a given maximum run-out index .....  | 49 |
| 15 | Joint histogram of daily air temperature and wind speed at 925 hPa .....   | 50 |
| 16 | Joint histogram of daily residual precipitation and snowfall.....  | 51 |
| 17 | Average atmospheric fields for the main avalanche season (Jan – Apr).....  | 52 |
| 18 | Low-level ensemble mean fields for days with major avalanche activity .....  | 53 |
| 19 | Upper-level ensemble mean fields for days with major avalanche activity.....   | 54 |
| 20 | Low-level ensemble mean fields for the days preceding major avalanche activity .   | 55 |
| 21 | Upper-level ensemble mean fields for the days preceding major avalanche activity   | 56 |
| 22 | Ensemble mean fields for the days preceding major avalanche activity with specific slope orientations .....              | 57 |
| 23 | Ensemble mean fields for days with major avalanche activity with specific slope orientations.....                        | 58 |
| 24 | Ensemble evolution of daily regional mean values towards the start of major avalanche activity in the Westfjords .....   | 59 |
| 25 | Ensemble evolution of daily regional mean values towards the start of major avalanche activity in Northern Iceland ..... | 60 |
| 26 | Ensemble evolution of daily regional mean values towards the start of major avalanche activity in Eastern Iceland .....  | 61 |
| 27 | Low-level evolution towards major avalanche activity in the Westfjords .....   | 62 |
| 28 | Upper-level evolution towards major avalanche activity in the Westfjords.....  | 63 |
| 29 | Low-level evolution towards major avalanche activity in Northern Iceland.....  | 64 |
| 30 | Upper-level evolution towards major avalanche activity in Northern Iceland .....   | 65 |
| 31 | Low-level evolution towards major avalanche activity in Eastern Iceland.....   | 66 |
| 32 | Upper-level evolution towards major avalanche activity in Eastern Iceland .....  | 67 |
| 33 | Low-level evolution towards severe snowstorm conditions in the Westfjords .....  | 68 |
| 34 | Upper-level evolution towards severe snowstorm conditions in the Westfjords .....  | 69 |
| 35 | Low-level evolution towards severe snowstorm conditions in Northern Iceland....  | 70 |
| 36 | Upper-level evolution towards severe snowstorm conditions in Northern Iceland .  | 71 |
| 37 | Low-level evolution towards severe snowstorm conditions in Eastern Iceland.....  | 72 |
| 38 | Upper-level evolution towards severe snowstorm conditions in Eastern Iceland ...   | 73 |
| 39 | Low-level evolution towards strong wind events in the Westfjords .....   | 74 |



|    |   |    |
|----|---|----|
| 40 | Upper-level evolution towards strong wind events in the Westfjords .....      | 75 |
| 41 | Low-level evolution towards strong wind events in Northern Iceland .....      | 76 |
| 42 | Upper-level evolution towards strong wind events in Northern Iceland.....     | 77 |
| 43 | Low-level evolution towards strong wind events in Eastern Iceland .....       | 78 |
| 44 | Upper-level evolution towards strong wind events in Eastern Iceland.....      | 79 |
| 45 | Low-level evolution towards heavy snowfall events in the Westfjords .....     | 80 |
| 46 | Upper-level evolution towards heavy snowfall events in the Westfjords.....    | 81 |
| 47 | Low-level evolution towards heavy snowfall events in Northern Iceland.....    | 82 |
| 48 | Upper-level evolution towards heavy snowfall events in Northern Iceland ..... | 83 |
| 49 | Low-level evolution towards heavy snowfall events in Eastern Iceland.....     | 84 |
| 50 | Upper-level evolution towards heavy snowfall events in Eastern Iceland .....  | 85 |
| 51 | Daily fields leading up to the avalanche cycle starting 4 Feb 1968.....       | 86 |
| 52 | Daily fields leading up to the avalanche cycle starting 8 Feb 1974.....       | 87 |
| 53 | Daily fields during the avalanche cycle starting 8 Feb 1974 .....             | 88 |
| 54 | Daily fields leading up to the avalanche cycle starting 19 Dec 1974.....      | 89 |
| 55 | Daily fields leading up to the avalanche cycle starting 12 Jan 1975 .....     | 90 |
| 56 | Daily fields leading up to the avalanche cycle starting 19 Mar 1987 .....     | 91 |
| 57 | Daily fields leading up to the avalanche cycle starting 31 Mar 1987 .....     | 92 |
| 58 | Daily fields leading up to the avalanche cycle starting 3 Apr 1994 .....      | 93 |
| 59 | Daily fields leading up to the avalanche cycle starting 16 Jan 1995 .....     | 94 |
| 60 | Daily fields prior to the avalanche cycle starting 23 Oct 1995 .....          | 95 |
| 61 | Daily fields during the avalanche cycle starting 23 Oct 1995.....             | 96 |
| 62 | Daily fields leading up to the avalanche cycle starting 11 Mar 1999 .....     | 97 |



# 1 Introduction

From the beginning of the settlement period, and continuing throughout the last century, snow avalanches have been one of the most deadly specific natural disaster in Iceland, surpassed in the resulting number of direct fatalities only by all types of accidents at sea, and by all weather related accidents on land (Björnsson, 1980; Jóhannesson, 2001).

In previous studies (Björnsson, 1980; Jóhannesson & Jónsson, 1996; Jónsson, 1998; Ólafsson, 1998; Thorsteinsson et al., 1999; Björnsson, 2002; Haraldsdóttir et al., 2004), the weather conditions associated with some individual avalanches, or the climatological conditions associated with avalanche activity in some regions of Iceland, have been established.

Ultimately, avalanches are released, when the gravitational pull on a substantial part of the snowpack exceeds friction of the snowpack with the ground, or the cohesion between different layers of snow. It is therefore clear from the outset, that even local atmospheric conditions can only serve as proxy variables for determining snowpack conditions. However, since at a given location the terrain is static, temporal variability within the snowpack is driven by atmospheric conditions, which determine the amount and type of falling snow, as well as the redistribution of snow by low-level wind. The atmosphere also provides boundary-conditions for metamorphism within the snowpack through surface air temperature, humidity, cloudiness, and forms of precipitation other than snow.

Therefore, building on the existing knowledge, the goal of this study is an analysis of the regional and large-scale atmospheric conditions associated with all well-documented major avalanche cycles in those settled regions of Iceland, that are particularly affected by avalanches. The nature of these weather conditions is determined in comparison with a corresponding non-avalanche or “background” cold-season climatology (described in detail in the following section), as well as with the atmospheric conditions associated with strong winds and heavy snowfall, either individually and combined, within corresponding regions of Iceland, that did not lead to the release of major avalanches at the locations considered here.

Although hazardous avalanches have been reported more widespread throughout Iceland (Björnsson, 1980), the three regions of the island, for which reliable and regular records about the occurrence and intensity of avalanches are available since the late 1950s, are the northern part of the Westfjords, including the communities of Bolungarvík, Flateyri, Ísafjörður, Súðavík, and Öndarfjörður, as well as around Siglufjörður in Northern Iceland, and around Neskaupstaður and Seyðisfjörður in Eastern Iceland. These communities are shown in Figures 1, 3, and 5, together with the regional scale terrain, and on higher-resolution maps in Figures 2, 4, and 6. Indicated also on these latter maps are the locations and orientations of the major avalanche slopes. Slope orientation, or aspect, is defined here as the direction towards which the negative terrain gradient points.

Björnsson (1980) estimated that about 80 – 90% of all avalanches in Iceland fall in cycles, defined as any number of individual avalanches that fell on the same or on consecutive days within the same region. In this study, a major avalanche cycle is considered to be one, for which the largest linear run-out index<sup>1</sup> is at least 13, or during which injuries or significant damage to buildings, roads, and other infrastructure incurred. Smaller avalanches, with run-out indices

---

<sup>1</sup>For a definition of run-out index used in this study see Arnalds et al. (2004).

of less than 13, are excluded from this study, since they are less likely to be correlated with specific large-scale weather patterns at the time of release. Taking into account these cases in climatological analyses might therefore mask relevant characteristics of atmospheric conditions that contribute to the release of large avalanches. Additionally, smaller avalanches are more likely to go unnoticed, at least at the time of their occurrence, introducing again uncertainties into attempts to relate these events to specific weather conditions.

Iceland experiences a maritime climate, with mild and wet winters, strong winds, and frequent precipitation, varying between rain and snow (Einarsson, 1984; Hanna et al., 2004). Under these climatic conditions, the relatively dense and homogenous snowpack usually results in direct-action avalanches, immediately linked to ongoing or very recent weather events (Sturm et al., 1995; McClung & Schaerer, 2006). In fact, it is known from the previous studies on avalanche activity in Iceland, that heavy snowfall and strong winds generally occur during or immediately preceding the release of large avalanches in Iceland. This enables a meaningful study of “avalanche weather conditions”, defined here as the atmospheric state on the day on which individual avalanches occurred, or as the average state throughout an extended avalanche cycle.

The occurrence of strong winds and heavy precipitation, and thus of avalanches, is closely linked to large-scale cyclonic storm systems. An extratropical cyclone, for the purpose of this study, is defined as a weather system with a closed depression in mean sea level air pressure (MSLP) of several hectopascal, and with associated warm, cold, and occluded fronts. Climatologically, cyclone activity over the northern North Atlantic Ocean, especially during the cold season, occurs between the semi-permanent Greenland and Azores Highs (e.g., Schneider et al., 2007). The region with prevailing low MSLP, between Iceland and the southern tip of Greenland, is generally referred to as the Icelandic Low (e.g., Serreze et al., 1993, 1997). The weather conditions over Iceland largely depend on the intensity and location of the individual cyclones, that make up this climatological low-pressure region (Einarsson, 1984).

In general terms, the development and life cycle of extratropical cyclones is well understood (e.g., Shapiro & Grønås, 1999). They are largely driven by a conversion of potential energy, present in horizontal temperature gradients, to kinetic energy. In the vicinity of Iceland, these temperature gradients are primarily associated with zonal asymmetries in the polar front, and with the cold waters of the East Greenland and East Icelandic Currents in the north and east, and the warm waters of the North Atlantic Drift in the south and west (Einarsson, 1984).

As described in quasi-geostrophic theory (Charney, 1947; Eady, 1949), a net poleward transfer of heat is required for part of the potential energy stored in horizontal temperature gradients to become available for conversion to kinetic energy. This baroclinic conversion process then manifests itself by descending cold air moving equatorwards, and ascending warm air moving polewards, forming the cold and warm front, respectively, of the developing cyclone. Above the boundary layer, the atmosphere is predominantly in geostrophic equilibrium, in which horizontal motion tends to follow isobars, and temperature gradients on isobaric surfaces are related to vertical wind shear. Warm or cold advection by geostrophic flow therefore only occurs if temperature varies on isobaric surfaces. In a state with coinciding isobaric and isothermal surfaces, temperature advection, and thus heat transport, are very limited, and no further conversion of potential to kinetic energy is possible. Therefore, in an ideal situation, maximum kinetic energy would be extracted from the atmosphere, by converting a given stratification into a barotropic

ground state, with vanishing wind shear between isobaric surfaces. Beyond that point, flow instabilities associated with horizontal shear can only grow by extracting kinetic energy from the mean flow (Lorenz, 1972). This requires “negatively” tilted troughs, which, in the northern hemisphere, deepen towards the northwest, against the westerly overlying flow. While this process can contribute to the intensification of cyclones, in extratropical regions, baroclinic instability is the dominant mechanism in initial cyclogenesis.

Traditionally in weather forecasting, the 500 hPa level is chosen to identify the location of the polar front. The wave pattern of geopotential height contours on that level allows an easy determination of minima and maxima of mean layer temperatures and vertical vorticity, with cold air and positive vorticity advection occurring downstream of troughs, counteracting each other in the forcing of vertical motion. On balance, upward motion usually occurs downstream of troughs, and often close to the following ridge.

On the northern hemisphere, cold advection by northerly flow is associated with a backing vertical wind profile, whereas warm advection by southerly flow is associated with veering. In both cases, the westerly wind component increases with height, developing into the jet stream near the tropopause, at a level oscillating between about 300 hPa in winter and 200 hPa in summer. For simplicity, the jet stream level is taken here to be at 250 hPa.

In an idealised situation of straight motion, jet streaks (i.e., speed maxima within the jet stream), are associated with divergence in their right entrance and left exit quadrants, due to temporary imbalances between the pressure gradient and Coriolis forces, as air accelerates and decelerates through the jet streak. Generally, however, the jet stream in the upper troposphere is curved. Under those circumstances, in the northern hemisphere, a jet streak located just upstream of a trough, amplifies the trough by creating divergence and ascent north of the jet axis to maintain or regain geostrophic balance and to counteract the increased centrifugal force. The opposite occurs with a jet streak downstream of a trough. Any pattern of divergence and convergence in the upper troposphere, by continuity, is associated with the opposite pattern at low levels, whereby the different levels are joined by columns of ascending and descending motion. This dynamically induced pattern of vertical motion may be modified by temperature advection, with low-level warm advection leading to divergence and rising motion across the entire exit region of the upper-level jet.

Taking into account the different levels of the atmosphere, a rapid formation or intensification of an extratropical surface cyclone can thus be expected to result from a vertical alignment of: (a) a low-level baroclinic zone, possibly associated with an enhanced west-to-east thermal gradient established through temperature advection along the frontal zones of an old (and possibly occluded) low; (b) a 500 hPa trough, providing positive vorticity advection; and (c) a 250 hPa jet streak, amplifying the trough, and creating low-level convergence and rising motion through upper-level divergence. Cyclogenesis and precipitation is then likely to develop within 24 hours just downstream of the trough.

The forcing of ascent by large-scale dynamics is not to be confused with convection, which may however be triggered by latent heat release during large-scale ascent, resulting in enhanced cloudiness and precipitation. Local ascent may also be due to orographic lift. For cold-season storms affecting Iceland, this is especially important for northerly and northeasterly off-shore winds impinging on the elevated terrain along the northern coast.

In the following discussion, these general considerations about extratropical storm development will be evaluated with regard to those cyclones responsible for major avalanche activity in Iceland, as well as creating adverse cold-season weather conditions, that do not lead to the release of avalanches.

## 2 Data and methodology

Most information about the occurrence of major avalanches in Iceland was taken from a list compiled by Tómas Jóhannesson at the Icelandic Meteorological Office in 2006, which only includes cases, for which the exact dates are known. Some additional well-documented cases for the Westfjords were obtained from Björnsson (2002), Haraldsdóttir (2002), and Arason et al. (2005). In all, 91 cases of major avalanche cycles are considered in this study, within the period starting at the beginning of the ERA-40 reanalyses produced by the European Centre for Medium-Range Weather Forecasts (ECMWF) in 1958, and ending with the 2005 – 06 winter season. These cases are separated into three different regions: the northern part of the Westfjords, the area around Siglufjörður in Northern Iceland, and Seyðisfjörður and Neskaupstaður in the east (see Table 1). Complete lists of cases, separated by region, are given in Tables 4 to 6. The exact locations are shown in Figures 1 to 6.

Terrain elevation of the avalanche slopes considered here generally increases from west to east. Ridge-top levels at the relevant locations in the northern part of the Westfjords vary between 600 and 850 metres above mean sea level (mASL), but mostly lie within 600 to 700 mASL. The slopes on both sides of Hnífsdalur reach about 600 mASL at the top. Likewise, the two ridges forming Tungudalur are at about 600 mASL, although to the north, the northern slope of Seljalandsdalur rises to 700 mASL. Similarly, the “active” slopes at Bolungarvík have tops between 600 and 700 mASL. The ridge-top levels on both sides of Öndarfjörður (Flateyri and Öndarfjörður community) and Skutulsfjörður (Ísafjörður and Kirkjubólshlíð) are about 700 mASL. At Súðavík, the ridge increases in height from north to south between about 600 and 850 mASL. At the relevant locations in Northern Iceland, ridge-top levels also vary between 600 and 850 mASL, but are mostly towards the upper end of this range. In Siglufjörður, the western side

*Table 1. Number of cases of avalanche cycles and extreme weather events in different regions. Also given are the numbers of extreme weather events, indicated by “NA”, that occurred without major avalanche activity.*

|  | Westfjords | North | East |
|--|------------|-------|------|
| Avalanche cycles (all cases)           | 34         | 34    | 23   |
| Avalanche cycles in separate regions   | 28         | 27    | 17   |
| Avalanche cycles with 5 day separation | 21         | 17    | 10   |
| Strong winds                           | 57         | 65    | 96   |
| Strong winds (NA)                      | 57         | 65    | 96   |
| Heavy snowfall                         | 45         | 70    | 39   |
| Heavy snowfall (NA)                    | 45         | 69    | 38   |
| Severe snowstorms                      | 61         | 64    | 37   |
| Severe snowstorms (NA)                 | 59         | 63    | 33   |

rises to about 650 mASL, with the highest point at 687 mASL. On the eastern side, the ridge rises from 600 mASL in the north to 850 mASL in the south. Hólsdalur, Skarðsdalur, and Skútudalur have ridge-top levels between 700 and 850 mASL. In Eastern Iceland, at Neskaupstaður, terrain tops are between 800 and 900 mASL, with a maximum at 930 mASL, whereas in Seyðisfjörður and Vestdalur the highest points lie between 1000 and 1150 mASL.

With these elevations, the 925 hPa level across the northern part of Iceland, oscillating between 180 and 1030 mASL in winter, around an average of 620 mASL, intersects the terrain at the upper parts of the main avalanche slopes. The 850 hPa level is typically above the highest terrain-tops, oscillating between 840 and 1700 mASL in winter, around an average of 1290 mASL. The 925 – 850 hPa thickness can therefore be taken as a measure of the average temperature within the avalanche starting zone. The wind at 925 and 850 hPa is an indicator of the direction of snow transport across ridges.

In the following analysis, “avalanche weather conditions” are compared with a corresponding “background climatology”. This contains fields for each day of the year with major avalanche activity within a given region, taking into account the previous and following 5 years during which within 5 days of that day no major avalanche activity was recorded at any of the observed locations. The 11-year period was chosen as a compromise between being long enough to average out anomalies on the specific day within individual years, but still short enough, that long-term climate trends are not significant. In that way, the weather conditions on each avalanche day are compared to representative current climate conditions. The 5-day gap around avalanche days was chosen to ensure synoptic separation between “avalanche” and “non-avalanche” weather conditions. If on a certain day of the year more than one major avalanche cycle is recorded in different years, that day is not counted repeatedly in the background climatology. Due to the small number of routinely observed avalanche slopes, “non-avalanche days” according to the collection of avalanche cycles considered here, may well include major avalanche activity elsewhere. Climatological comparisons between avalanche and non-avalanche weather conditions are therefore only meaningful at the specific locations, for which regular reports are available. The results obtained in this study do not necessarily translate to even nearby slopes, that are not routinely observed.

In “static” comparisons between composite fields for avalanche and non-avalanche days in different regions, presented in Sections 4 and 5, all major avalanche cycles are taken into account that are limited to one region. For the study of atmospheric evolution towards the beginning of avalanche cycles, presented in Section 6, the number of cases is further reduced to those, that are separated from each other by at least 5 days without reported avalanche activity in any of the regions (see Table 1). These selection criteria lead to the exclusion of some notable cases from the climatological analyses, which are discussed individually in Section 7.

The sources for meteorological data are the ERA-40 and ERA-Interim reanalyses produced by ECMWF (Uppala et al., 2005; Simmons et al., 2006; Berrisford et al., 2009). ERA-40, for complete years, is available for the 1958 – 2001 period. The ERA-Interim reanalysis project starts on 1 January 1989.

The variables used here are MSLP, geopotential height at 925, 850, 500, and 250 hPa, air temperature at 925 hPa, wind at 925 and 850 hPa, total precipitation (the sum of large-scale and convective precipitation), and snowfall (the sum of large-scale and convective snowfall). All

fields are available at a uniform 1-degree resolution in latitude and longitude. Over Iceland, this amounts to a physical grid-spacing of around 45 km in longitude, and 111 km in latitude. All variables, with the exception of precipitation, are provided as 6-hourly analysis fields valid at 00, 06, 12, and 18 UTC (which is local time in Iceland throughout the year). Daily averages are then calculated from the four 6-hourly fields of each day.

Precipitation amounts are derived from short-term forecasts, whereby total accumulation amounts are given from the beginning until the end of the forecast. To reduce spin-up effects, 24 hour accumulation throughout day  $D_0$  is calculated as the difference between the total accumulation from a 36 hour forecast starting at 12 UTC on day  $D_0 - 1$ , and the total accumulation from a 12 hour forecast starting at 12 UTC on day  $D_0 - 1$ . Units of total precipitation are millimetres of water per square metre, and millimetres of water equivalent in the case of snowfall. Occasionally, it is useful to analyse the difference between total precipitation and snowfall. As Einarsson (1984) points out, the classification of precipitation type in Iceland, even based on human observations and measurements, is difficult, since a considerable part of precipitation falling between observation times is mixed. In fact, it is estimated that in the northern part of the island during winter 15 – 45% of the total precipitation is of mixed type. Therefore, during the cold season, the residual between total precipitation and snowfall, as classified in the reanalysis data, cannot simply be classified as rain. However, the relative magnitude of snowfall, compared with either the total or residual precipitation, can be interpreted as a measure of the “dryness” of snow.

To extend any study beyond either the ERA-40 or ERA-Interim period, at some point between 1989 and 2001, a transition needs to be made between the two reanalyses. For this study, this is complicated by the fact that, over and in the vicinity of Iceland, significant differences exist between coinciding ERA-40 and ERA-Interim fields with regard to some variables (see Figures 7 and 8 as examples). In these figures, grid-point time-series are selected at ( $-19^\circ\text{E}$ ,  $65^\circ\text{N}$ ) for central Iceland, ( $-23^\circ\text{E}$ ,  $66^\circ\text{N}$ ) for the Westfjords, ( $-19^\circ\text{E}$ ,  $66^\circ\text{N}$ ) for Northern Iceland, and ( $-14^\circ\text{E}$ ,  $65^\circ\text{N}$ ) for Eastern Iceland. Compared with interannual fluctuations, there are large discontinuities in the zonal wind component at 925 hPa between ERA-40 and ERA-Interim over the northern and eastern part of the island, with winds during the ERA-40 period being more easterly at the northern coast, and less westerly at the eastern coast than during the ERA-Interim period (not shown). To a lesser extent, 925 hPa winds over the centre of the island are less easterly during the ERA-40 than during the ERA-Interim period. There are no significant discontinuities over the Westfjords. The latitudinal wind component at 925 hPa over the centre of the island, as well as at the northern coast, is about  $1 \text{ m s}^{-1}$  less southerly in the ERA-40 than in the ERA-Interim (not shown). To a lesser extent, this is also true at the eastern coast, with only small differences over the Westfjords. Related to these differences between ERA-40 and ERA-Interim in the annual mean values of individual velocity components, there are also significant discontinuities in the corresponding averages of wind speed (see Figure 7). Annual wind speed at 925 hPa, over the centre of the island, is almost  $2 \text{ m s}^{-1}$  higher in the ERA-40 than in the ERA-Interim, more than  $1 \text{ m s}^{-1}$  higher at the northern and eastern coast, and about  $1 \text{ m s}^{-1}$  over the Westfjords. Over the northwest, there is a discontinuity in the direction of long-term trends of annual wind speed, switching from positive in the ERA-40 to negative in the ERA-Interim. Qualitatively the same discontinuities, although to a lesser extent, exist at 850 hPa (not shown), suggesting that differences in reanalysed horizontal wind are due to differences in the treatment of terrain and boundary-layer processes, rather than model dynamics. There are no significant discontinuities in total annual precipitation amounts. However, with the exception of



Eastern Iceland, where snowfall amounts are relatively small, significantly less annual snowfall is analysed in the ERA-40 compared with ERA-Interim (see Figure 8). For the other variables relevant to this study, differences between ERA-40 and ERA-Interim are negligible in relation to interannual fluctuations.

As described by Simmons et al. (2006) and Berrisford et al. (2009), compared with ERA-40, several improvements in the ECMWF operational system were employed for the ERA-Interim reanalysis project, leading to systematically improved forecast performance, especially with regard to the hydrological cycle. The most far-reaching changes include the introduction of a higher spatial resolution of the numerical weather prediction model, and more extensive use of different satellite data. In general, ERA-Interim can therefore be considered to be more reliable, and was used here from its beginning in 1989 until 2006, with ERA-40 covering the earlier period since 1958. To minimise discontinuities in horizontal wind and snowfall, ERA-40 data for these variables are transformed in such a way, that the linear approximations of annual averages and standard deviations of the ERA-40 and ERA-Interim grid-point time-series have the same value in 1989.

For a 6-hourly ERA-40 grid-point time-series  $S$ , annual averages and standard deviations are calculated for the years 1958 – 1989, whereas for a corresponding ERA-Interim grid-point time-series  $S_i$ , annual averages and standard deviations are calculated for the years 1989 – 2006. Linear approximations to the time-series of ERA-40 and ERA-Interim annual averages have values  $\bar{S}_{89}$  and  $\bar{S}_{i89}$ , respectively, in 1989, whereas the linear approximations to the time-series of annual standard deviations have values  $\sigma_{89}$  and  $\sigma_{i89}$ . The corrected ERA-40 time-series is then given by

$$\tilde{S} = \frac{\sigma_{i89}}{\sigma_{89}} (S - \bar{S}_{89}) + \bar{S}_{i89} . \quad (1)$$

For wind speed and snowfall, only values above zero are corrected. Consequently, only values above zero are taken into account in calculating annual averages and standard deviations. When combining the two reanalyses, the data for 1989 is omitted from the corrected ERA-40 time-series. This linear trend matching is less sensitive to the choice of the transition year, than matching the annual values of the two time-series at the transition point. The corrected ERA-40 annual time-series, together with the linear trends, are also shown in Figures 7 and 8.

In the following analysis, regional averages are calculated by taking into account grid-points at ( $-23^\circ\text{E}$ ,  $66^\circ\text{N}$ ) and ( $-22^\circ\text{E}$ ,  $66^\circ\text{N}$ ) for the Westfjords, and ( $-19^\circ\text{E}$ ,  $66^\circ\text{N}$ ) and ( $-18^\circ\text{E}$ ,  $66^\circ\text{N}$ ) for Northern Iceland. Regional time-series for Eastern Iceland are taken at ( $-14^\circ\text{E}$ ,  $65^\circ\text{N}$ ). As mentioned in the introduction, and shown in Figures 1 to 6, this is related to the locations at which avalanches are routinely observed. Additionally, regional averages are calculated within the domain  $-24 \leq \lambda \leq -14^\circ\text{E}$  and  $65 \leq \phi \leq 66^\circ\text{N}$ , with longitude  $\lambda$  and latitude  $\phi$ , covering all three regions across the northern part of the island. For all regional averages on the regular angular grid, grid-point values are weighted by the cosine of latitude, to take into account the area represented by each grid-point.

Based on these regional averages, strong wind events are then defined as those consecutive cold season (Jan – Apr) days, during which the 925 hPa regionally averaged wind speed exceeds the cold season 95th percentile, excluding calm conditions. Here, January through April is chosen as reference period, to coincide with the main avalanche season (as discussed in the following section). Additionally, strong wind events are limited to those days, on which snowfall amounts

are within the lowest 5% of the cold season, excluding days without snowfall. The explicit limit values used for the different regions are given in Table 2.

Heavy snowfall events are defined as those consecutive days in any season, during which daily snowfall exceeds the 95th percentile of all days with snowfall, and during which 925 hPa wind speeds are within the lowest 50% throughout the whole year, excluding calm conditions. Heavy snowfall tends to be associated with intense storm systems and strong winds. Therefore, only few cases exist of heavy snowfall and lower wind speed limits.

As a third category of weather extremes, severe snowstorms are defined as those consecutive days, during which daily snowfall and 925 hPa wind speeds simultaneously exceed their respective 95th percentile throughout the whole year, excluding days without snowfall and calm conditions.

These extreme weather conditions are considered here for comparisons with those weather conditions, that are associated with major avalanche activity, rather than for comparisons of extreme weather conditions between different regions. Therefore, the extreme weather ensembles are not restricted to those cases, that exceed climatological limits in only one of the regions, as in the case of avalanche cycles. However, to insure synoptic independence, the ensembles of extreme events are restricted to those cases, that are separated from the previous event in each category by at least 5 days. Additionally, for comparisons with the prevailing weather conditions leading to major avalanche cycles, ensembles are restricted to those cases, that are not associated with any known major avalanche activity. The total number of cases for each category of extreme weather events, with and without avalanche activity, is given in Table 1.

### 3 Occurrence of severe snowstorms and major avalanches

As discussed in the introduction, it is well established that a combination of current or recent heavy snowfall and strong wind is conducive to the natural release of avalanches in a region characterised by maritime climatic conditions such as Iceland.

The number of cold season days with strong low-level winds but without significant snowfall, and the annual number of days with heavy snowfall and below-median wind speeds in different regions of Iceland is shown in Figure 9. There is no consistency between “windy” or “snowy” years, based on the annual number of extreme events, defined with regard to the long-term

*Table 2. Limit values for the definition of extreme regional averages of 925 hPa wind speed and daily snowfall for the whole year and the cold season (January through April).*

|                       | Percentile | Westfjords | North | East | All Regions |
|-----------------------|------------|------------|-------|------|-------------|
| 925 hPa Speed (year)  | 50         | 10.4       | 7.8   | 9.2  | 8.3         |
| 925 hPa Speed (year)  | 95         | 22.2       | 17.2  | 19.0 | 16.2        |
| 925 hPa Speed (JFMA)  | 95         | 23.7       | 18.6  | 20.3 | 17.6        |
| Daily snowfall (JFMA) | 5          | 0.04       | 0.04  | 0.06 | 0.01        |
| Daily snowfall (year) | 90         | 4.98       | 5.14  | 4.63 | 3.56        |
| Daily snowfall (year) | 95         | 6.63       | 7.27  | 6.64 | 4.94        |

climate. The annual number of days with snowstorm conditions, combining strong low-level winds and heavy snowfall, is shown in Figure 10. Again, since strong winds during the cold season and heavy snowfall can occur separately, there is no consistency between years with a high number of “windy” and “snowy” days, with those years with a high number of “snowstorm” days. Taking into account all regions, the periods with a relatively high number of snowstorm days are, most notably, 1958 to 1960, 1979 to 1982, the 1989 to 1992, 1995, and 1998.

Previously, Alexander et al. (2005) studied the occurrence of severe storm events over Iceland, defined as those weather conditions associated with absolute MSLP changes of at least 10 hPa over 3 hours. For the January through March winter season they found a large number of severe storms (more than 8) in 1976, 1989, and 1993, whereas no severe storm events, according to this definition, were found in 1960, 1965 – 66, 1974, 1977 – 78, 1980, 1987.

Comparing these results with those shown in Figures 9 to 10, again there is varying consistency between “stormy” years based on different definitions of storminess. For example, 1976 and 1993, which had a relatively high occurrence of rapid MSLP changes, were unremarkable across the northern part of Iceland with regard to the occurrence of strong cold season winds and heavy snowfall. Conversely, 1980, which had no occurrence of rapid MSLP changes, had a relatively high number of days with snowstorm conditions across the northern part of Iceland. Also, 1987 was unremarkable with regard to the occurrence of extreme winds and snowfall.

What this comparison demonstrates, is the diversity of what might be considered “stormy” cold season weather, which provides some difficulties for defining a representative measure of storminess for a given application. With regard to avalanche activity in Iceland, based on the previous studies, a direct measure of heavy snowfall combined with strong winds, or snowstorms as defined here, appears to be most appropriate. However, as shown in Figure 10, in all regions, the majority of days with severe snowstorm conditions is not associated with major avalanche activity. Based on these results alone it is clear, that a combination of heavy snowfall and strong winds is not sufficient for the release of major avalanches. This is consistent with previous studies linking the occurrence of avalanches in the Westfjords to local weather conditions (Björns-son, 2002; Haraldsdóttir et al., 2004), in which it was found that avalanche predictions based on locally measured snow accumulation and wind speed lead to high false alarm rates.

The annual occurrence of days with major avalanche activity, as defined in the previous section, is shown in Figure 11. Due to days with simultaneous avalanche activity in different regions, the sum of the occurrences in individual regions, in some years, exceeds the total number of days. As pointed out by Jónsson (1998), fewer avalanches occur in Eastern Iceland than in the Westfjords, due to higher temperatures and less frequent northeasterly storms in the east. Within well-documented history, four years stand out with major avalanche activity occurring on 13 or more days in any of the three regions: 1974, with the most severe avalanche activity and several fatalities in Eastern Iceland, but including also a severe 7-day cycle in the Westfjords; 1994, with the highest number of major avalanche days in the Westfjords; 1995, with the highest number of avalanche related fatalities in recent history in Iceland; and 2001, during which avalanche activity was spread out mostly over individual days in all three regions. Although, as noted above, the avalanche activity in 1974 occurred mostly in February, March, and December, no severe storms, defined based on rapid pressure changes, occurred during that winter. Nor was there a particularly high number of days with heavy snowfall or snowstorms. Similarly,

1994 – 95 had an average number of cases with rapid MSLP changes, as reported by Alexander et al. (2005). Also, 1994 was unremarkable with regard to the number of days with strong winds, heavy snowfall, and snowstorms. However, 1995 clearly stands out as the year with the highest number of days with snowstorm conditions in the Westfjords and Northern Iceland, where most of the avalanches fell during that year.

As shown in Figure 12, in the Westfjords and in Northern Iceland, most major avalanche activity has been recorded in January, whereas in the east, the highest occurrence of major avalanches is in February. To date, no hazardous avalanches have been recorded in June through September.

As shown in Figure 13, in Northern Iceland, most major avalanches associated with a given cycle fall within one day. In the Westfjords, and to a lesser extent in the east, hazardous avalanche activity, once started, tends to occur over an extended period of time of up to 8 days.

As shown in Figure 14, despite the selection criteria described in the introduction, putting an emphasis on avalanche cycles with maximum recorded run-out indices above 13, there are still some hazardous cases with smaller run-out indices. For these histograms, run-out indices were rounded to the nearest integer. Those recorded as being greater than 13.5 are counted as 14, whereas those greater than 15.5 are counted as 16. In the Westfjords, most run-out indices have been precisely determined, and approximately follow a normal distribution with a maximum at 15. In Northern and Eastern Iceland, many run-out indices are recorded with lower bounds of either 13.5 or 15.5, and are therefore not normally distributed.

## **4 Weather conditions associated with major avalanche cycles**

In the previous section it was shown, that the annual occurrence of strong winds, heavy snowfall, and snowstorms is only inconsistently related to the number of major avalanches that fell from regularly observed slopes that year. In this section, the weather conditions during avalanche activity will be analysed in more detail.

Figure 15 shows the difference between the joint histogram of daily air temperature and wind speed at 925 hPa for days with major avalanche activity, and the corresponding histogram for days during the main avalanche season from January through April without the occurrence of major avalanches. In all regions, the distribution of daily values associated with major avalanches is shifted from that of non-avalanche daily values towards lower temperatures and higher wind speeds. However, there is considerable overlap. Based on local station records in the Westfjords, this has previously been documented by Björnsson (2002).

Daily amounts of snowfall and residual precipitation, as defined in Section 2, during the main avalanche season from January through April are shown in Figure 16. With the exception of Eastern Iceland, major avalanches are associated with a greater amount of snowfall than of residual precipitation. In the east, two types of avalanches occur, associated with either predominantly snowfall or residual precipitation. The latter are slush flows, that occur during periods of heavy rainfall on an existing snowpack, or with rapid snowmelt. For one particular location in the Westfjords, these types of avalanches have been investigated by Decaulne & Sæmundsson (2006).

The greatest snow amount, and consequently the strongest gravitational pull for a given inclination, is likely to be found on the upper parts of lee side slopes, particularly in places with concave shape, such as gullies, ravines, and river valleys. If avalanches are triggered by current weather events, simultaneous avalanche activity at nearby locations might be expected to occur on slopes with similar aspects. However, as shown in Tables 4 to 6, many avalanche cycles, especially the most severe ones, are widespread and simultaneously involve slopes with a wide range of aspects. On these days, threshold values for the release of avalanches are exceeded regardless of wind direction. Therefore, in this section, no distinction will be made between avalanches occurring on slopes with significantly different aspects. For those avalanche cycles, that were limited to slopes with similar aspects, the associated large-scale weather patterns are analysed in the following section.

To establish avalanche-related atmospheric conditions in different regions of Iceland, comparisons will be made with specific background climatologies, as described in Section 2. To get an impression of the more general prevailing weather patterns during the main avalanche season from January through April, average atmospheric fields for this period of the year are shown in Figure 17. The dominant weather feature is the Icelandic Low, already mentioned in the introduction, located southwest of Iceland. Associated with that are southeasterly near-surface winds impinging on the southern coast. Consistent with the warm advection from the south, the prevailing off-shore winds rapidly veer with height to southwest on the 850 hPa level, located at a geopotential height of around 1320 m over Iceland. Over the land, average winds are weak from variable directions. Up to the 500 and 250 hPa levels, southwesterly winds intensify over and around Iceland, with wind directions remaining fairly constant. On the 500 hPa level and above, a shallow trough is situated to the west of Greenland, just upstream of a narrow zone of strong low-level baroclinicity, with a low ridge situated over Iceland and towards the southeast. Precipitation over the northern part of the island is mostly snow, with average daily rates of about 2 mm. Over the southern part, daily snow and residual precipitation amounts are approximately equal at 2 mm each. Interpreting residual precipitation as rain, these findings are consistent with those reported by Björnsson (1980) and Einarsson (1984) based on station records. Off-shore along the south coast, precipitation falls mostly as rain.

Compared with the cold-season climatology, as well as with the specific background climatologies, there are some distinct differences in the composite large-scale weather patterns associated with the release of avalanches across the northern part of Iceland.

As shown in Figures 18 and 19, for avalanche activity in all three regions, the prevailing low-pressure centre is shifted from its long-term climatological position in the southwest, to the southeast of Iceland. Consequently, low-level winds are shifted from southeast to northeast. For small and medium-size avalanches during two winters in the Westfjords, this has previously been documented by Haraldsdóttir et al. (2004). The cyclone centre is shifted progressively towards southeast for avalanches in the Westfjords, Northern Iceland, and Eastern Iceland. The intensity of the composite low, in absolute terms, is weakest for avalanches in Northern Iceland, and strongest for the Westfjords, consistent with the relative intensities of the composite upper-level jet stream. For the Westfjords and Eastern Iceland, the composite closed circulation extends to 500 hPa, tilting towards the northwest. In relative terms, compared with the background climatology, the composite low associated with avalanche activity in Eastern Iceland is most intense. Average boundary-layer temperature perturbations are small. For all three regions,

low-level baroclinicity over the northern part of Iceland is weak. Consequently, winds between the surface and 850 hPa change little with height, and are northeasterly throughout (not shown). The regions with the highest low-level baroclinicity are the cold front extending southwest from the composite cyclone centres, and the warm front extending eastwards. In all three regions, on average, snowfall accounts for about 80% of the total precipitation during avalanche activity.

There are significant qualitative differences for the three different regions between the transitions from the day preceding each of the major avalanche cycles (shown in Figures 20 and 21), to the atmospheric conditions during avalanche activity.

For the Westfjords, under the combined influence of an intense low-level baroclinic zone and a strong jet stream, the composite surface cyclone remains stationary and intensifies, with increased low-level wind speed from a steady northeast direction. On average, snowfall is higher on the preceding days, than during avalanche activity. Together with the increased average wind speed, this suggests that snowdrift rather than current intense precipitation is important for the release of at least some avalanches, which has previously been pointed out by Haraldsdóttir et al. (2004), and will be further discussed in the following sections.

For Northern Iceland, mid- and upper-level tropospheric winds are relatively weak on the preceding days. The already poorly defined composite surface cyclone weakens further during avalanche activity and moves slightly northeastwards, while low-level wind speeds from northeast decrease. Snowfall is moderate on the preceding days, and only slightly higher during avalanche activity. Nonetheless, in contrast with the Westfjords, it appears as if snowfall rather than wind may often be the dominant triggering mechanism in that region. However, this result may not be robust, considering the limited number of avalanche cases available for analysis.

For Eastern Iceland, comparing preceding days and days with avalanche activity, the composite surface cyclone weakens and moves east-northeastwards, steered by a mid-level cyclone. Consequently, surface winds shift from east to northeast, weakening slightly. During avalanche activity, snowfall decreases compared with the preceding days, suggesting that the changing direction of snowdrift may be partially responsible for the release of at least some of the avalanches.

## **5 Weather conditions for specific slope aspects**

As mentioned in the previous section, overall snow accumulation in the typical starting zones of major avalanche slopes not only depends on the actual snowfall, but also on the wind driven deposition of snow, or the erosion of the existing snowpack. Strong winds are therefore responsible for creating an inhomogeneous snow distribution over complex terrain, with excessive accumulation and avalanche danger in specific locations, even if the equivalent homogenous snow amount is insufficient to release hazardous avalanches.

As seen in the previous section, surface winds associated with cyclonic storm systems turn from southeast to northeast, while winds above the boundary-layer turn from southwest to northeast, with a shift of the cyclone centre from southwest of Iceland to the southeast. This is typically the case as cyclones, forming in the wake of the southern tip of Greenland, intensify. Considering the potential significance of snowdrift for the triggering of large avalanches, it is possible that slopes with different aspects become active at different times. As discussed previously, for many of the worst avalanche cycles, based on large-scale daily wind fields, this is not the case. However,

some avalanche cycles in each region are restricted to slopes with similar aspects. The prevailing wind conditions associated with these are analysed in this section. Thereby, the start dates of avalanche activity on specific slopes, as shown in Tables 4 to 6, are used, rather than the start dates of the corresponding avalanche cycles. As before, slope aspect is defined as the direction towards which the negative terrain gradient points.

For avalanche activity in all three regions, differences between the 925 and 850 hPa wind fields are small, without significant differences in wind speed, and only slightly veering wind directions with height over the northern and eastern part of Iceland (not shown).

## 5.1 Skutulsfjörður

As shown in Figure 2, major avalanches in the Westfjords occur on slopes with a wide range of aspects, and most of the hazardous avalanche activity is widespread. However, within Skutulsfjörður, opening towards the northeast, seven cases have been recorded only on the northwestern side of Ísafjörður, whereas three cases have been recorded only on the southeastern side of Kirkjubólshlíð. The occurrence of fewer major avalanches on slopes with a northern aspect was explained by Jónsson (1998) through the higher temperatures associated with southerly winds that are required to deposit rather than remove snow on these slopes.

Figures 22 and 23 show the average 925 hPa wind field and snowfall on the days preceding and during avalanche activity, respectively, on either northwest or southeast slopes in Skutulsfjörður. For the southeast slope, snowfall amounts are moderate before and during avalanche activity, with strong but steady ridge-top level winds blowing into the fjord from the northeast. For the northwest slope, more so than for the overall composite fields discussed in the previous section, snow falls almost exclusively during the preceding day with intermediate winds from east-northeast, and almost calm conditions during avalanche activity. Since the large-scale wind direction is consistent with the orientation of the fjord, local winds are likely to be similar. Snowdrift can therefore be expected to take place mostly parallel to the slopes, rather than from the windward to the lee side of the ridges on either side of the fjord.

For the southeast slopes in Skutulsfjörður, residual precipitation amounts (not shown) are insignificant before and during avalanche activity. For the northwest slopes, residual precipitation is slightly larger at the edges of the Westfjords, shifting from northeast during the preceding days, to southwest during avalanche activity. However, the total precipitation amounts associated with major avalanche activity on both sides of Skutulsfjörður is dominated by dry snow.

## 5.2 Siglufjörður

Siglufjörður, located in the central part of Northern Iceland, opens towards the north-northeast (see Figure 4). Thirteen major avalanche cycles have been recorded only on the western side of the fjord, with aspects varying between northeast and east-southeast, whereas twelve cases have been recorded only on the eastern side, with westerly aspects.

As shown in Figures 22 and 23, for avalanche activity on either side of the fjord, average snowfall during the preceding days is intermediate, increasing considerably during avalanches on the western side, but decreasing during avalanches on the eastern side. Residual precipitation amounts are generally small, but slightly increase during avalanche activity on the western side

of the fjord. Overall, dry snow dominates. Average winds before and during avalanche activity on either side of the fjord are steady from northeast, with low wind speeds for avalanches on the western side, and intermediate winds for those on the eastern side. The slopes on the eastern side are slightly leeward with respect to the overlying flow. The release of avalanches there, without current snowfall, is therefore likely to be triggered by snowdrift from the windward side of the ridges east of the fjord. Winds below ridge-top level within the fjord can be expected to be channelled from the north. The release of avalanches on the windward western side, occurring with heavy current snowfall, may therefore also be triggered by sideways snowdrift along the slopes.

### 5.3 Eastern Iceland

In Seyðisfjörður, Vestdalur, and Neskaupstaður, ten major avalanche cycles have been recorded only on slopes with east-southeast to southerly aspects, whereas in Seyðisfjörður, ten cases have been recorded only on a slope with west-northwest aspect (see Figures 5 and 6).

As shown in Figures 22 and 23, for avalanche activity on slopes with either of the two general orientations, snowfall is intermediate during the preceding days, and heavier than during the occurrence of avalanches, especially on the southeastern slopes. Residual precipitation is only significant for the west-northwestern slope, where it is intermediate on the days preceding avalanche activity, but decreases during the release of avalanches. There, snowfall and residual precipitation amounts, on average, are approximately equal, consistent with the occurrence of slush flows on these slopes. Average winds before and during avalanche activity on slopes with either of the two orientations are intermediate throughout, turning northeast to north for avalanches on southeastern slopes, and east to northeast for avalanches on the west-northwest slope. For the southeastern slopes, the decrease in current snowfall during avalanche activity and the change from windward to lee suggest that the triggering mechanism is largely due to snowdrift. On the west-northwest slope, the largest snow amount is deposited with leeward winds on the day preceding the release of avalanches. Avalanches are then released with approximately along-slope winds, possibly due to sideways deposit of snow into ravines.

## 6 Development of avalanche weather conditions

Separately for each region, Figures 24 to 26 show ensemble 5-day histories leading up to the first day of each avalanche cycle, which is separated by at least five days from the previous cycle. In addition to total precipitation and snowfall, the percentage of snowfall relative to the total precipitation is calculated as a measure of the dryness of snow. The corresponding ranges in maximum values of temperature, wind speed, total precipitation, snowfall, and residual precipitation are listed in Table 3.

In the Westfjords (see Figure 24), average and median regional wind speeds at 925 hPa are consistently above  $10 \text{ m s}^{-1}$  during the 6-day period. On average, wind gradually strengthens towards the beginning of avalanche cycles, turning northeast in almost all cases. Temperature at 925 hPa (not shown) is almost exclusively below freezing. For most cases, total precipitation is predominately snow throughout the 6-day period, on average reaching a maximum on the day preceding avalanche activity. In one case, the highest daily snowfall amount during the period was as low as 1 mm. However, half of the cases had daily snowfall maxima above 8 mm.



In Northern Iceland (see Figure 25), average and median regional wind speeds at 925 hPa are around  $10 \text{ m s}^{-1}$  during the 6-day period, and increase towards the beginning of avalanche cycles. Wind directions are mixed, but mostly around northeast on days with the highest precipitation and snowfall amounts. Temperature at 925 hPa in one case reaches well above freezing, but is mostly below freezing. The highest daily snowfall amounts for the most part are somewhat larger than those in the Westfjords, but in one case a daily maximum as low as 2 mm fell within the 5 days leading up to the release of avalanches.

In Eastern Iceland (see Figure 26), average and median regional wind speeds at 925 hPa increase to above  $10 \text{ m s}^{-1}$  towards the beginning of avalanche cycles, turning northeast in all cases. Temperature at 925 hPa remains almost exclusively below freezing. Nonetheless, as seen previously, in several cases, the proportion of snow in total precipitation is well below 60%, leading up to the release of avalanches. The highest daily snowfall amounts during the 6-day period are similar to those in Northern Iceland, with considerably higher maximum residual precipitation amounts.

Despite a considerable variability among and even within different regions, the range of weather conditions leading up to the release of major avalanches, derived from reanalyses, is similar to that reported by Björnsson (1980), based on local station records. In that study it was pointed out that the release of dry-snow avalanches in any of the three regions is associated with, or preceded within 4 – 6 days by maximum surface wind speeds of  $10 - 30 \text{ m s}^{-1}$  (6 – 10 on the Beaufort scale), maximum daily snowfall amounts of 15 – 25 mm, and temperatures just below freezing. However, as noted in Section 3, consistent with previous studies, these are not sufficient criteria for the release of major avalanches, and cannot serve as predictive threshold values without missing some significant cases, and with high false alarm rates otherwise.

This can be demonstrated by comparing the “avalanche ensembles” discussed so far, with meteorologically comparable ensembles of 6-day periods that did not lead to the release of major avalanches, during which nonetheless daily snowfall reaches 15 mm at least once, daily average wind speed at 925 hPa is consistently above  $5 \text{ m s}^{-1}$ , and daily average temperature at 925 hPa is consistently below freezing. Further restrictions are, that individual 6-day periods are separated from each other by at least 5 days, and no major avalanches occurred during the 6-day period, nor during the 5 days leading up to it and following it. For periods during which these criteria are

*Table 3. Lowest / median / highest maximum values of daily mean 925 hPa temperature ( $T_{\max}$ ), daily mean 925 hPa wind speed ( $S_{\max}$ ), daily total precipitation ( $TP_{\max}$ ), daily snowfall ( $SF_{\max}$ ), and daily residual precipitation ( $RP_{\max}$ ), for ensembles of time-series leading up to the release of avalanches (A), or without avalanches (NA). The number of cases in each ensemble is shown in parentheses.*

|                     | $T_{\max}$ [°C]    | $S_{\max}$ [ $\text{m s}^{-1}$ ] | $TP_{\max}$ [mm] | $SF_{\max}$ [mm] | $RP_{\max}$ [mm] |
|---------------------|--------------------|----------------------------------|------------------|------------------|------------------|
| Westfjords (A, 21)  | -9.4 / -3.0 / 2.5  | 13.5 / 24.5 / 33.1               | 3 / 11 / 28      | 2 / 8 / 19       | 0 / 3 / 18       |
| Westfjords (NA, 11) | -9.3 / -2.7 / -0.2 | 12.8 / 22.3 / 28.6               | 17 / 19 / 39     | 15 / 16 / 26     | 1 / 4 / 24       |
| North (A, 17)       | -7.7 / -1.1 / 4.8  | 9.1 / 14.9 / 21.0                | 6 / 13 / 30      | 2 / 9 / 25       | 2 / 4 / 12       |
| North (NA, 21)      | -8.8 / -1.8 / -0.3 | 10.3 / 16.2 / 28.1               | 19 / 22 / 57     | 15 / 18 / 41     | 2 / 6 / 16       |
| East (A, 10)        | -7.6 / -1.8 / 1.0  | 8.8 / 20.5 / 22.5                | 5 / 10 / 20      | 4 / 6 / 13       | 1 / 5 / 17       |
| East (NA, 11)       | -7.1 / -2.5 / -0.7 | 13.5 / 18.6 / 23.5               | 19 / 24 / 36     | 15 / 19 / 27     | 2 / 7 / 14       |

satisfied for more than 6 days, the period is chosen such, that the highest daily snowfall occurs as close to the end of the 6-day period as possible.

As can be seen from Figures 24 to 26, as well as from Table 3, in all three regions, the highest daily total precipitation and snowfall amounts of the non-avalanche ensembles greatly exceed those of the avalanche ensembles. Also, generally, snow has a higher percentage in total precipitation for the non-avalanche ensembles. In Northern and Eastern Iceland, wind speeds at 925 hPa are similar in the two ensembles. In the Westfjords, contrary to the avalanche ensembles, wind speed generally decreases during the 6-day periods that do not lead to the release of major avalanches. However, in general, avalanche prediction based on regional averages of precipitation, wind speed, and temperature is unreliable.

The same ambiguity between avalanche and non-avalanche storm conditions in any of the three regions can be seen on a larger scale. Compared with the discussion in Section 4, the ensemble of avalanche cycles here is reduced to those cases that are separated from each other by at least 5 days. Additionally, only the first day of avalanche activity is taken into consideration.

For the Westfjords, the atmospheric evolution leading up to the release of major avalanches is shown in Figures 27 and 28. At 5 days prior to the release of avalanches, a weak composite low-pressure region is located south and especially northeast of Iceland, with a low-level baroclinic zone extending towards the southwest and east. At that time, mid- and upper-level forcing is weak, without composite troughs or ridges over the North Atlantic, and only a weak jet stream. This is due to significant variability among individual cases at that stage of the development towards the release of avalanches. Over the following days, in response to the differential temperature advection by the pre-existing low-level circulation within the baroclinic zone, a mid- and upper-level trough begins to form, while a new low forms southwest of Iceland. The composite surface cyclone intensifies just downstream of the trough axis until the day prior to avalanche activity, while moving east.

As shown in Figures 29 to 32, weather conditions over Northern and Eastern Iceland, leading to the release of avalanches in these regions, are similar. For Northern Iceland, at 5 days prior to the start of avalanche cycles, a composite cyclone is located east of the southern tip of Greenland. Over the next 3 days, it intensifies and moves eastwards. Then however, in contrast with the situation for the Westfjords, the composite cyclone weakens towards the release of avalanches. This is consistent with the results discussed in the previous section for a larger ensemble of avalanche cases, and taking into account all avalanche days for each cycle. For Eastern Iceland, at 4 days prior to the start of avalanche cycles, a new composite cyclone forms southwest of the island. It intensifies steadily until the start of avalanche activity, while moving slowly eastwards. The situation differs from that for the Westfjords primarily in the location of the composite low, being about 500 km further southeast.

As shown in Figures 33 and 34, some notable differences exist between the composite atmospheric evolution leading up to snowstorm conditions over the Westfjords that are not associated with avalanche activity, compared with that leading up to the release of major avalanches in that region. The magnitude and orientation of the 925 – 850 hPa mean layer temperature gradient across the northern North Atlantic are similar, but the absolute layer thickness is about 10 m higher for snowstorms, implying warmer low-level temperatures. The new composite surface cyclone forms southwest of Iceland, as for avalanches occurring in the same region. It and

the upper-level flow change little for the next 3 days. Then, the daily central pressure drops by 5 hPa, followed by a further drop of 10 hPa, and a shift towards the northeast, with the onset of snowstorm conditions. At the same time, the mid- and upper-level trough intensifies. The central pressure value of the composite low associated with snowstorm conditions is similar to that associated with the release of avalanches, but the pressure gradient, low-level winds, and snowfall are considerably stronger.

As shown in Figures 35 to 38, the formation of the composite surface cyclone, responsible for snowstorm conditions over Northern and Eastern Iceland, is less focussed than that for the Westfjords until the last day prior to the onset of snowstorm conditions. The reason for that is weak and almost zonal mid- and upper-level flow. The mid- and upper-level trough axis is rotated progressively towards the east, for snowstorm conditions in the Westfjords, in Northern, and in Eastern Iceland.

Despite the differences between “avalanche weather conditions” in different regions, as well as the differences between the atmospheric evolution towards either the release of avalanches or non-avalanche snowstorm conditions for any one of the regions, the composite large-scale weather patterns during the last 3 days are basically the same in all cases, with a cyclone forming southeast of Iceland, rather than in the cold-season climatological location in the southwest, and intensifying by a combination of low-level baroclinic instability, mid-level positive vorticity advection, and upper-level divergence. This is consistent with the findings of Jóhannesson & Jónsson (1996), who pointed out that even the weather conditions associated with the catastrophic Súðavík and Flateyri avalanches in 1995 were not extreme within the context of the long-term storm climate of the Westfjords.

However, there are significant differences in the formation of strong winds or heavy snowfall individually, compared with storms combining both. In the case of strong wind events over all three regions (see Figures 39 to 44), the composite surface cyclone develops near the southern tip of Greenland. The strong southwesterly winds over Iceland are driven by the strong pressure gradient between this cyclone and an anticyclone over the North Sea. The mid- and upper-level flow is dominated by a ridge over the eastern half of the North Atlantic. In contrast, heavy snowfall events with below-median wind speeds over all three regions (see Figures 45 to 50) are associated with an elongated composite low-pressure zone between the southern tip of Greenland, and the northern tip of the Scandinavian Peninsula, suggesting that individual cyclones are located either towards the southwest or northeast of Iceland, rather than towards the southeast, as under snowstorm conditions. Mid- and upper-level forcing is relatively weak, with a shallow trough over the western half of the North Atlantic, and a low ridge of the eastern half.

## **7 Weather associated with individual avalanche cycles**

For comparison with the climatological analyses presented so far, this section briefly describes the weather conditions leading up to some important or unusual individual avalanche cycles, that were not included in the ensembles discussed in the previous sections, due to avalanche activity occurring simultaneously in different regions, or because avalanche cycles are separated by less than 5 days without avalanche activity. Some details of these cases are also listed in Tables 4 to 6.

On 4 Feb 1968, major avalanches were released simultaneously in the Westfjords and in Northern Iceland, on slopes with different aspects. As shown in Figure 51, ignoring differences in the absolute values, this individual case closely followed the composite pattern of atmospheric evolution towards the start of avalanche cycles in the Westfjords (see again Figures 27 and 28). Two days prior to release, a surface cyclone formed southwest of Iceland under a strong mid-level temperature gradient, with a ridge to the north of the island, and a trough towards the south. Within the next day, the northern ridge was eroded by low-level northwesterly cold advection from Greenland. Rapid intensification of the surface cyclone occurred south of Iceland, due to mid-level positive vorticity advection associated with the newly formed trough, and upper-level divergence associated with the older trough further east. Heavy precipitation started on the day on which avalanches were released, primarily in the form of snow over the Westfjords, but with a significant amount of residual precipitation over Northern Iceland.

On 8 – 15 Feb 1974, one of the most active cycles on record affected the Westfjords and Eastern Iceland, on slopes with a wide range of aspects. Avalanche activity began in Eastern Iceland on 8 Feb. As shown in Figure 52, a small amount of snow fell on the preceding day with northeasterly winds, which intensified and turned easterly on the first day of release. Over the next 4 days (9 – 12 Feb), intermediate but sustained snowfall occurred over northern Iceland (see Figure 53). Avalanche activity in the Westfjords began on 10 Feb, and continued until the 12th, with strong northeasterly winds. The troposphere at different levels was highly variable throughout the entire cycle, without establishing any stable pattern. Consequently, relevant surface cyclones were located south, east, and northeast of Iceland at different stages of the evolution.

On 19 – 21 Dec 1974, an avalanche cycle affected Northern and Eastern Iceland, on slopes with east-southeast to southerly aspects. As shown in Figure 54, it deviated significantly from the composite evolution discussed in the previous section. Three days prior to the release of the first avalanche, strong east-northeasterly low-level winds existed over the northern part of Iceland, associated with an intense cyclone to the south, downstream of a negatively tilted mid-level trough. Under the influence of an upper-level jet streak, this trough moved rapidly eastwards. The surface cyclone weakened, as a ridge built behind the mid-level trough, but reformed south of Iceland on the first day of avalanche activity, with easterly low-level winds over the affected regions. Weak but continuous snowfall existed throughout the 3 days leading up to the avalanche cycle.

On 12 – 14 Jan 1975, an avalanche cycle affected Northern and Eastern Iceland, associated with widespread impact. As shown in Figure 55, the troposphere was unstable and highly variable until the start of avalanche activity. Then, a mid- and upper-level trough moved eastwards over a low-level baroclinic zone, located southwest of Iceland, leading to explosive development of a surface cyclone just downstream of the trough axis, with a drop in centre pressure of about 30 hPa in one day. Strong easterly low-level winds existed across Iceland during the first day of release, with heavy snowfall in the east, and moderate snowfall in the north.

Between 19 Mar and 3 Apr 1987, two major avalanche cycles affected the Westfjords, associated with widespread impact. There was an unusual atmospheric evolution during that period, with a continuous cyclone moving repeatedly east and west across the North Atlantic. As shown in Figure 56, during the days leading up to the first cycle (16 – 19 Mar), the surface cyclone was initially located south of Iceland, and intensified as it moved southeast over the North Sea. At the

start of avalanche activity, it was farther removed from Iceland than is usually the case, resulting in weak northerly low-level winds over the Westfjords. Only a small amount of snow fell during the preceding 3 days. Over the next 4 days (20 – 23 Mar, not shown), the cyclone maintained its intensity while moving northwest, bringing increased snowfall to the Westfjords. During that period, low-level winds turned from northerly to easterly. Over the following 4 days (24 – 27 Mar, not shown), the cyclone moved southeast again, rapidly intensifying over Scotland, with little precipitation over the Westfjords. As shown in Figure 57, during the days leading up to the second cycle (28 – 31 Mar), the cyclone over Scotland moved northeast and dissolved, while a new low formed north of Iceland. This cycle started during a rapid intensification of this cyclone, with heavy snowfall and strong northerly low-level winds over the Westfjords.

On 3 – 5 Apr 1994, an avalanche cycle affected the Westfjords, on slopes with southeast to southerly aspects. It is an unusual case, as it appears to involve delayed-action avalanches. As shown in Figure 58, “typical” avalanche weather conditions existed 3 days prior to the release of the first avalanche, with an intense cyclone situated southeast of Iceland, and moderate snowfall, and strong northeasterly low-level winds over the Westfjords. Moderate to weak snowfall continued over the next 2 days, but the low-pressure centre and the low-level winds over the Westfjords weakened considerably until the start of avalanche activity. The cyclone intensified again on the second day of avalanche activity (not shown), but snowfall remained weak.

On 16 – 22 Jan 1995, a severe avalanche cycle affected the Westfjords and Northern Iceland, associated with widespread impact. As shown in Figure 59, 3 days prior to the release of the first avalanche, an intense cyclone existed between Greenland and Iceland, extending from the surface to mid-levels. A band of heavy precipitation was located in the frontal zone between the cyclone and a high pressure region over the Bay of Biscay, with a mid- and upper-level ridge over the eastern part of the North Atlantic. Together with low-level cold advection from Greenland, a jet streak over Iceland caused eastward motion of the mid-level trough. On the day prior to the release of avalanches, a surface cyclone formed southwest of Iceland. However, in contrast with the composite evolution discussed in the previous section, the surface cyclone moved northeast rather than east. Avalanche activity began, when the cyclone intensified rapidly just off the northern coast of Iceland under the influence of strong upper-level divergence, generating heavy snowfall and strong northeasterly winds over the northern part of the island.

On 23 – 26 Oct 1995, an avalanche cycle in the Westfjords was responsible for the highest number of avalanche related fatalities in recent history in Iceland. This case has been discussed in detail by Thorsteinsson et al. (1999). For a direct comparison with the other avalanche cycles discussed here, the atmospheric conditions leading up to and during this event are shown in Figures 60 and 61. Despite the catastrophic impact from avalanches with the highest run-out indices on record, the associated large-scale weather conditions, as represented by the European reanalyses, were not unusually severe, as far as location and central pressure of the dominant cyclone were concerned, as well as wind speed and snowfall amounts before and during avalanche activity.

On 11 – 13 Mar 1999, an avalanche cycle affected the Westfjords and Northern Iceland, associated with widespread impact. The atmospheric conditions associated with this cycle are distinctly different from the composite evolution discussed in the previous section. As shown in Figure 62, 3 days prior to the release of the first avalanche, a ridge was located between

Greenland and Iceland. Over the next day, it was eroded by mid- and upper-level cold air advection from the Canadian Archipelago, and a sudden shift of the Arctic Vortex from Baffin Island to south of Iceland, with cyclonic circulation extending throughout the troposphere. Moderate snowfall and easterly winds across the northern part of Iceland started on the day prior to the start of avalanche activity.

## 8 Summary

In this study, based on ECMWF reanalysis data, the regional and large-scale atmospheric conditions associated with well-documented major avalanche cycles at various locations in three regions of Iceland have been analysed. Comparisons were made with the non-avalanche cold-season climatology, as well as with the atmospheric conditions associated with severe snow storm conditions in corresponding regions, that did not lead to the release of major avalanches at the locations considered here.

Compared with the non-avalanche cold-season climatology, there are some distinct differences in the composite large-scale weather patterns associated with the release of avalanches across the northern part of Iceland. For avalanche activity, the prevailing low-pressure centre is shifted from its long-term climatological position in the southwest, to the southeast of Iceland. Consequently, low-level winds are shifted from southeast to northeast.

However, despite these clear differences between “avalanche weather conditions” and the non-avalanche cold-season climatology, the composite atmospheric fields, and the range of synoptic situations that lead to the release of major avalanches, as represented by the European reanalyses, do not show large-scale characteristics, that distinguish them from severe snowstorms, that are not associated with major avalanche activity.

As demonstrated in previous studies (Björnsson, 1980, 2002), the same ambiguity between avalanche and non-avalanche storm conditions exists based on nearby meteorological surface station measurements. Weather conditions associated with major avalanche activity, while generally characterised by strong winds and heavy snowfall, are often not extreme. Conversely, only a small subset of the most intense snowstorms leads to the release major avalanches on routinely observed slopes, where a combination of heavy snowfall and strong wind is not sufficient for the release of major avalanches. Overall, therefore, even in a maritime climate, the correlation between the release of avalanches and recent or current large-scale weather conditions, as well as nearby surface station measurements, is poor.

Nonetheless, there are some distinct differences in the prevailing weather conditions leading up to and during the release of major avalanches in different regions. For the Westfjords, on average, snowfall is higher on the preceding days, than during avalanche activity. Together with an increased average wind speed, this suggests that snowdrift rather than current intense precipitation is important for the release of at least some avalanches. For Northern Iceland, winds are often relatively weak on the preceding days, and weaken further during avalanche activity. Snowfall is moderate on the preceding days, and only slightly higher during avalanche activity. Nonetheless, in contrast with the Westfjords, it appears as if snowfall rather than wind is often the dominant triggering mechanism in that region. For Eastern Iceland, comparing preceding days and days with avalanche activity, surface winds shift from east to northeast, weakening slightly. During avalanche activity, snowfall decreases compared with the preceding days, suggesting that the

changing direction of snowdrift may be responsible for the release of some avalanches. With the exception of Eastern Iceland, major avalanches are associated with a greater amount of snowfall than the total amount of other types of precipitation. In the east, two types of major avalanches occur, associated with either predominantly snowfall or other types of precipitation (slush flows).

Also, within a given region, or even within an individual fjord, for avalanche activity on opposing slopes, distinct differences are detectable in large-scale reanalysis fields, mostly in the low-level wind conditions and snowfall. Therefore, despite a limited predictive value, the large-scale weather conditions are closely enough related to the release of avalanches to identify, after the fact, the dominant triggering mechanism in individual cases, and over time, the prevalent triggering mechanism within a given region.

For reliable predictions of avalanches, however, more parameters are needed to sufficiently characterise snowpack stability. This includes the shape of ice crystals, affecting their mechanical properties within the snowpack, such as stacking and interlocking, as well as temperature and liquid water content, affecting bonding among ice crystals. These characteristics are affected by in-cloud thermodynamic properties, and the atmospheric temperature profile between the level of snow formation and the ground. Although direct-action avalanches are less dependent on the temperature within the snowpack, they do depend on the type of surface onto which the fresh snow falls (e.g., rocks, soft or hard-packed existing snowpack). These considerations require detailed information about the local history of wind, temperature, humidity, cloudiness, and precipitation, and are beyond the scope of this investigation.

## References

- Alexander, L. V., Tett, S. F. B., & Jonsson, T. (2005). Recent observed changes in severe storms over the United Kingdom and Iceland. *Geophys. Res. Lett.*, *6*, L13704.
- Arason, P., Arnalds, P., Sauermoser, S., & Sigurðsson, H. P. (2005). *Hættumat fyrir Súðavík* (Report 05006). Reykjavik, Iceland: Icelandic Meteorological Office.
- Arnalds, P., Jónasson, K., & Sigurðsson, S. (2004). Avalanche hazard zoning in Iceland based on individual risk. *J. Glaciol.*, *38*, 285-290.
- Berrisford, P., Dee, D., Fielding, K., Fuentes, M., Kållberg, P., Kobayashi, S., & Uppala, S. (2009). *The ERA-Interim archive* (ERA Report Series No. 1). Reading, United Kingdom: European Centre for Medium Range Weather Forecast.
- Björnsson, H. (1980). Avalanche activity in Iceland, climatic conditions, and terrain features. *J. Glaciol.*, *26*(94), 13-23.
- Björnsson, H. (2002). *Veður í aðdraganda snjóflóðahrina á norðanverðum Vestfjörðum* (Report 02019, VÍ-ÚR14). Reykjavik, Iceland: Icelandic Meteorological Office.
- Charney, J. G. (1947). The dynamics of long waves in a baroclinic westerly current. *J. Meteorol.*, *4*(5), 135-162.
- Decaulne, A., & Sæmundsson, Þ. (2006). Meteorological conditions during slush-flow release and their geomorphological impact in Northwestern Iceland: A case study from the Bíldudalur Valley. *Geogr. Ann.*, *88A*(3), 187-197.
- Eady, E. (1949). Long waves and cyclone waves. *Tellus*, *1*, 33-52.
- Einarsson, M. Á. (1984). Chapter 7: Climate of iceland. In H. van Loon (Ed.), *Climates of the oceans* (Vol. 15, p. 673-697). Amsterdam, Netherlands: Elsevier.
- Hanna, E., Jónsson, T., & Box, J. E. (2004). An analysis of Icelandic climate since the Nineteenth Century. *Int. J. Climatol.*, *24*, 1193-1210.
- Haraldsdóttir, S. H. (2002). *Snjóflóðasaga Flateyrar og Önundarfjarðar* (Report 02036). Reykjavik, Iceland: Icelandic Meteorological Office.
- Haraldsdóttir, S. H., Ólafsson, H., Durand, Y., Giraud, G., & Mérindol, L. (2004). A system for prediction of avalanche hazard in the windy climate of Iceland. *Ann. Glaciol.*, *38*, 319-324.
- Jóhannesson, T. (2001). Náttúruhamfarir á Íslandi. *Orkuþing*, <http://www.samorka.is/doc/1043>, 9 pages.
- Jóhannesson, T., & Jónsson, T. (1996). *Weather in Vestfirðir before and during several avalanche cycles in the period 1949 to 1995* (Report 96015). Reykjavik, Iceland: Icelandic Meteorological Office.
- Jónsson, T. (1998). *Hlutfallslíkur snjóflóðaátta á Vestfjörðum og Austfjörðum* (Report 98013). Reykjavik, Iceland: Icelandic Meteorological Office.



- Lorenz, E. N. (1972). Barotropic instability of Rossby wave motion. *J. Atmos. Sci.*, 29, 258-264.
- McClung, D., & Schaerer, P. (2006). *The avalanche handbook, 3rd edition*. Seattle, Washington, USA, 345 pages: The Mountaineers Books.
- Ólafsson, H. (1998). *Veður fyrir snjóflóðahrinur í Neskaupstað 1974 – 1995* (Report 98015). Reykjavik, Iceland: Icelandic Meteorological Office.
- Schneiderreit, A., Blender, R., Fraedrich, K., & Lunkeit, F. (2007). Icelandic climate and North Atlantic cyclones in ERA-40 reanalyses. *Meteorol. Z.*, 16(1), 17-23.
- Serreze, M. C., Box, J. E., Barry, R. G., & Walsh, J. E. (1993). Characteristics of Arctic synoptic activity, 1952 – 1989. *Meteorol. Atmos. Phys.*, 51, 147-164.
- Serreze, M. C., Carse, F., Barry, R. G., & Rogers, J. C. (1997). Icelandic Low cyclone activity: Climatological features, linkages with the NAO, and relationships with recent changes in the Northern Hemisphere circulation. *J. Climate*, 10, 453-464.
- Shapiro, M., & Grønås, S. (Eds.). (1999). *The life cycles of extratropical cyclones*. Boston, Massachusetts, USA, 359 pages: American Meteorological Society.
- Simmons, A., Uppala, S., Dee, D., & Kobayashi, S. (2006). ERA-Interim: New ECMWF reanalysis products from 1989 onwards. *ECMWF Newsletter*, 110, 25-35.
- Sturm, M., Holmgren, J., & Liston, G. E. (1995). A seasonal snow cover classification system for local to global applications. *J. Climate*, 8, 1261-1283.
- Thorsteinsson, S., Kristjánsson, J. E., Røsting, B., Erlingsson, V., & Ulfarsson, G. F. (1999). Diagnostic study of the Flateyri avalanche cyclone, 24 – 26 October 1995, using potential vorticity inversion. *Mon. Wea. Rev.*, 127, 1072-1088.
- Uppala, S. M., Kållberg, P. W., Simmons, A. J., et al. (2005). The ERA-40 re-analysis. *Q. J. R. Meteorol. Soc.*, 131, 2961-3012.

*Table 4. Start dates and duration in number of days of all major avalanche cycles considered in this study, that occurred in the northern part of the Westfjords. Also given is the largest run-out index (ROI) recorded for each cycle, and the main locations affected. Slope orientations and avalanche dates for specific slopes are given in parentheses. Slope orientation, or aspect, is defined as the direction towards which the negative terrain gradient points.*

| Start Date  | Dur. | Max. ROI | Locations affected   |
|-------------|------|----------|--|
| 14 Mar 1958 | 2    | 15.0     | Flateyri (SW, 14.03.), Öndarfjörður (NNE, 14-15.03.)   |
| 28 Jan 1966 | 4    | n/a      | Widespread damage  |
| 4 Feb 1968  | 1    | n/a      | Flateyri (SW)  |
| 7 Nov 1969  | 4    | 15.4     | Flateyri (SW, 10.11.), Ísafjörður (SE, 10.11.), Öndarfjörður, several other locations  |
| 12 Feb 1973 | 3    | 15.0     | Ísafjörður (SE, 12.02.), Kirkjubólshlíð (NW, 12.02.), Súðavík (ESE, 14.02.), Tungudalur (S, 13.02.)  |
| 8 Feb 1974  | 7    | 17.0     | Flateyri (SW, 11.02.), Ísafjörður (SE, 10&12.02.), Öndarfjörður, several other locations   |
| 4 Feb 1977  | 2    | > 13.5   | Flateyri (SW, 05.02.), Öndarfjörður (NNE, 04.02.; E, 05.02.)   |
| 29 Nov 1979 | 1    | 15.0     | Flateyri (SW)  |
| 2 Jan 1983  | 5    | 14.7     | Súðavík (ESE, 06.01.), Öndarf. (WNW&NNE, 02-06.01.)  |
| 14 Dec 1983 | 1    | 14.7     | Hnífsdalur (SE)  |
| 4 Jan 1984  | 1    | 12.3     | Ísafj. (SE), Kubbi (NNE), Öndarf. (WNW&NNE)  |
| 23 Dec 1985 | 1    | 13.0     | Hnífsdalur (NNW, SE), Ísafjörður (SE), Kubbi (NW), Öndarfjörður (NNW)  |
| 19 Mar 1987 | 8    | 14.0     | Flateyri (SW, 24-26.03.), Hnífsdalur (SE, 23.03.), Ísafjörður (SE, 24.03.), Kirkjubólshlíð (NW, 23-24.03.), Öndarfjörður (NNW&NNE, 19.03.; NNE, 21.03.), several other locations |
| 31 Mar 1987 | 4    | 15.5     | Flateyri (SW, 01-02.04.), Tungudalur (S, 02-03.04.), Súðavík (ESE, 31.03)  |
| 25 Feb 1989 | 2    | 13.9     | Hnífsdalur (SE, 26.02.), Ísafjörður (SE, 26.02.), Kirkjubólshlíð (NW, 26.02.), Öndarfjörður (NNW, 26.02.; NNE, 25.02.)   |
| 23 Jan 1990 | 8    | 14.1     | Flateyri (SW, 25&28-30.01.), Hnífsdalur (SE, 27.01.), Ísafjörður (SE, 27.01.), Öndarfjörður (WNW, 30.01.; NNE, 23-24&28.01.), several other locations                            |
| 5 Jan 1991  | 1    | 13.2     | Flateyri (SW), Öndarfjörður (NNE)  |
| 17 Mar 1991 | 3    | 13.2     | Flateyri (SW, 17-18.03.), Tungudalur (S, 19.03.)   |
| 12 Nov 1991 | 3    | 14.6     | Flateyri (SW, 12-13.11.), Hnífsdalur (SE, 13-14.11.), Ísafjörður (SE, 13-14.11.), Tungudalur (S, 13.11.)   |
| 11 Jan 1994 | 3    | > 15.5   | Kirkjubólshlíð (NW, 13.01.), Syðridalur (WNW, 11-13.01.)   |
| 3 Apr 1994  | 3    | 16.7     | Bolungarvík (S, 03.04.), Hnífsdalur (SE, 04-05.04.), Ísafjörður (SE, 05.04.), Tungudalur (S, 04-05.04.)  |

Table 4. Continued.

| Start Date  | Dur. | Max. ROI | Locations affected   |
|-------------|------|----------|--|
| 10 Apr 1994 | 4    | > 13.5   | Bolungarvík (S, 10-13.04.),<br>Kirkjubólshlíð (NW, 10&13.04.), Kubbi (NW, 13.04.)  |
| 16 Dec 1994 | 3    | 16.0     | Hnífsdalur (SE, 17-18.12.), Ísafjörður (SE, 17-18.12.),<br>Kirkjubólshlíð (NW, 16.12.), Kubbi (NW, 18.12.),<br>Súðavík (ESE, 18.12.)   |
| 16 Jan 1995 | 7    | 16.0     | Flateyri (SW, 18&22.01.), Ísafjörður (SE, 16-18.01.),<br>Kirkjubólsh. (NW, 19.01.), Korpudalur (SSW, 18.01.),<br>Súðavík (ESE, 16.01.), Öndarfjörður (NNE, 18.01.),<br>several other locations |
| 23 Oct 1995 | 4    | 18.6     | Flateyri (SW, 26.10.), Hnífsdalur (SE, 23.10.),<br>Ísafjörður (SE, 23.10.), Kirkjubólsh. (NW, 23&25.10.),<br>Tungudalur (S, 23.10.), several other locations                                   |
| 21 Feb 1997 | 2    | 13.6     | Bolungarvík (S&E, 21.02.), Flateyri (SW, 22.02.),<br>Hnífsd. (SE, 22.02.), Ísafjörður (SE, 21-22.02.),<br>Kirkjubólshlíð (NW, 22.02.)  |
| 20 Feb 1999 | 3    | 16.0     | Flateyri (SW, 21.02.), Hnífsdalur (SE, 21.02.),<br>Ísafjörður (SE, 20-21.02.), Kirkjubólshlíð (NW, 21.02.),<br>Öndarfjörður (NNE, 21.02), several other locations                              |
| 11 Mar 1999 | 3    | 15.0     | Flateyri (SW, 11.03.), Ísafjörður (SE, 11-12.03.),<br>Kirkjubólshlíð (NW, 11.03.), Tungudalur (S, 13.03.),<br>several other locations  |
| 8 Jan 2000  | 1    | 14.8     | Flateyri (SW)  |
| 28 Feb 2000 | 2    | 16.0     | Flateyri (SW), Hnífsdalur (SE, 28.02.),<br>Ísafjörður (SE, 28-29.02.), Tungudalur (S, 29.02.),<br>several other locations  |
| 4 Mar 2001  | 1    | 14.9     | Flateyri (SW), Hnífsdalur (SE), Ísafjörður (SE),<br>Kirkjubólshlíð (NW)  |
| 26 Mar 2001 | 3    | 13.5     | Flateyri (SW, 27.03.), Hnífsdalur (SE, 28.03.),<br>Súðavík (ESE, 26-27.03.)  |
| 30 Apr 2002 | 3    | 14.0     | Bolungarvík (E), Flateyri (SW), Hnífsdalur (SE)  |
| 1 Jan 2005  | 6    | 16.5     | Widespread damage  |

*Table 5. Start dates and duration in number of days of all major avalanche cycles considered in this study, that occurred in Northern Iceland. Also given is the largest run-out index (ROI) recorded for each cycle, and the main locations affected. Slope orientations and avalanche dates for specific slopes are given in parentheses. Slope orientation, or aspect, is defined as the direction towards which the negative terrain gradient points.*

| Start Date  | Dur. | Max. ROI | Locations affected   |
|-------------|------|----------|--|
| 26 Dec 1963 | 1    | 12.4     | Siglufjörður (ESE)   |
| 4 Feb 1968  | 1    | 13.8     | Siglufjörður (ESE)   |
| 14 Feb 1971 | 1    | 12.9     | Siglufjörður (ESE)   |
| 19 Dec 1973 | 1    | 15.0     | Siglufjörður (ESE)   |
| 19 Dec 1974 | 1    | 13.9     | Siglufjörður (ESE)   |
| 12 Jan 1975 | 3    | n/a      | Widespread damage  |
| 26 Feb 1978 | 1    | > 15.5   | Skútudalur (W)   |
| 29 Mar 1978 | 1    | > 13.5   | Skútudalur (W)   |
| 23 May 1979 | 1    | > 13.5   | Hestskarðshnjúkur (W&SW)   |
| 6 Mar 1983  | 1    | > 13.5   | Skútudalur (W)   |
| 26 Nov 1983 | 1    | > 15.5   | Hestskarðshnjúkur (W&SW), Skútudalur (ENE)   |
| 8 Jan 1984  | 1    | 13.3     | Siglufjörður (ESE)   |
| 22 Jan 1984 | 2    | > 15.5   | Skútu. (ENE, 22-23.01.), Staðarhóls. (W, 22-23.01.)  |
| 11 Feb 1988 | 3    | 13.0     | Hólsdalur (NW, 13.02.), Siglufjörður (ESE, 13.02.), Skútudalur (ENE, 13.02.), several other locations      |
| 14 Apr 1988 | 2    | > 13.5   | Hólsdalur (NW, 14-15.04.), Skútudalur (W, 14.04), Staðarhólshnjúkur (W, 14-15.04.)                         |
| 18 Apr 1988 | 1    | > 13.5   | Skútudalur (W)   |
| 21 Jan 1994 | 3    | 13.5     | Siglufjörður (ESE)   |
| 19 Dec 1994 | 1    | 14.4     | Siglufjörður (ESE)   |
| 16 Jan 1995 | 1    | > 13.5   | Skútudalur (W)   |
| 18 Jan 1995 | 1    | 13.4     | Siglufjörður (ESE)   |
| 30 Jan 1995 | 1    | > 13.5   | Skútudalur (ENE), Strákar (NE)   |
| 22 Feb 1995 | 1    | > 13.5   | Skútudalur (W)   |
| 25 Feb 1995 | 1    | > 13.5   | Skútudalur (W)   |
| 3 Jan 1996  | 4    | 13.0     | Siglufjörður (ESE, 03.01.), Skarðsd. (S, 05-06.01.), Skútudalur (W, 03.01.), Staðarhólshnjúkur (W, 03.01.) |
| 19 Jan 1997 | 2    | > 13.5   | Nesskriður (W, 19.01.), Skútudalur (ENE, 19-20.01.; W, 19.01.)   |
| 21 Feb 1998 | 2    | > 13.5   | Skútudalur (W)   |
| 20 Jan 1999 | 1    | n/a      | Siglufjörður (ESE)   |
| 12 Mar 1999 | 1    | 13.0     | Siglufjörður (ESE), Skarðsdalur (S)  |
| 7 Dec 2000  | 2    | > 13.5   | Hestskarðshnjúkur (W&SW)   |
| 1 Apr 2001  | 1    | > 13.5   | Siglufjörður (ESE), Staðarhólsh. (W), Strákar (NE)   |
| 3 Apr 2001  | 1    | 14.7     | Siglufjörður (ESE)   |
| 6 Apr 2001  | 1    | > 13.5   | Hestskarðshn. (W&SW), Skútud. (W, ENE)   |
| 12 Jan 2004 | 7    | 16.9     | Héðinsfjörður, several other locations   |
| 19 Feb 2006 | 1    | n/a      | Skútudalur (W)   |

*Table 6. Start dates and duration in number of days of all major avalanche cycles considered in this study, that occurred in Eastern Iceland. Also given is the largest run-out index (ROI) recorded for each cycle, and the main locations affected. Slope orientations and avalanche dates for specific slopes are given in parentheses. Slope orientation, or aspect, is defined as the direction towards which the negative terrain gradient points.*

| Start Date  | Dur. | Max. ROI | Locations affected                                  |
|-------------|------|----------|---|
| 1 Mar 1960  | 3    | > 15.5   | Seyðisfjörður (WNW)                                 |
| 22 Feb 1966 | 2    | > 15.5   | Seyðisfjörður (WNW)                                 |
| 27 Mar 1967 | 1    | 11.0     | Seyðisfjörður (ESE)                                 |
| 5 Apr 1973  | 1    | > 13.5   | Seyðisfjörður (WNW)                                 |
| 8 Feb 1974  | 8    | 12.9     | Seyðisfjörður (ESE 08-12.02., WNW 15.02.)           |
| 18 Mar 1974 | 2    | > 15.5   | Seyðisfjörður (WNW)                                 |
| 19 Dec 1974 | 3    | > 15.5   | Neskaupstaður (SE - S), Seyðisfjörður (SE)          |
| 12 Jan 1975 | 3    | n/a      | Widespread damage                                   |
| 26 Apr 1977 | 1    | 12.9     | Seyðisfjörður (WNW; slush flows)                    |
| 28 Mar 1978 | 1    | 12.2     | Seyðisfjörður (WNW; slush flows)                    |
| 23 Jan 1986 | 1    | > 15.5   | Seyðisfjörður (WNW)                                 |
| 2 Feb 1988  | 1    | > 13.5   | Seyðisfjörður (WNW)                                 |
| 4 Feb 1988  | 3    | 11.0     | Seyðisfjörður (ESE)                                 |
| 14 Feb 1988 | 1    | 13.6     | Seyðisfjörður (WNW; slush flows)                    |
| 15 Apr 1988 | 1    | > 15.5   | Seyðisfjörður (SE)                                  |
| 25 Feb 1990 | 3    | 16.4     | Seyðis. (WNW, 25-27.02.), Neskaup. (SE - S, 27.02.) |
| 17 Mar 1995 | 3    | 11.0     | Seyðisfjörður (ESE)                                 |
| 27 Feb 2000 | 2    | 9.0      | Seyðisfjörður (ESE)                                 |
| 2 Jan 2001  | 2    | 13.8     | Seyðisfjörður (ESE)                                 |
| 6 Jan 2001  | 1    | 14.8     | Seyðisfjörður (ESE)                                 |
| 1 Mar 2001  | 1    | > 13.5   | Seyðisfjörður (WNW)                                 |
| 28 Mar 2001 | 4    | > 13.5   | Seyðisfjörður (SE), Vestdalur (SE)                  |
| 3 Apr 2006  | 8    | 15.0     | Seyðisfjörður (ESE)                                 |

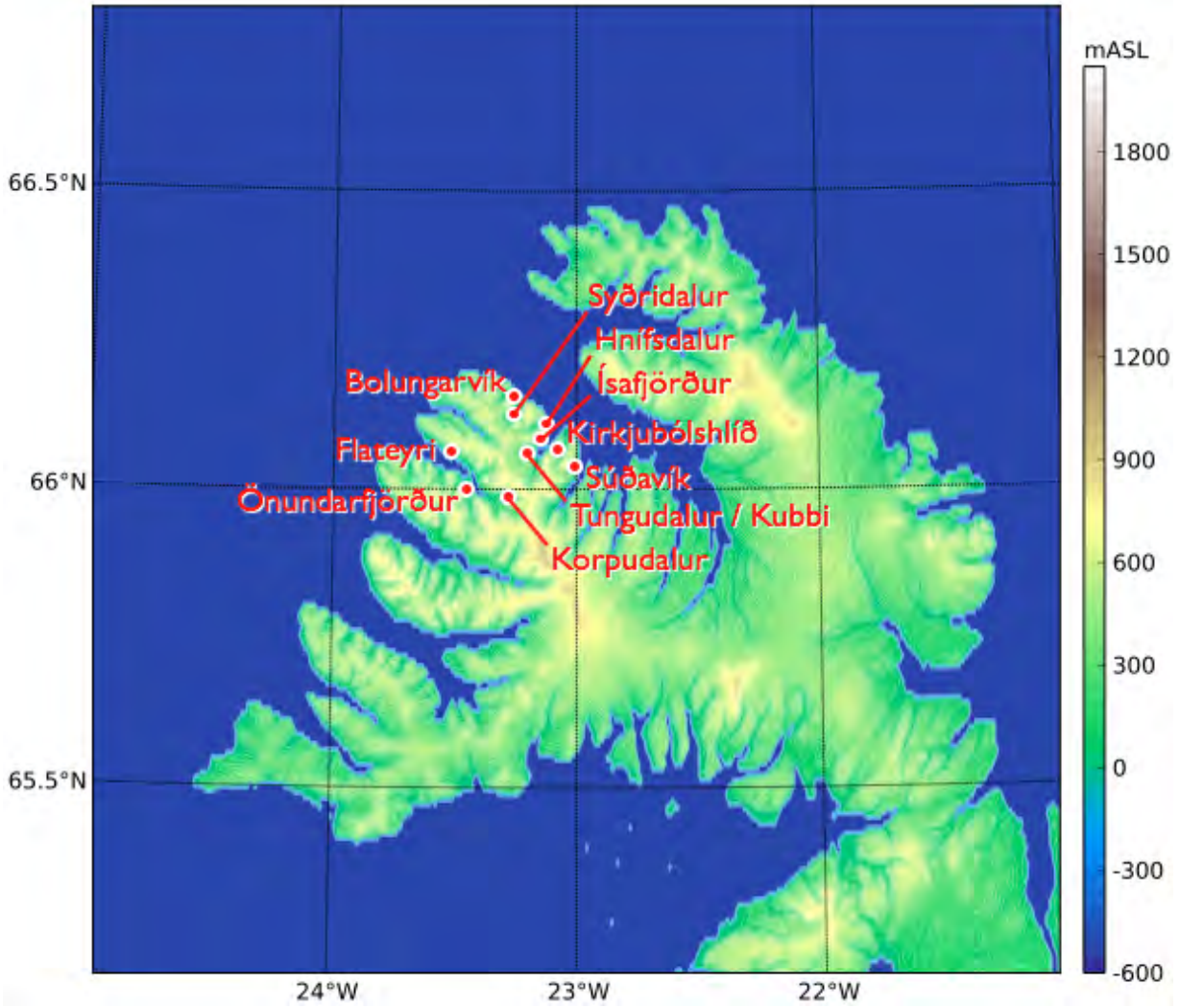


*Figure 1. Topographic map of the Westfjords, indicating those locations, for which major avalanches have been recorded.*



Figure 2. Location and downslope orientation (black arrows) of major avalanche slopes in the Westfjords.

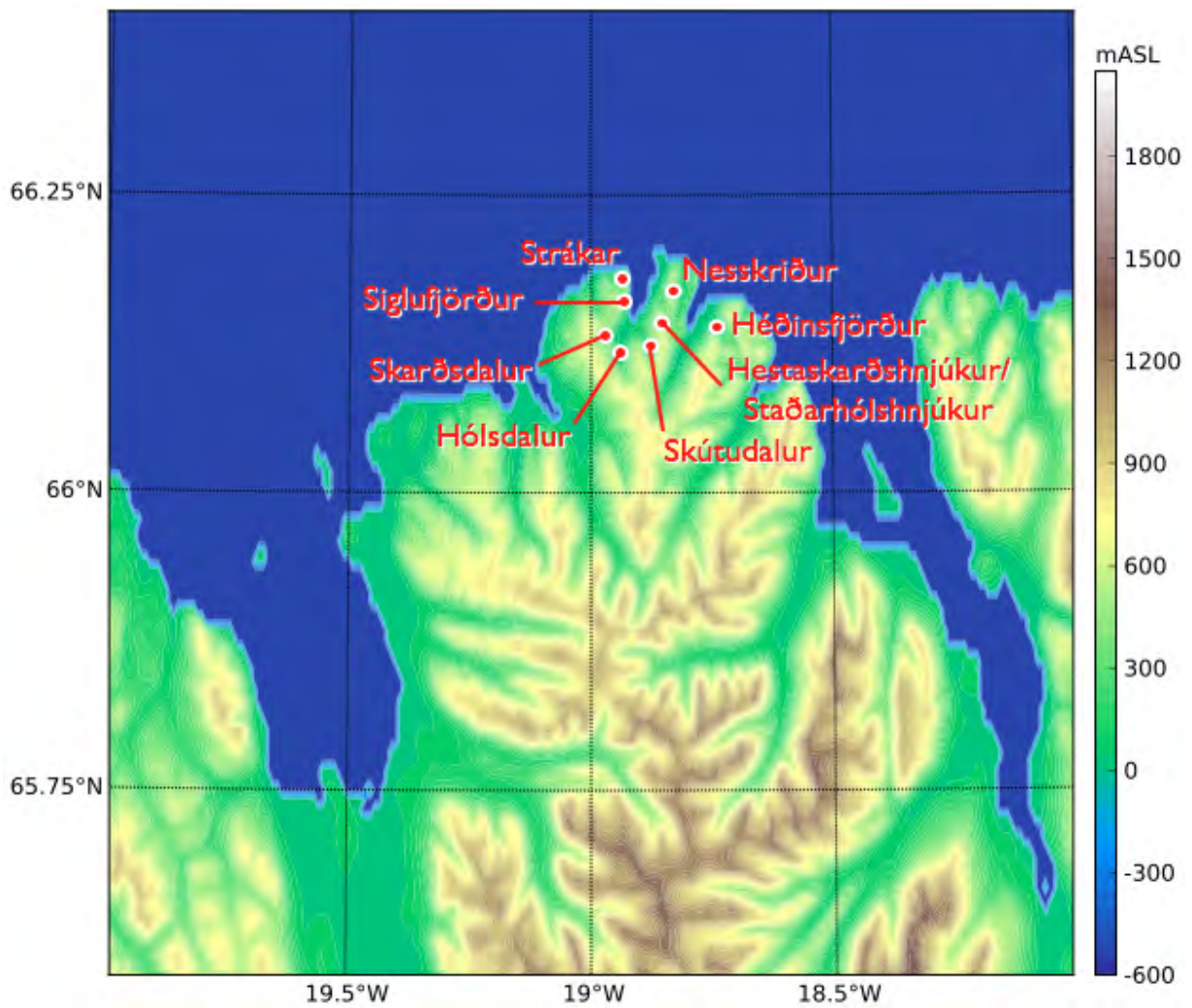


*Figure 3. Topographic map of Northern Iceland, indicating those locations, for which major avalanches have been recorded.*





Figure 4. Location and downslope orientation (black arrows) of major avalanche slopes in Northern Iceland.

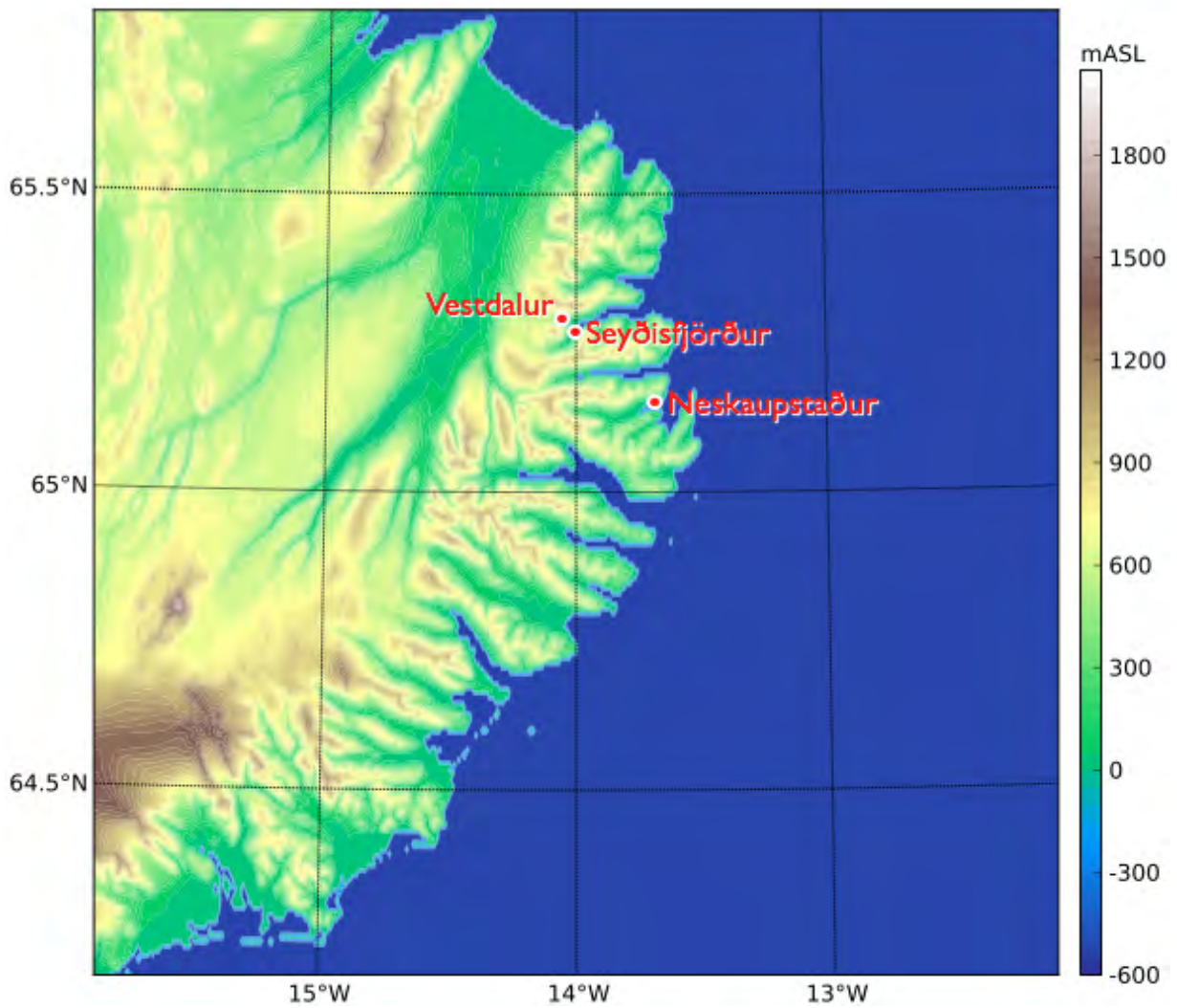


*Figure 5. Topographic map of Eastern Iceland, indicating those locations, for which major avalanches have been recorded.*

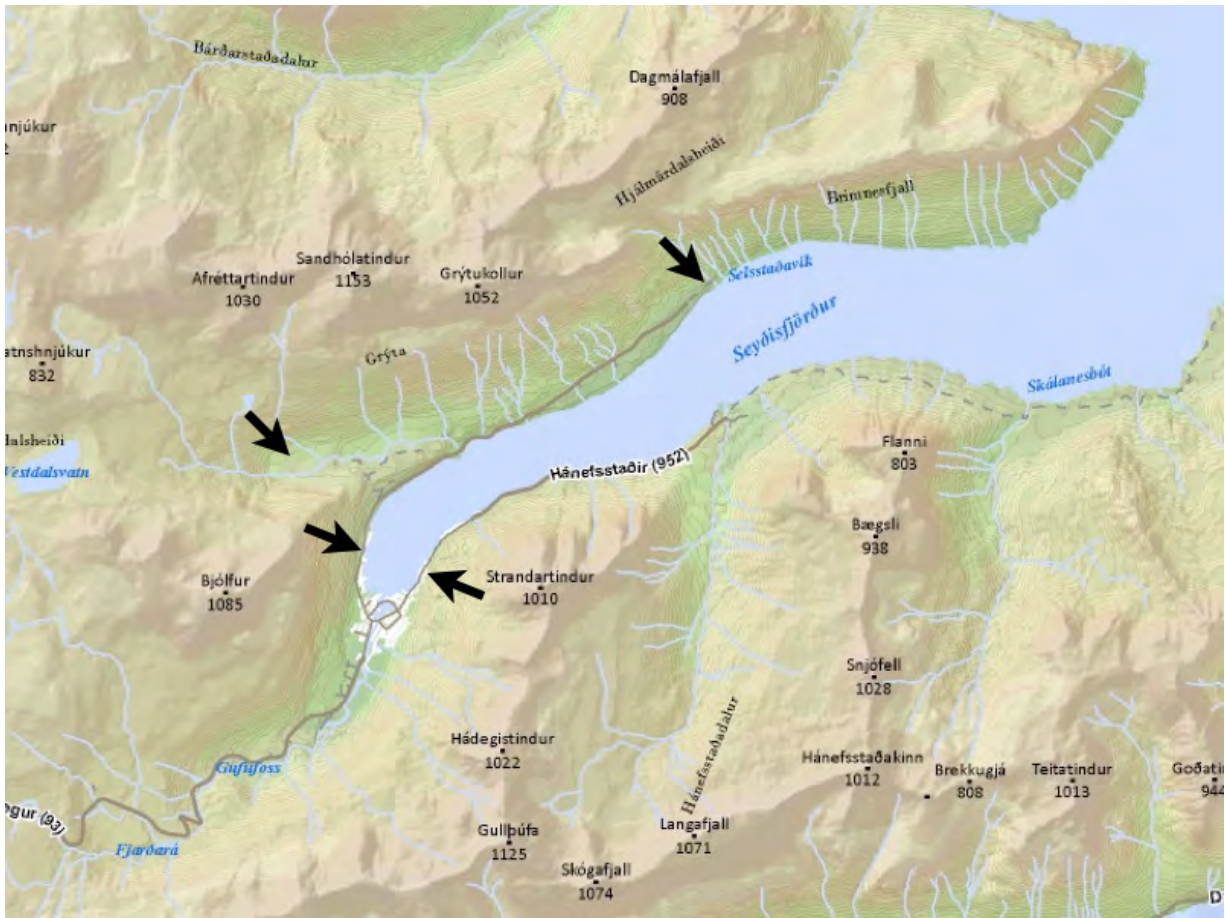


Figure 6. Location and downslope orientation (black arrows) of major avalanche slopes in Seyðisfjörður.

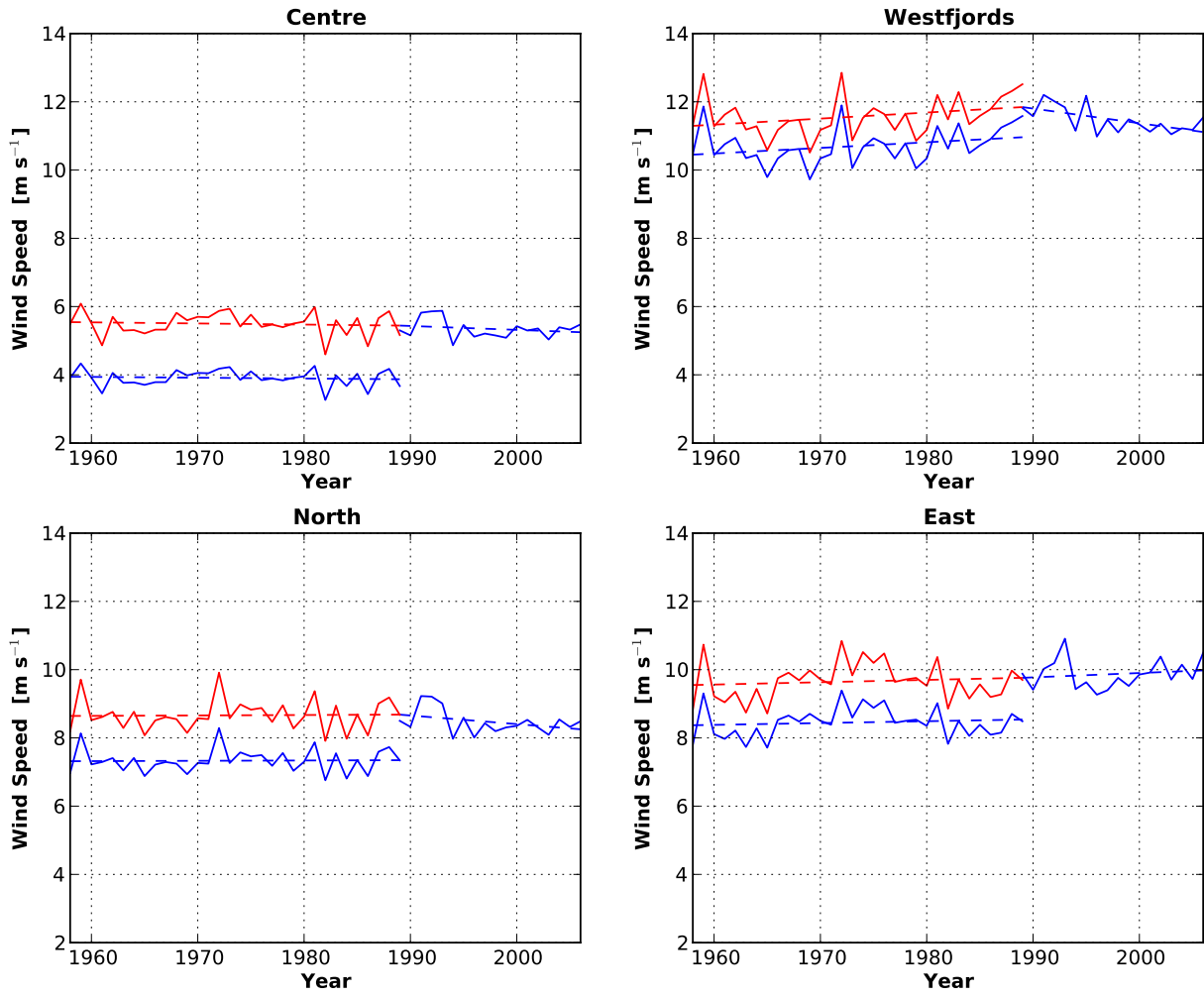


Figure 7. Annual averages of regional mean wind speed at 925 hPa in different parts of Iceland based on the original (blue lines) and corrected (red lines) ERA-40 and ERA-Interim reanalyses (see Section 2).

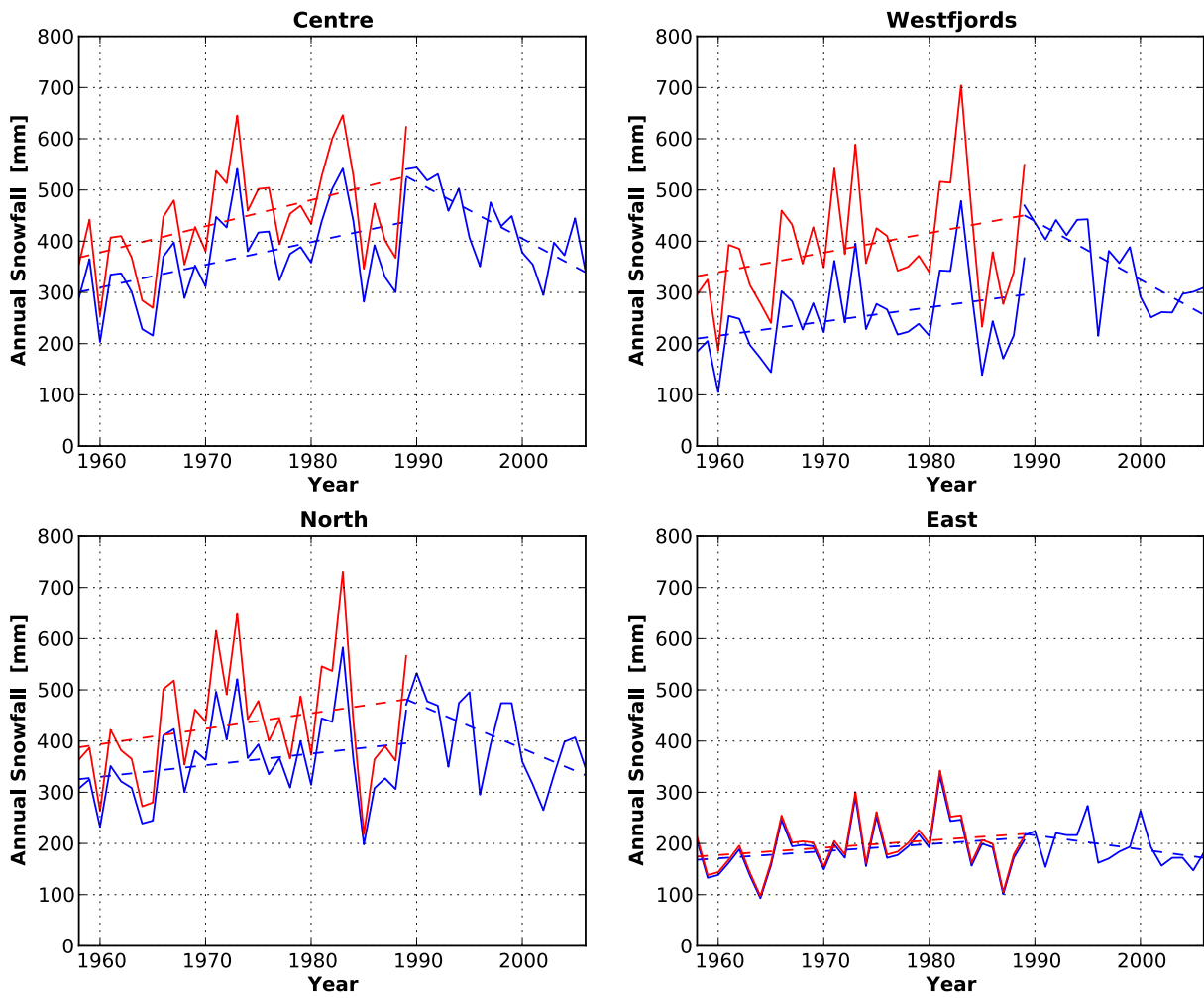


Figure 8. Regional averages of annual snowfall in different parts of Iceland based on the original (blue lines) and corrected (red lines) ERA-40 and ERA-Interim reanalyses (see Section 2).

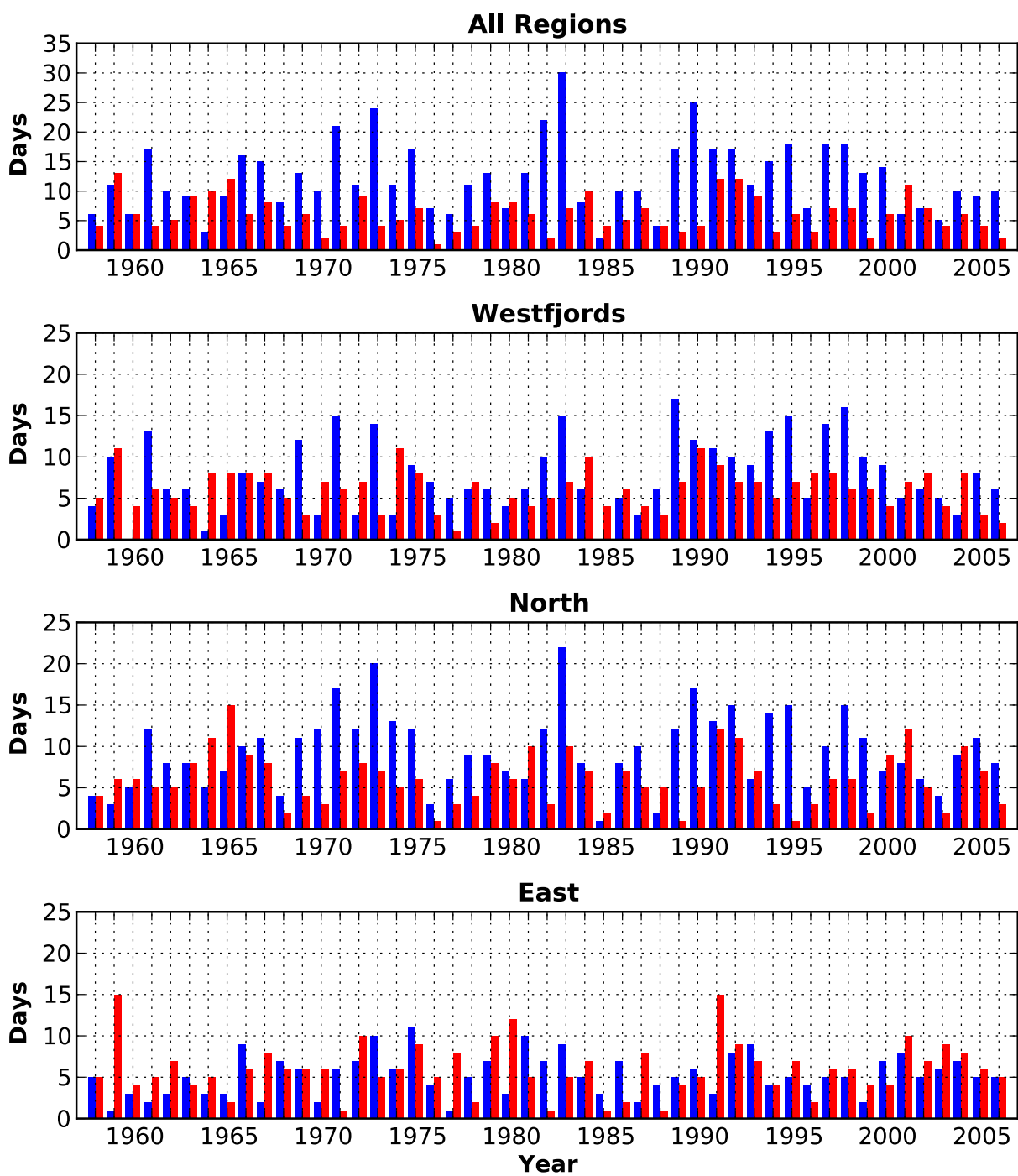


Figure 9. Annual number of days with heavy snowfall (blue bars) and strong winds (red bars) in different parts of Iceland.

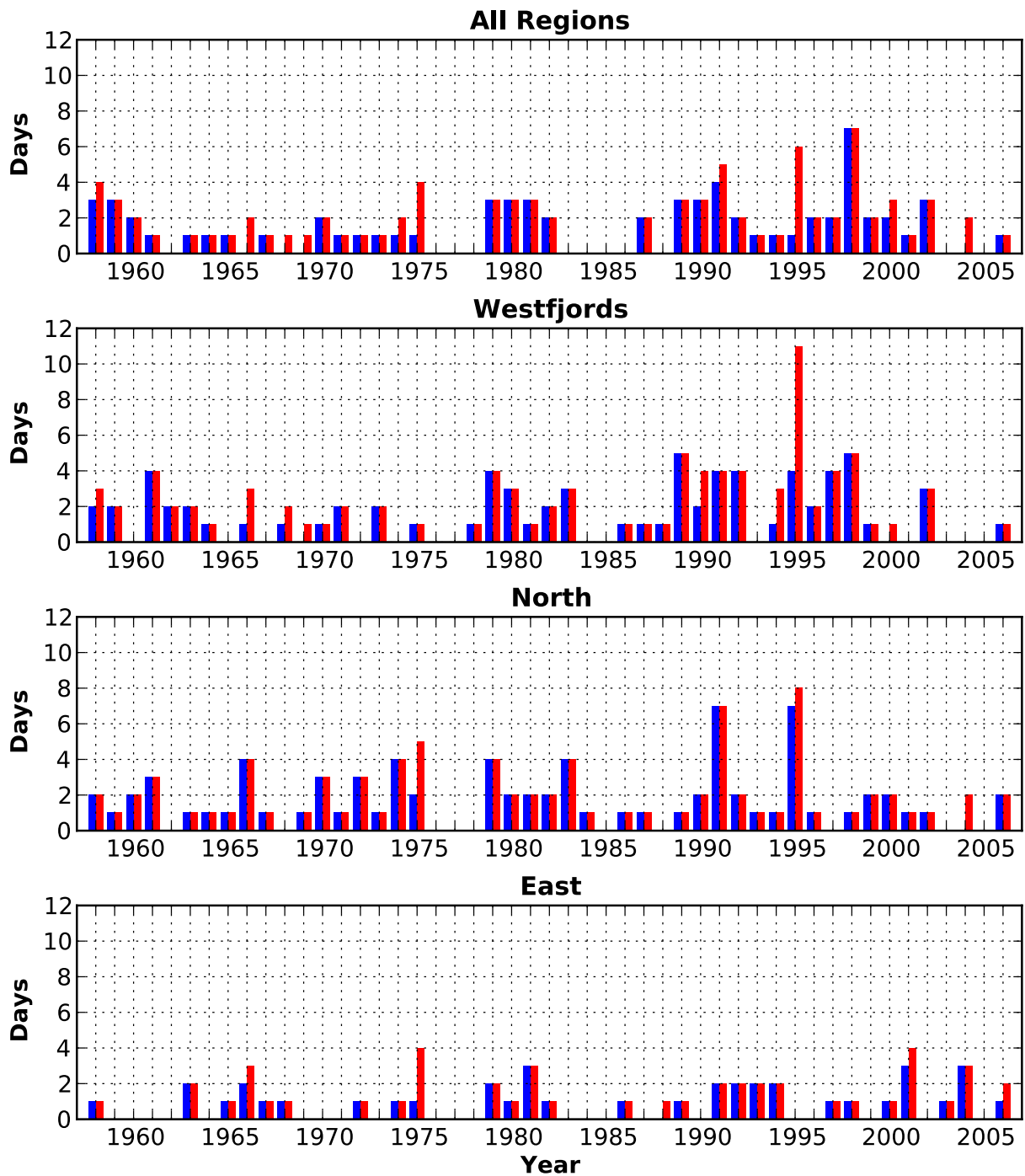


Figure 10. Annual number of days with severe snowstorm conditions without (blue bars) and potentially with (red bars) major avalanche activity in different parts of Iceland.

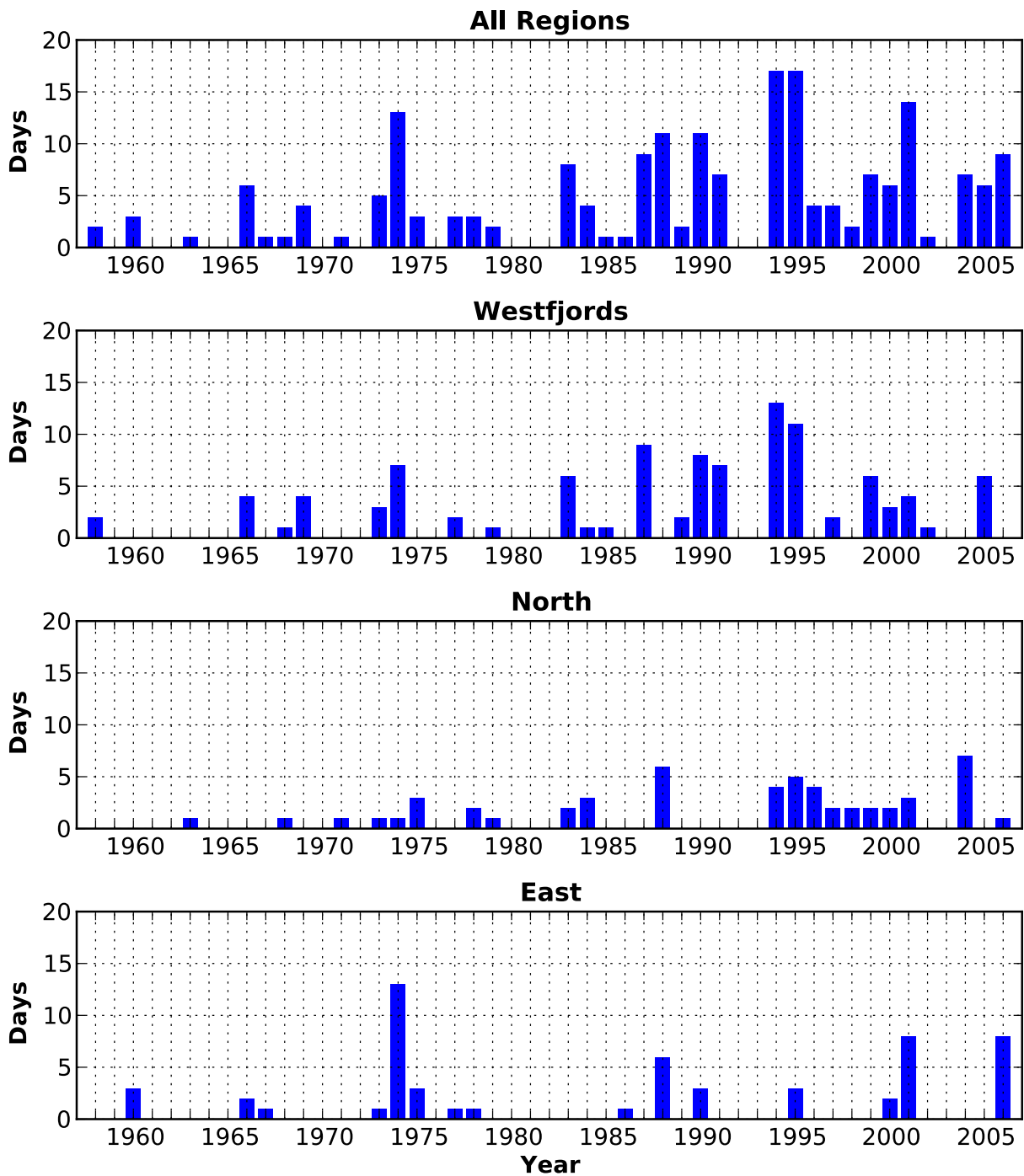


Figure 11. Annual number of days with large or destructive avalanches in different parts of Iceland.



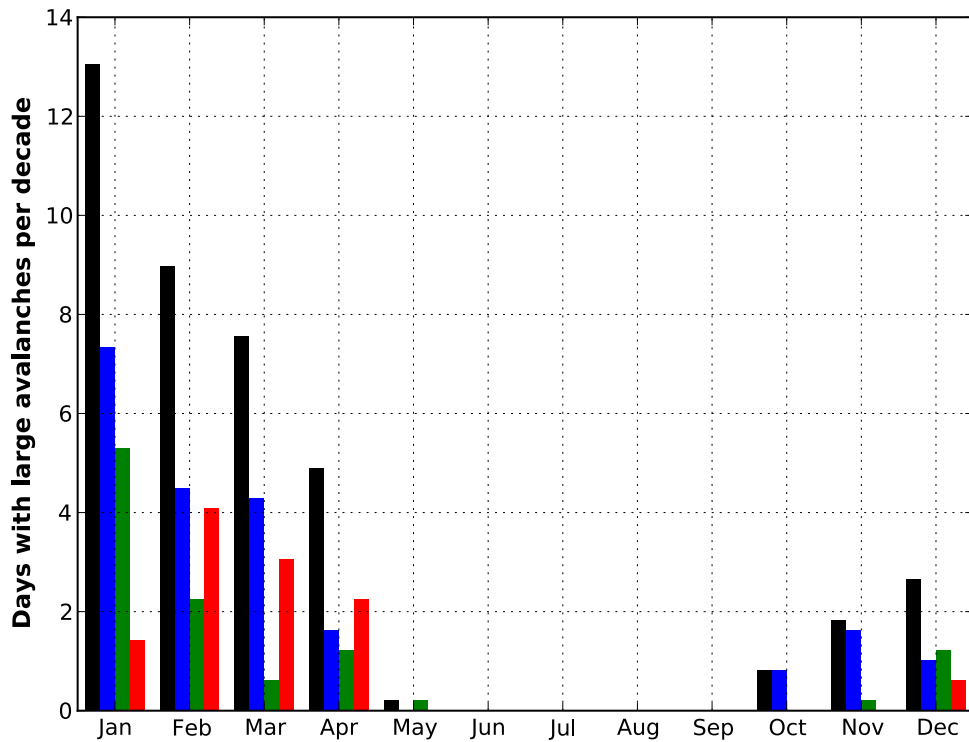


Figure 12. Seasonal distribution of 91 well-documented cases within the 1958 – 2006 study period of large or destructive avalanches at all observed locations (black bars), the northern part of the Westfjords (blue bars), Northern Iceland (green bars), and Eastern Iceland (red bars).

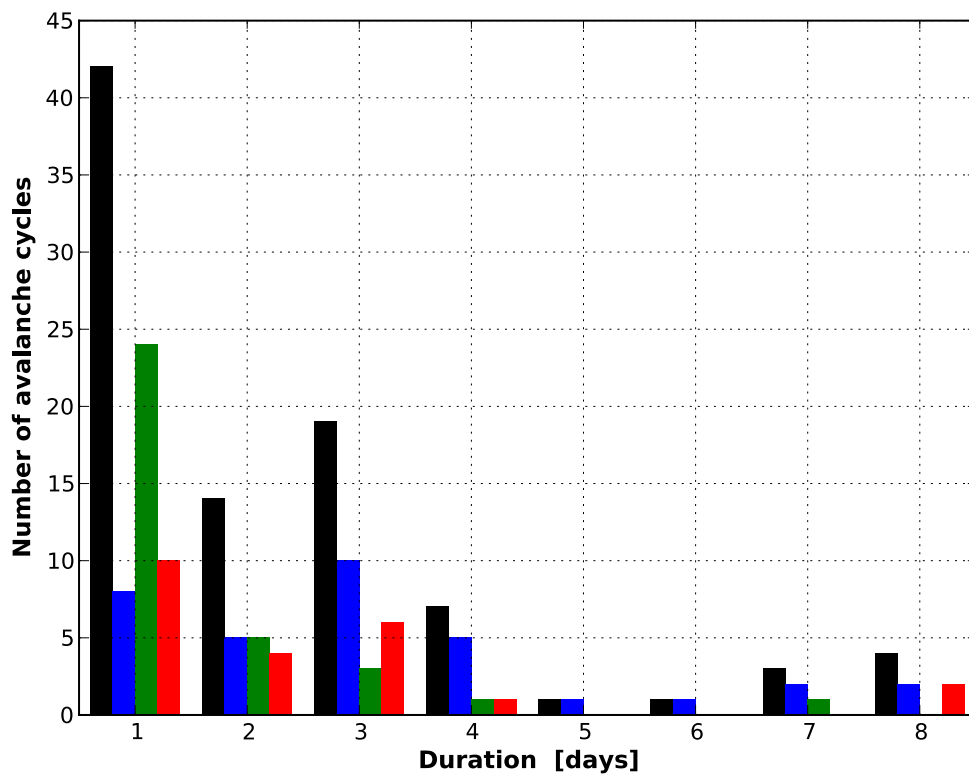


Figure 13. Occurrence of avalanche cycles with a given duration at all observed locations (black bars), the northern part of the Westfjords (blue bars), Northern Iceland (green bars), and Eastern Iceland (red bars).

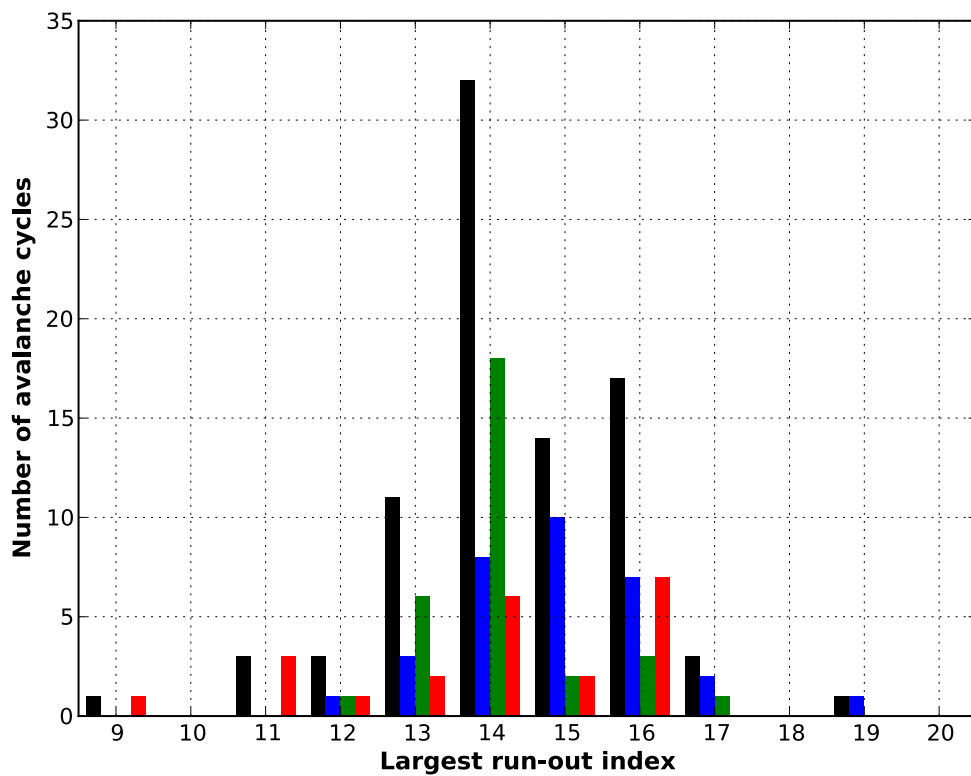


Figure 14. Occurrence of avalanche cycles with a given maximum run-out index at all observed locations (black bars), the northern part of the Westfjords (blue bars), Northern Iceland (green bars), and Eastern Iceland (red bars).

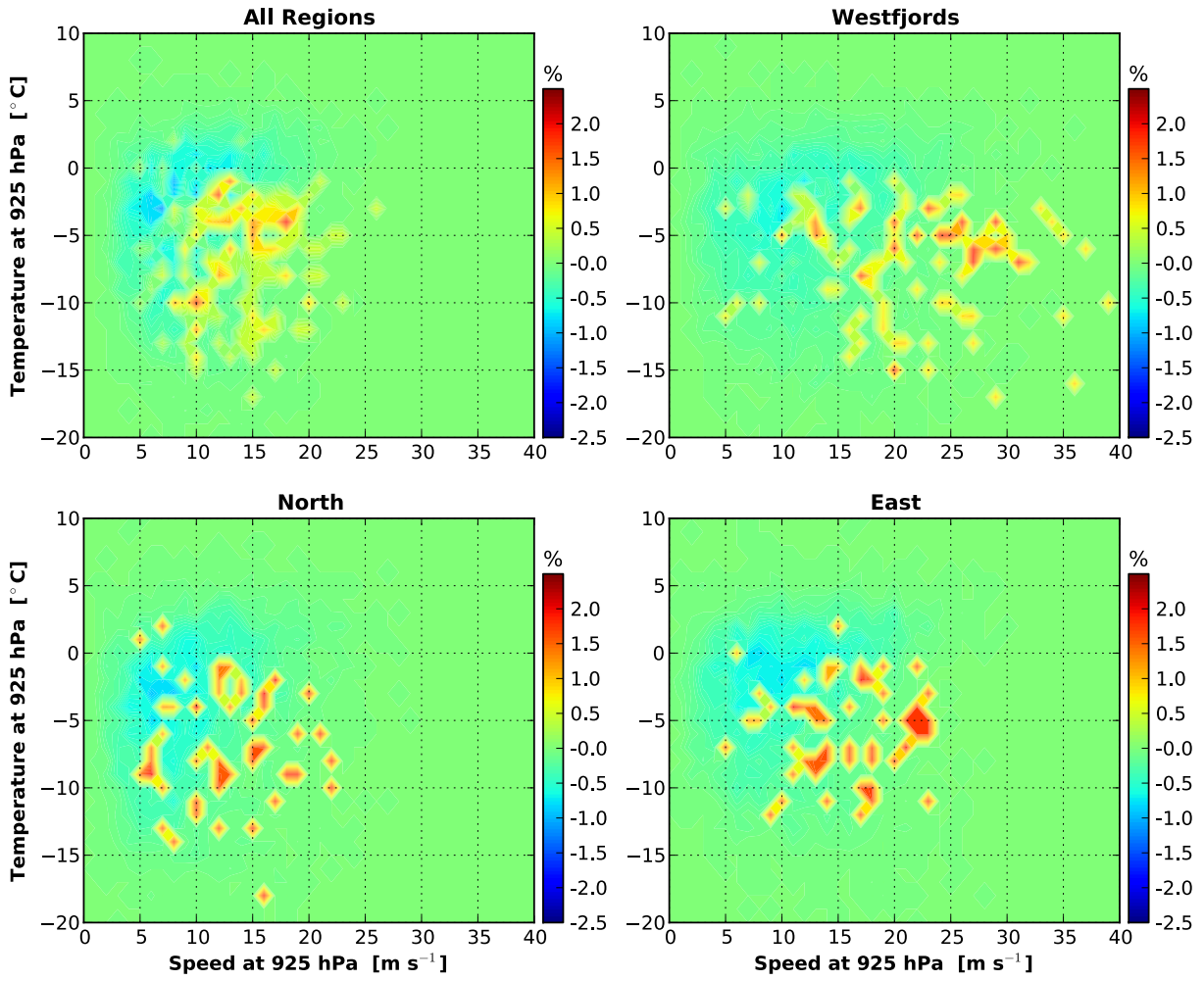


Figure 15. Difference between the joint histogram of daily air temperature and wind speed at 925 hPa for days with major avalanche activity, and the corresponding histogram for days during the main avalanche season (Jan – Apr) without the occurrence of major avalanches.

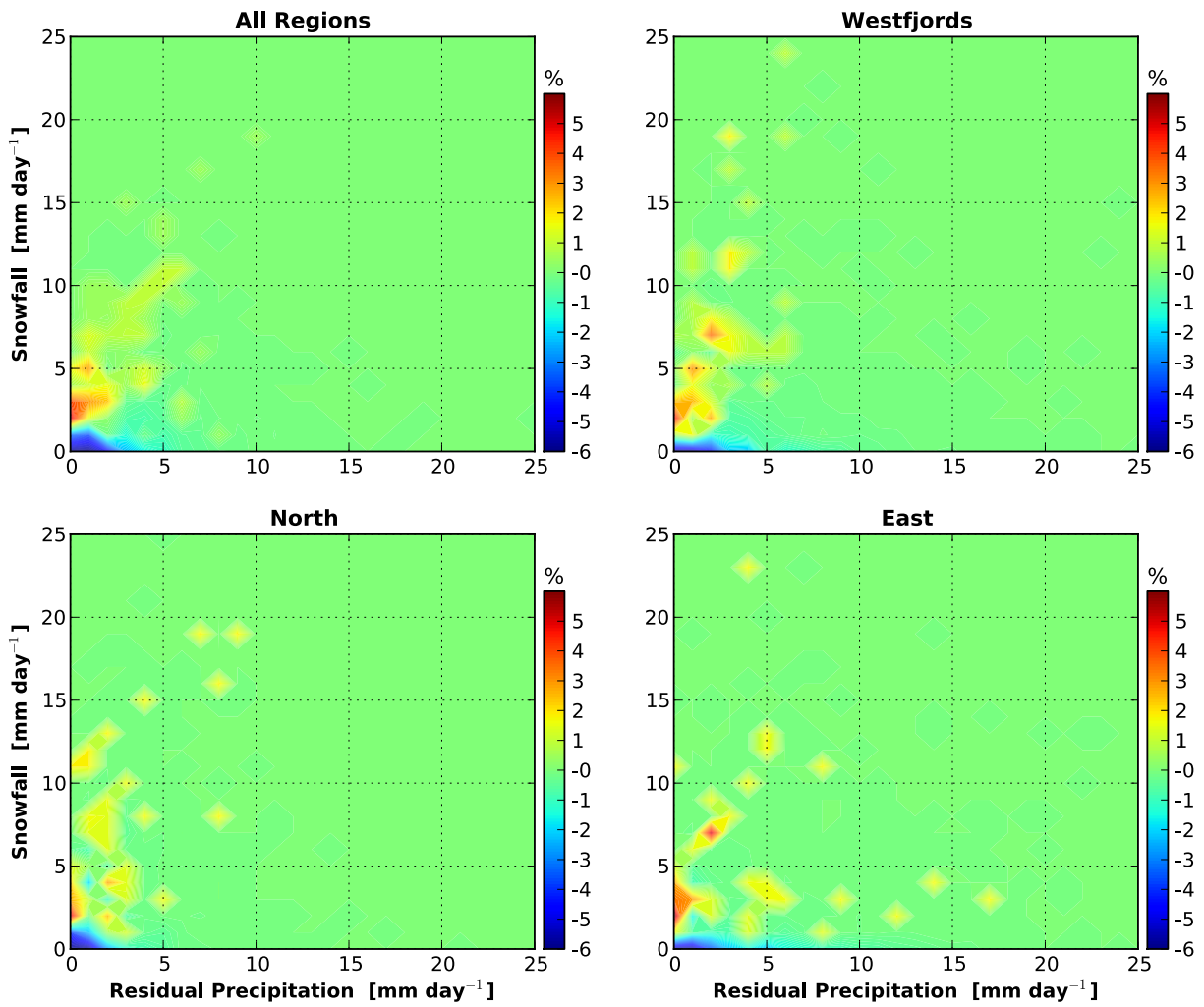


Figure 16. Difference between the joint histogram of daily residual precipitation and snowfall for days with major avalanche activity, and the corresponding histogram for days during the main avalanche season (Jan – Apr) without the occurrence of major avalanches.

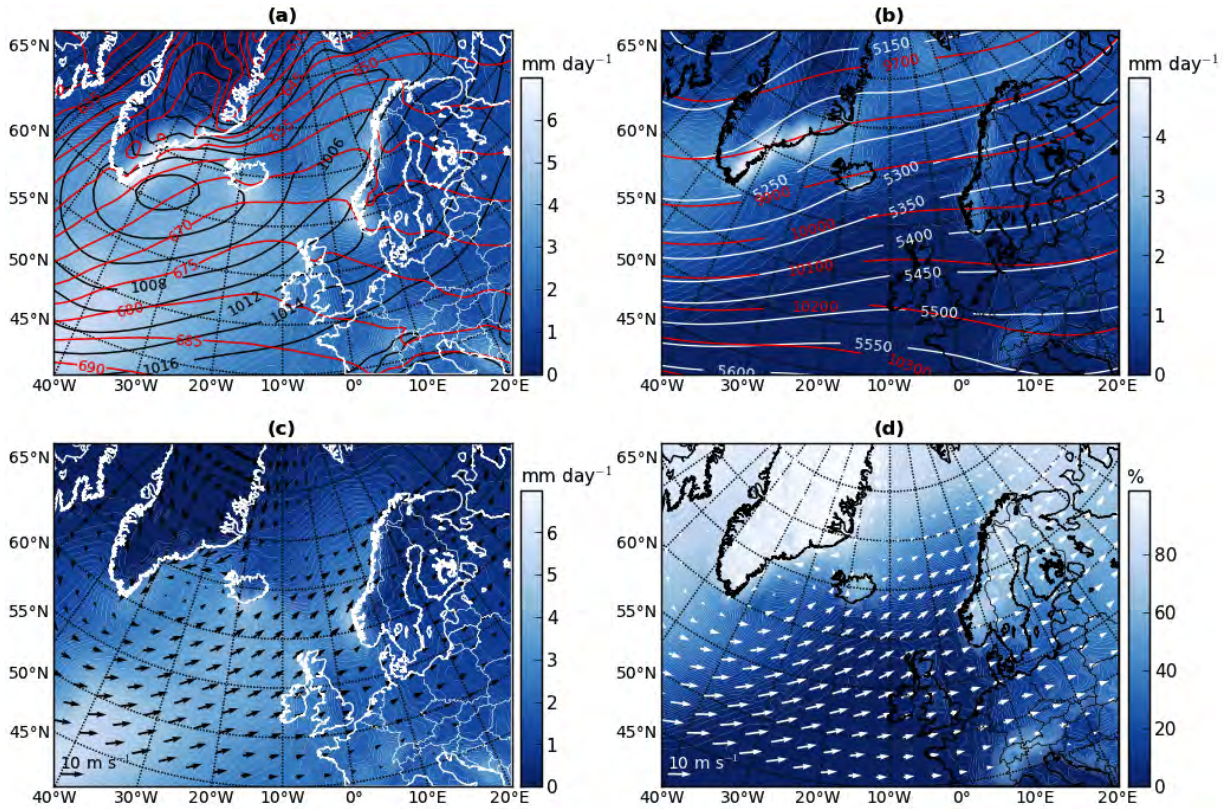


Figure 17. Average atmospheric fields for the main avalanche season (Jan – Apr) within the period 1958 – 2006: (a) mean sea level pressure (black contour lines), 925 – 850 hPa layer thickness (red contour lines), and total daily precipitation (coloured contours); (b) 500 hPa geopotential height (white contour lines), 250 hPa geopotential height (red contour lines), and daily snowfall (coloured contours); (c) daily residual precipitation, and 925 hPa wind field; (d) percent snowfall relative to total precipitation, and 850 hPa wind field.

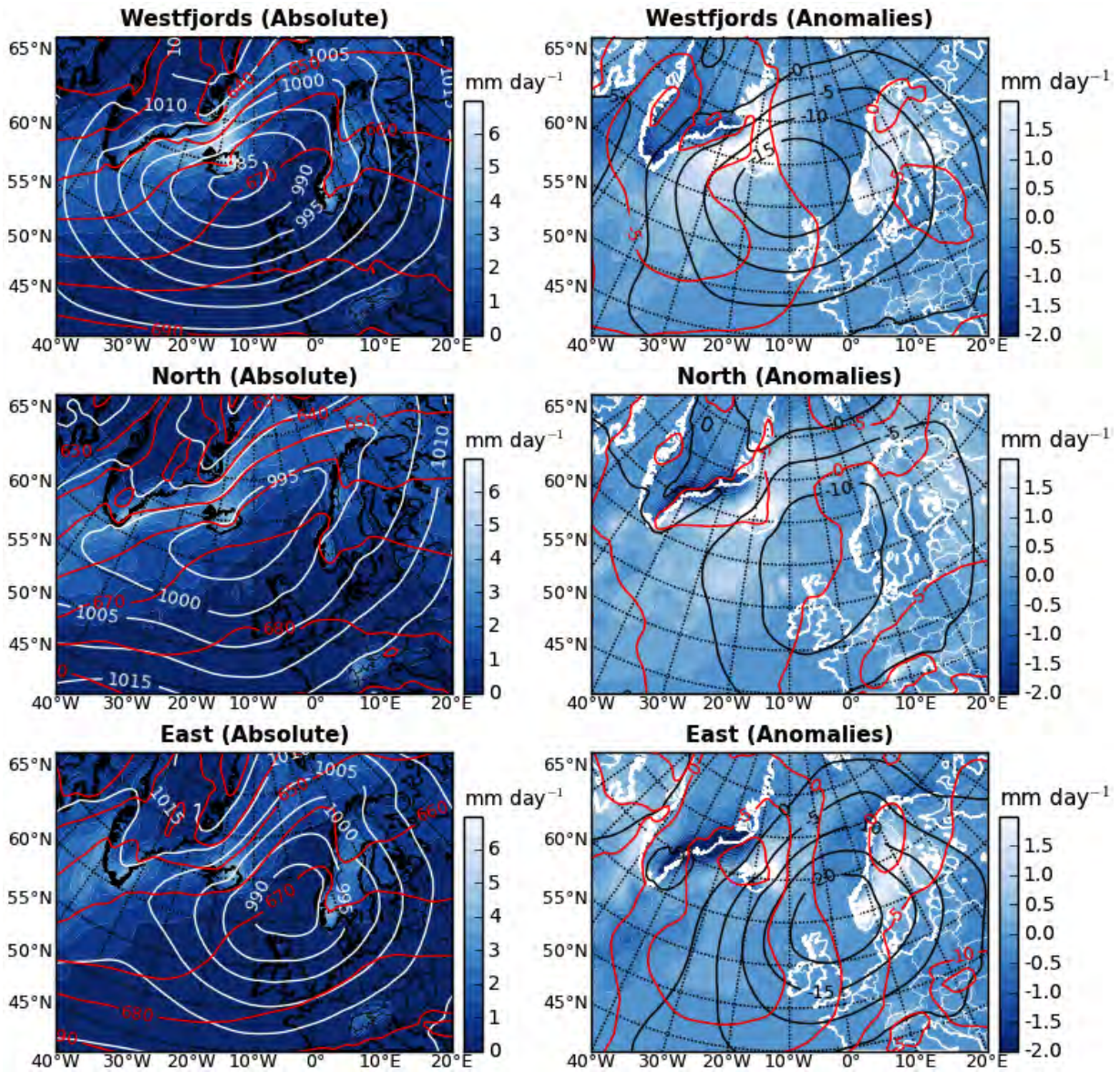


Figure 18. Ensemble mean fields for days with major avalanche activity in different regions of Iceland: mean sea level pressure (white contour lines), 925 – 850 hPa layer thickness (red contour lines), and daily snowfall (coloured contours). Anomalies are deviations from the background climatology (see Section 2).

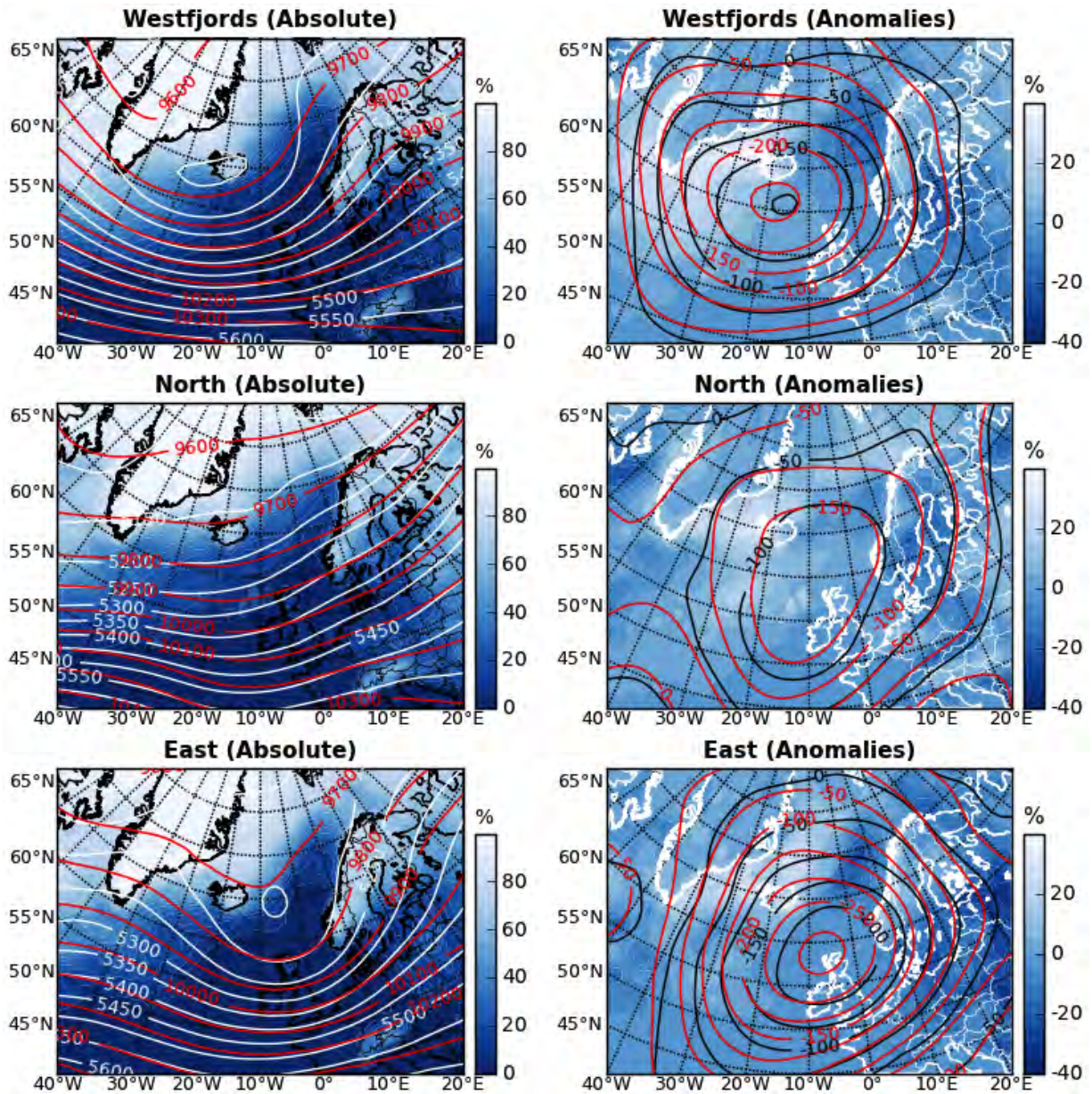


Figure 19. Ensemble mean fields for days with major avalanche activity in different regions of Iceland: 500 hPa geopotential height (white contour lines), 250 hPa geopotential height (red contour lines), and percent snowfall relative to total precipitation (coloured contours). Anomalies are deviations from the background climatology (see Section 2).



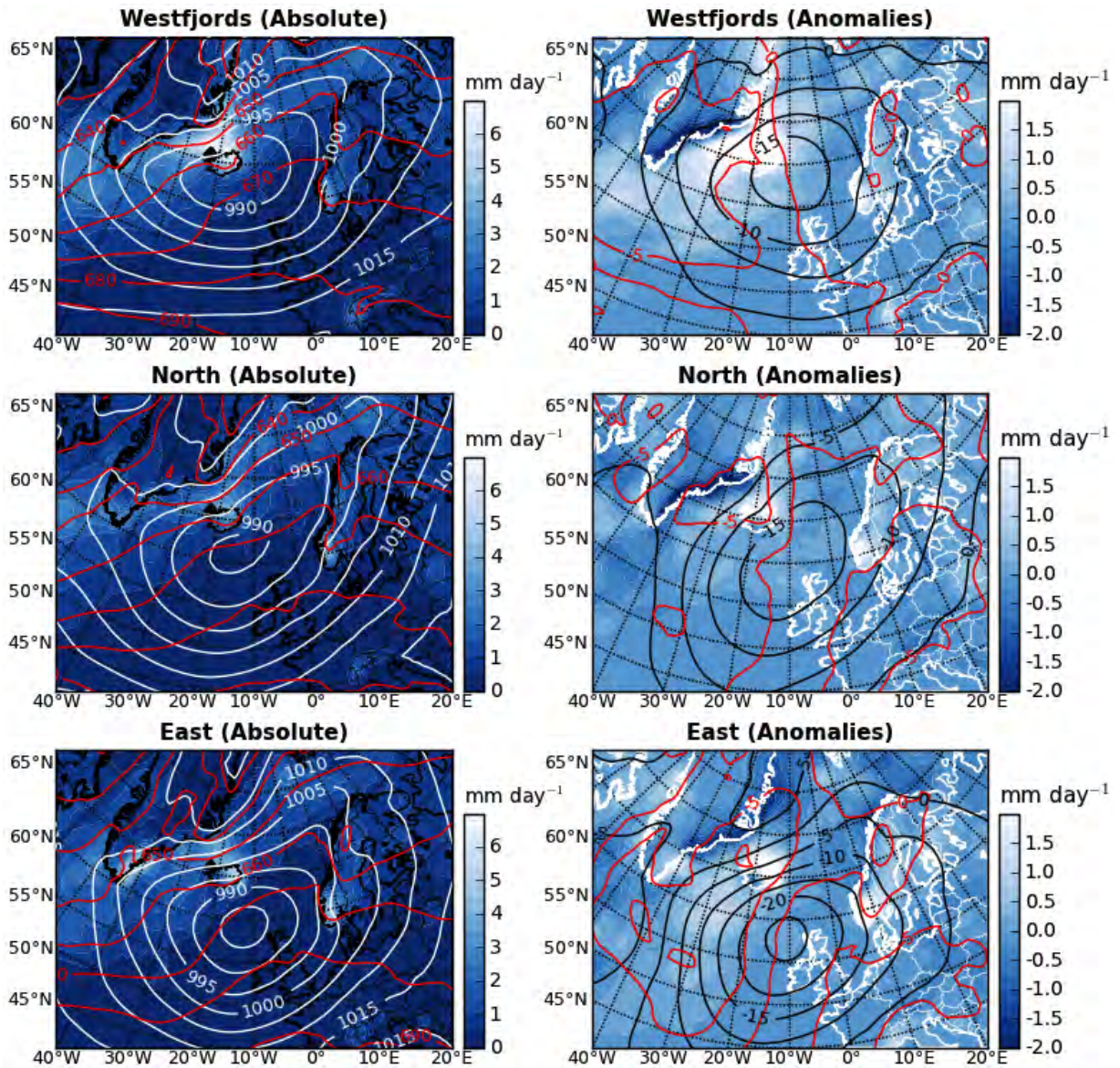


Figure 20. Ensemble mean fields for the days preceding major avalanche activity in different regions of Iceland: mean sea level pressure (white contour lines), 925 – 850 hPa layer thickness (red contour lines), and daily snowfall (coloured contours). Anomalies are deviations from the background climatology (see Section 2).

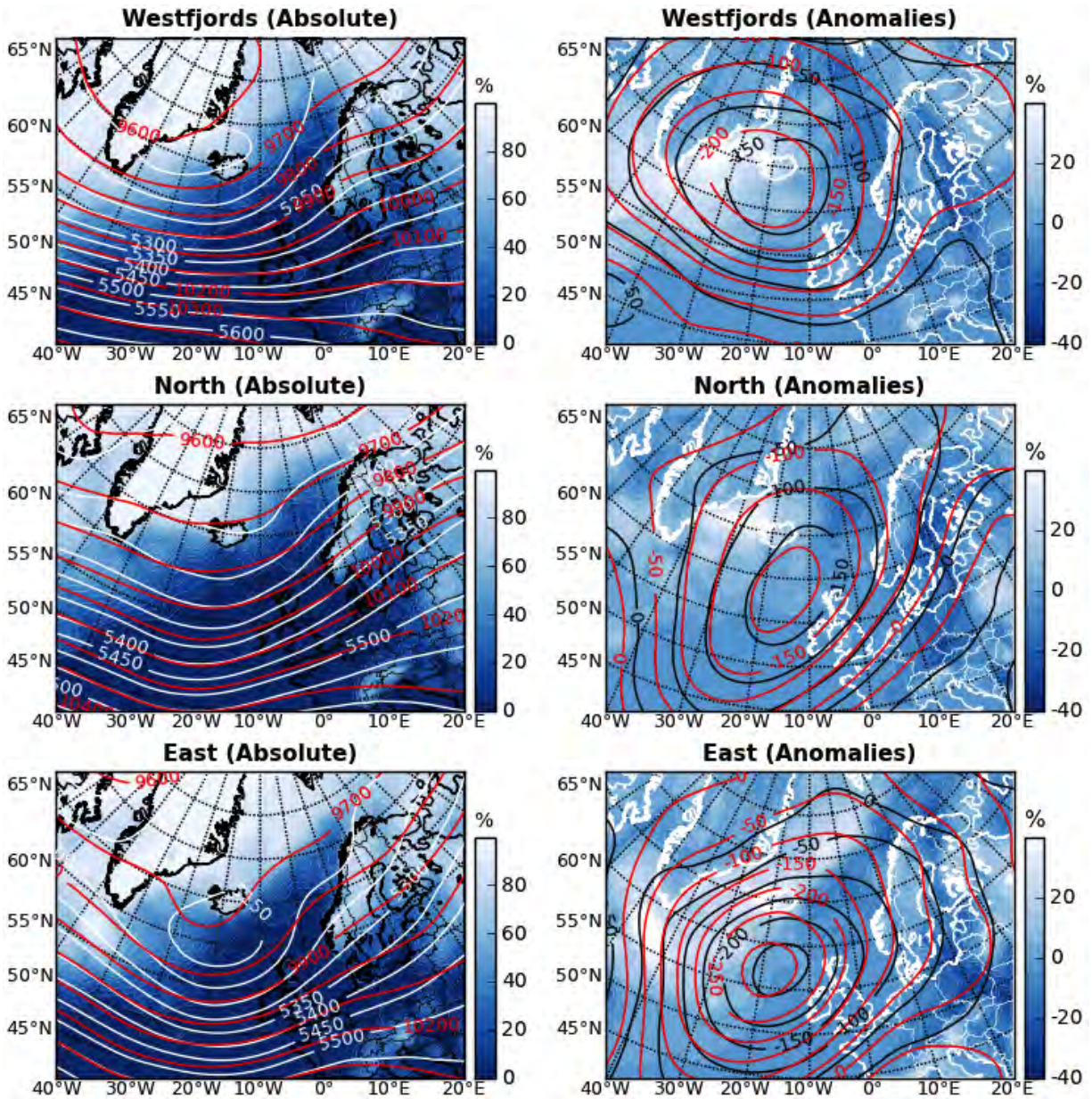


Figure 21. Ensemble mean fields for the days preceding major avalanche activity in different regions of Iceland: 500 hPa geopotential height (white contour lines), 250 hPa geopotential height (red contour lines), and percent snowfall relative to total precipitation (coloured contours). Anomalies are deviations from the background climatology (see Section 2).

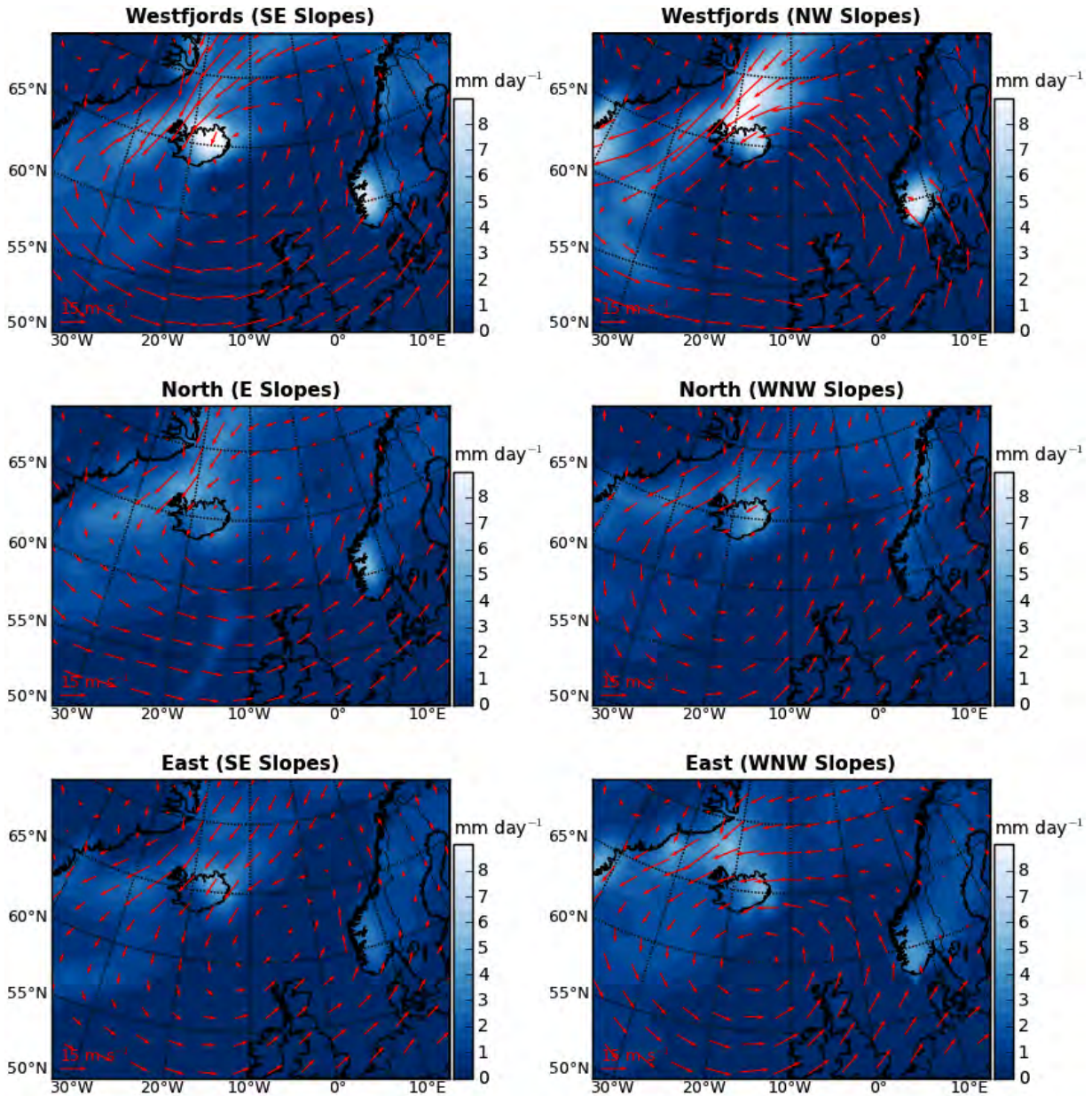


Figure 22. Ensemble mean fields for the days preceding major avalanche activity in different regions of Iceland, limited to specific slope orientations: daily snowfall, and 925 hPa wind field.

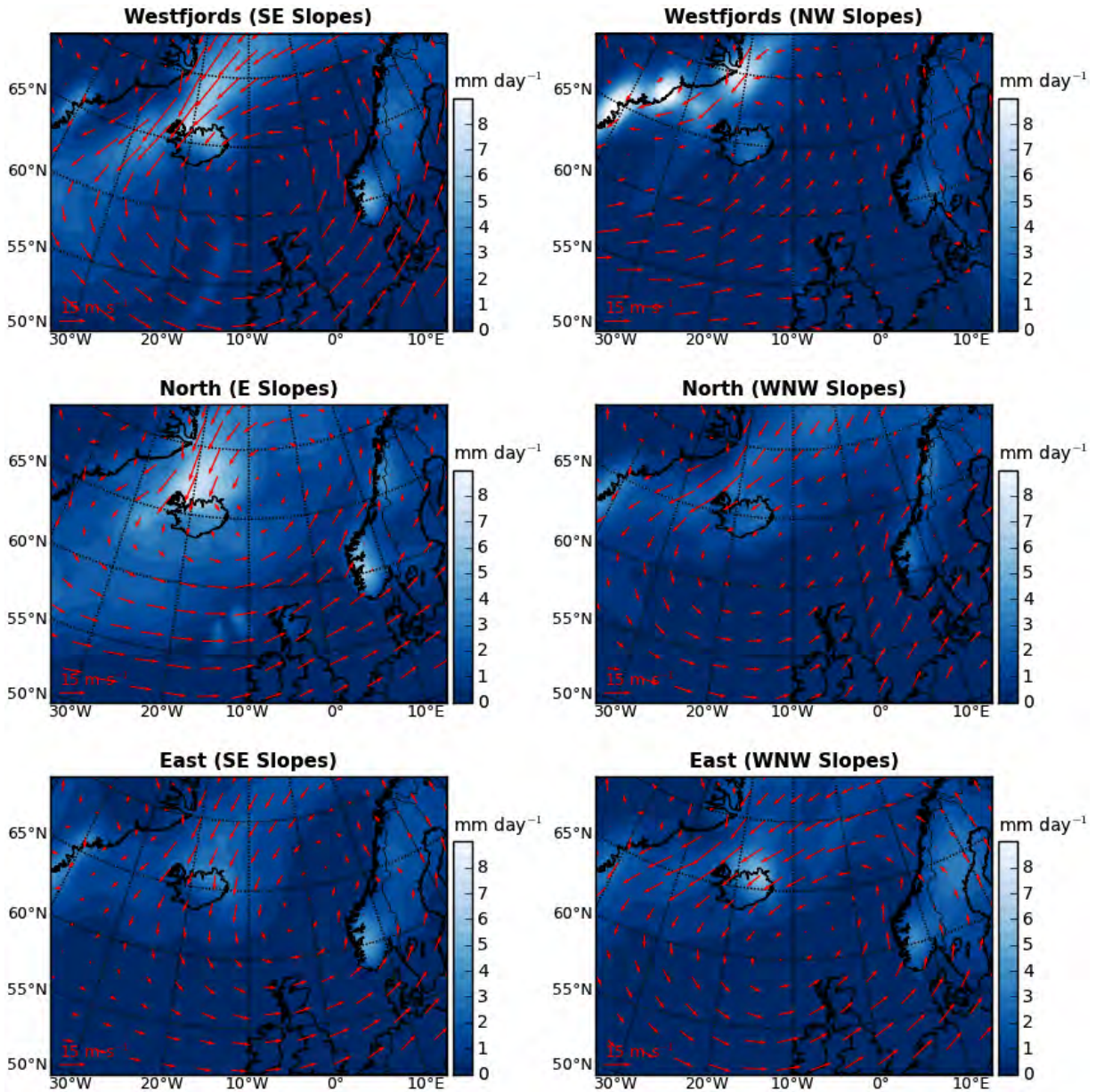


Figure 23. Ensemble mean fields for days with major avalanche activity in different regions of Iceland, limited to specific slope orientations: daily snowfall, and 925 hPa wind field.

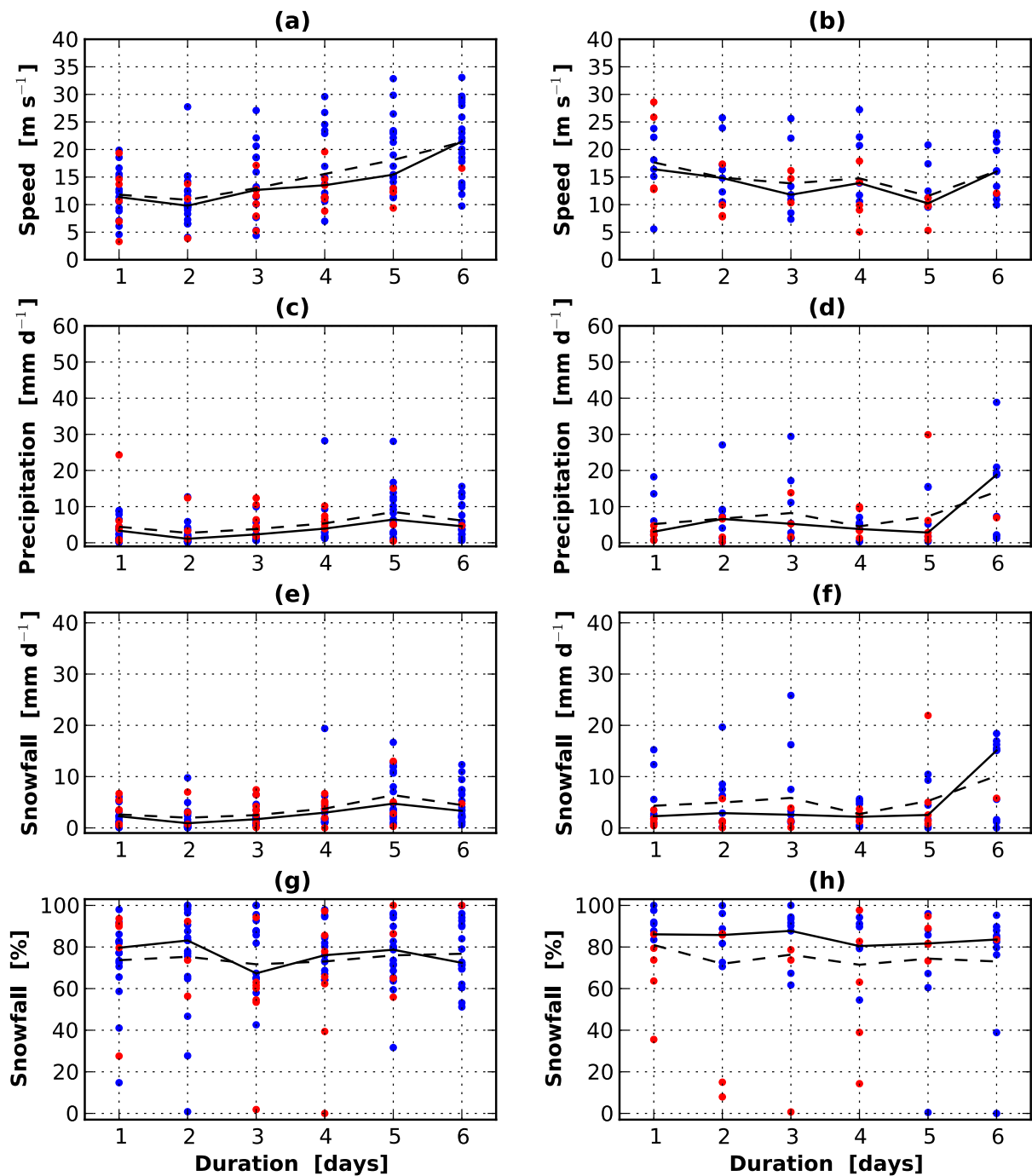


Figure 24. Left column: ensemble evolution of daily regional mean values towards the start of major avalanche activity in the Westfjords on day 6. Right column: evolution of meteorologically comparable ensembles, that were not associated with major avalanche activity (see Section 6). Red dots represent values associated with southwesterly winds ( $135 < \text{wind direction} \leq 315$  degrees), blue dots represent values associated with northeasterly winds ( $\text{wind direction} > 315$  degrees, or  $\leq 135$  degrees). Ensemble medians are shown by the solid lines. Ensemble averages are shown by the dashed lines.

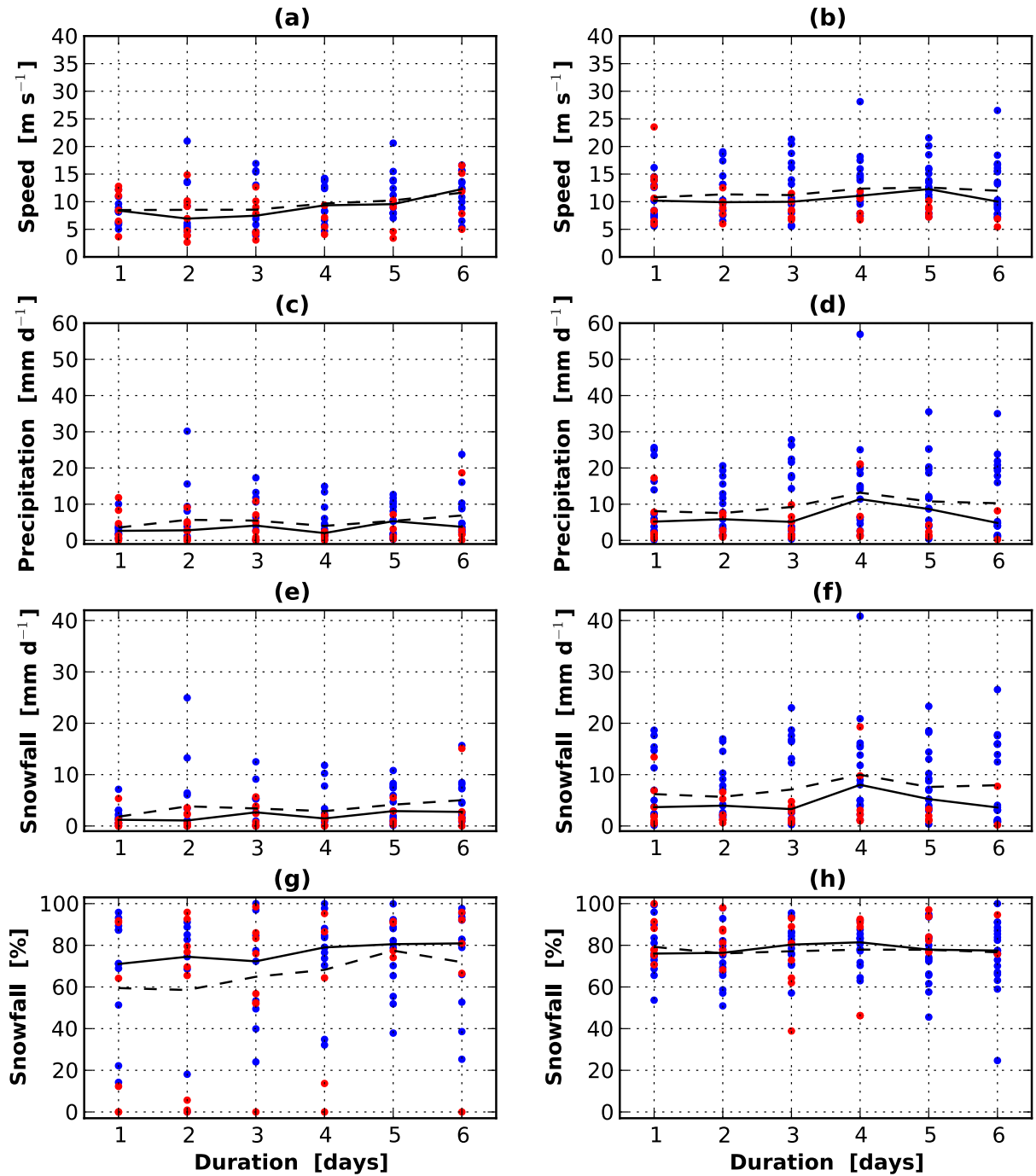


Figure 25. Left column: ensemble evolution of daily regional mean values towards the start of major avalanche activity in Northern Iceland on day 6. Right column: evolution of meteorologically comparable ensembles, that were not associated with major avalanche activity (see Section 6). Red dots represent values associated with southwesterly winds ( $135 < \text{wind direction} \leq 315$  degrees), blue dots represent values associated with northeasterly winds ( $\text{wind direction} > 315$  degrees, or  $\leq 135$  degrees). Ensemble medians are shown by the solid lines. Ensemble averages are shown by the dashed lines.

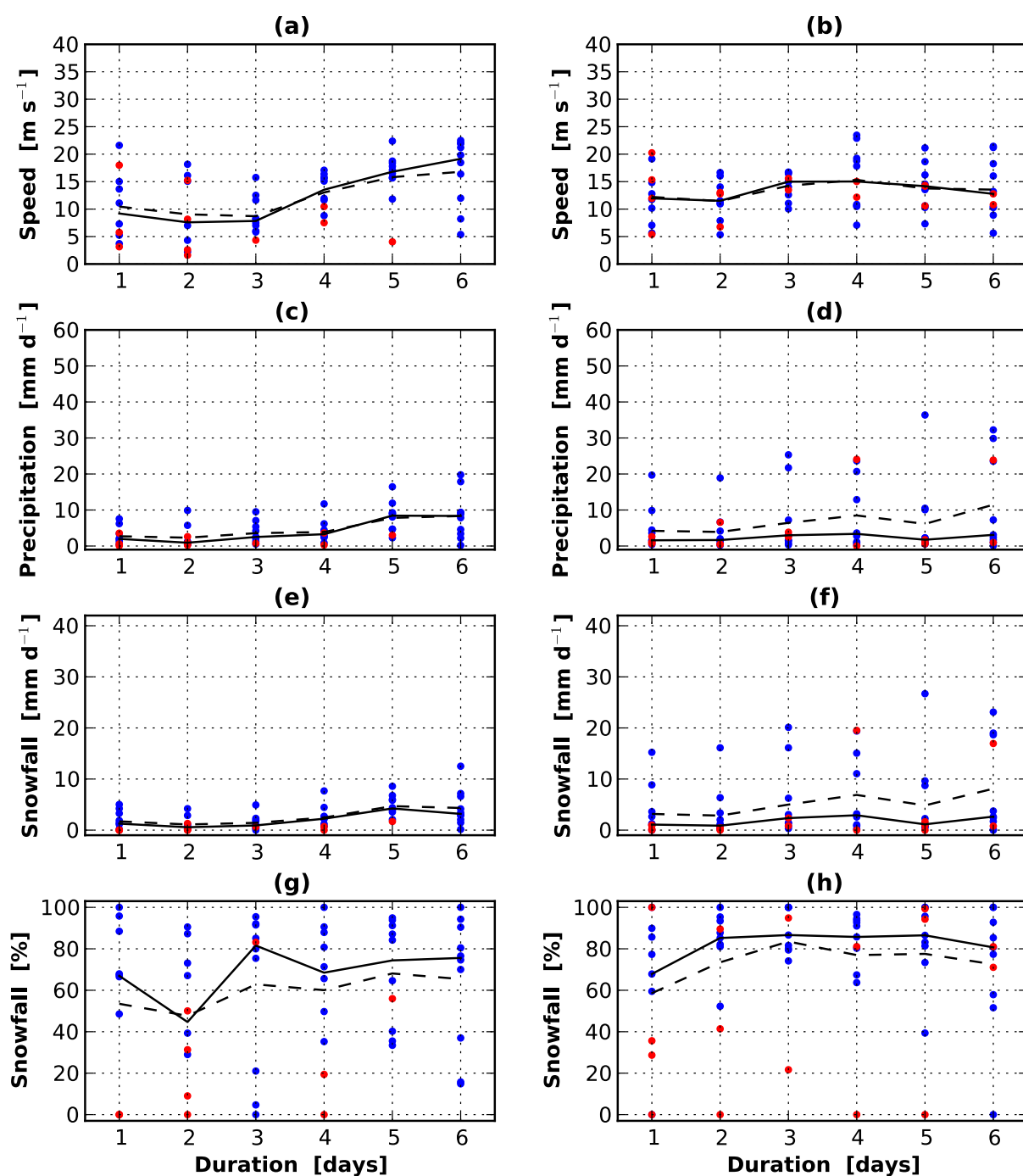


Figure 26. Left column: ensemble evolution of daily regional mean values towards the start of major avalanche activity in Eastern Iceland on day 6. Right column: evolution of meteorologically comparable ensembles, that were not associated with major avalanche activity (see Section 6). Red dots represent values associated with southwesterly winds ( $135 < \text{wind direction} \leq 315$  degrees), blue dots represent values associated with northeasterly winds ( $\text{wind direction} > 315$  degrees, or  $\leq 135$  degrees). Ensemble medians are shown by the solid lines. Ensemble averages are shown by the dashed lines.

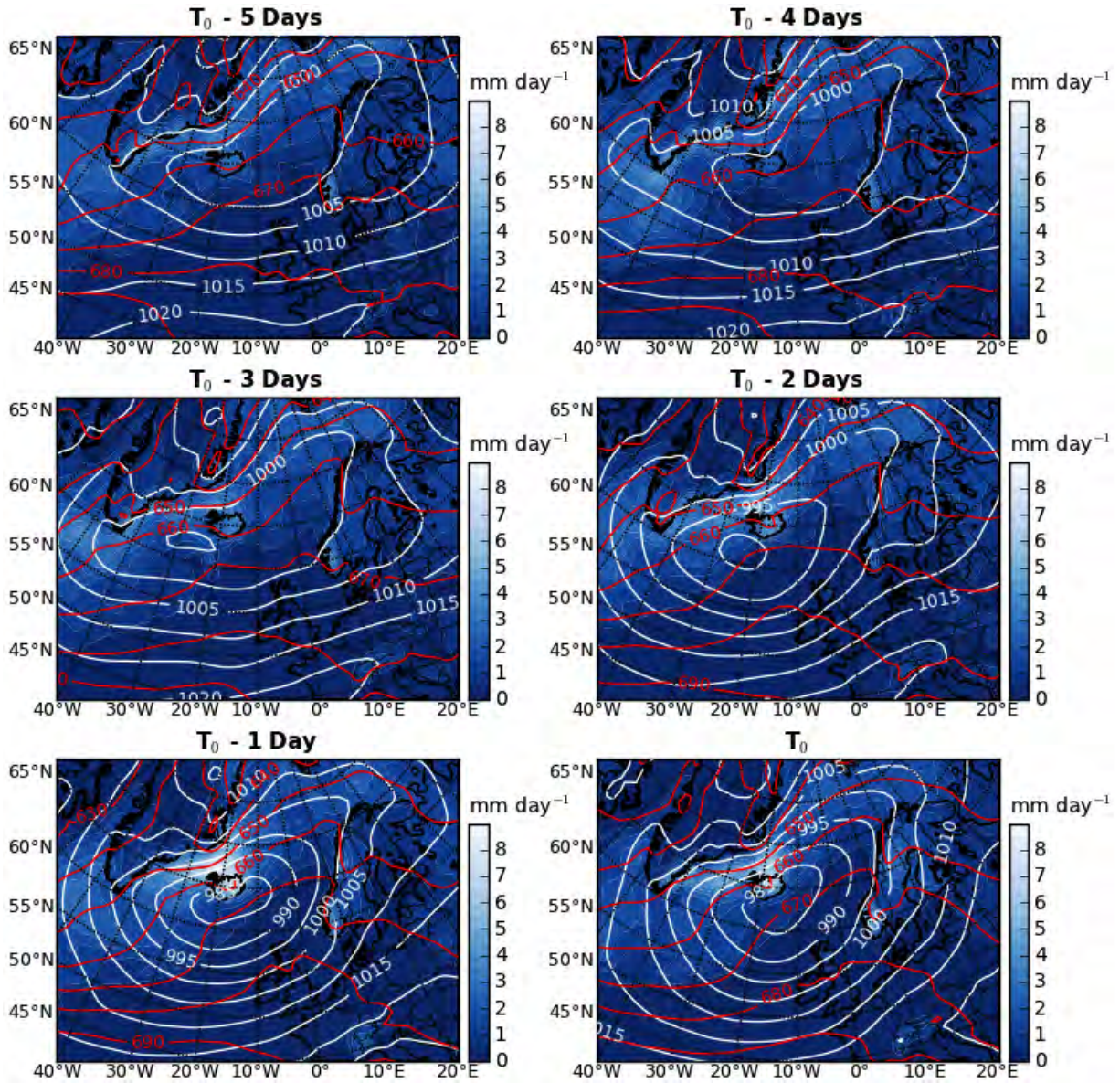


Figure 27. Ensemble mean evolution towards the start of major avalanche activity in the Westfjords on day  $T_0$ : mean sea level pressure (white contour lines), 925 – 850 hPa layer thickness (red contour lines), and daily snowfall (coloured contours).



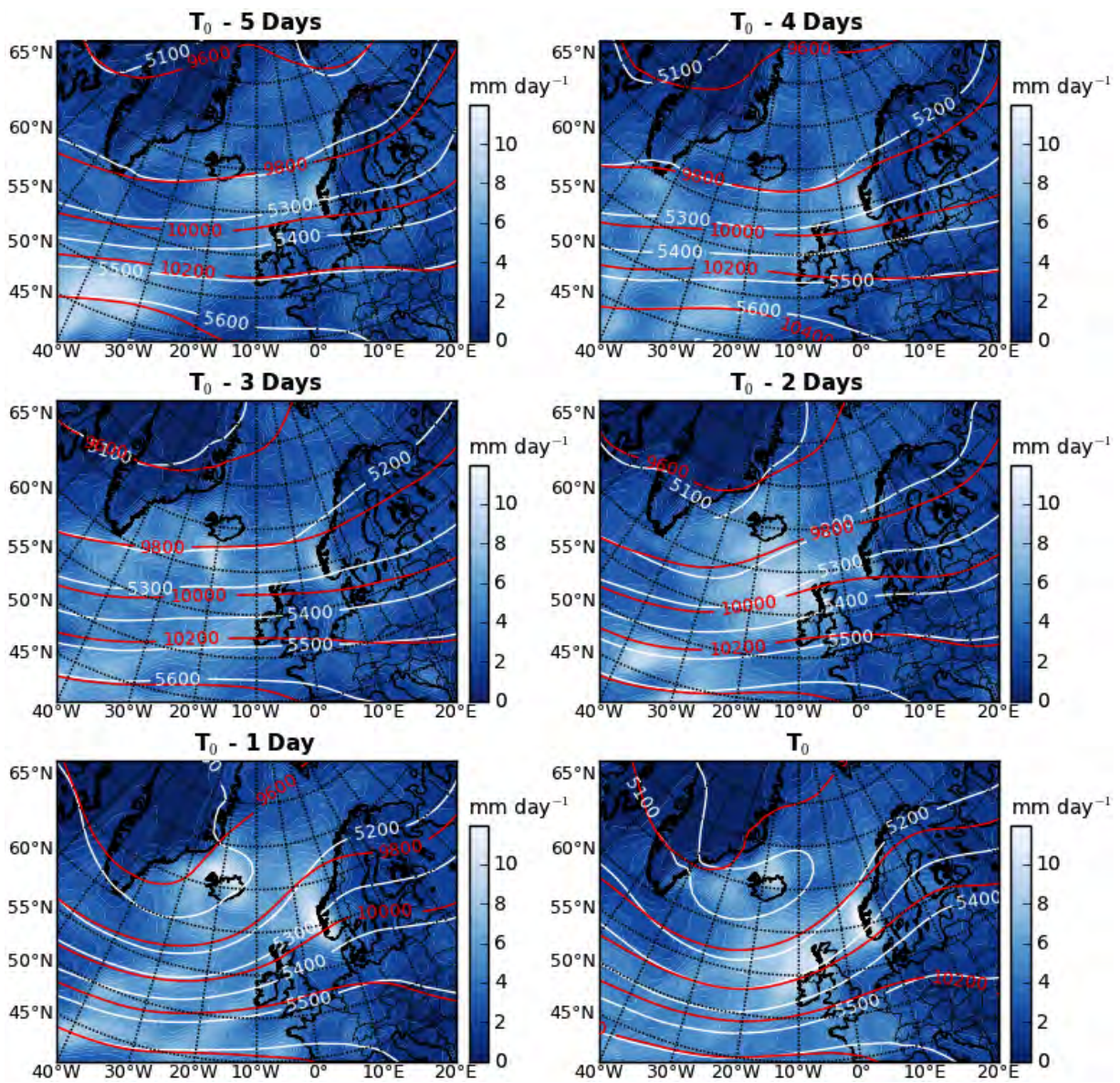


Figure 28. Ensemble mean evolution towards the start of major avalanche activity in the Westfjords on day  $T_0$ : 500 hPa geopotential height (white contour lines), 250 hPa geopotential height (red contour lines), and total daily precipitation (coloured contours).

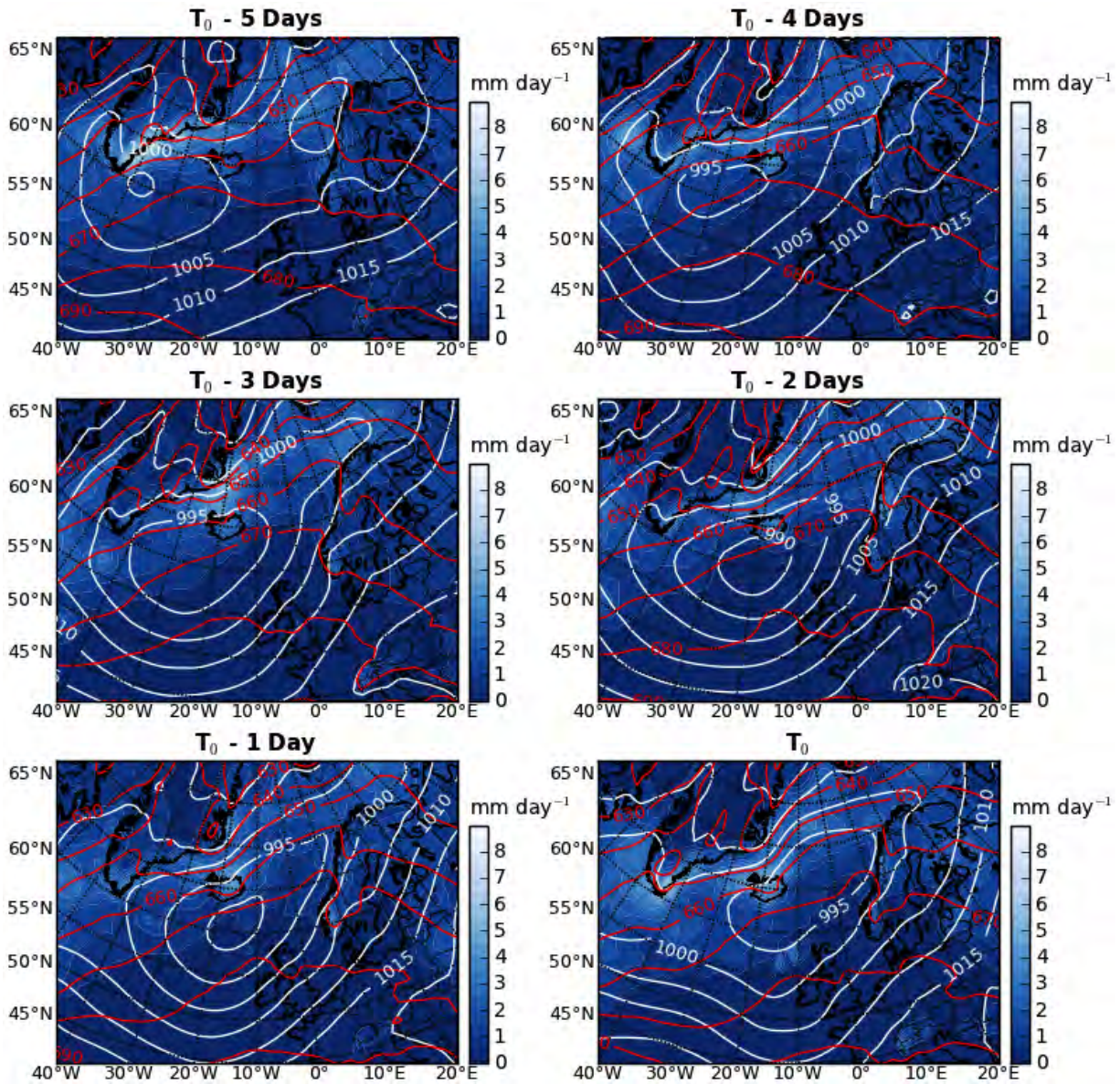


Figure 29. Ensemble mean evolution towards the start of major avalanche activity in Northern Iceland on day  $T_0$ : mean sea level pressure (white contour lines), 925 – 850 hPa layer thickness (red contour lines), and daily snowfall (coloured contours).

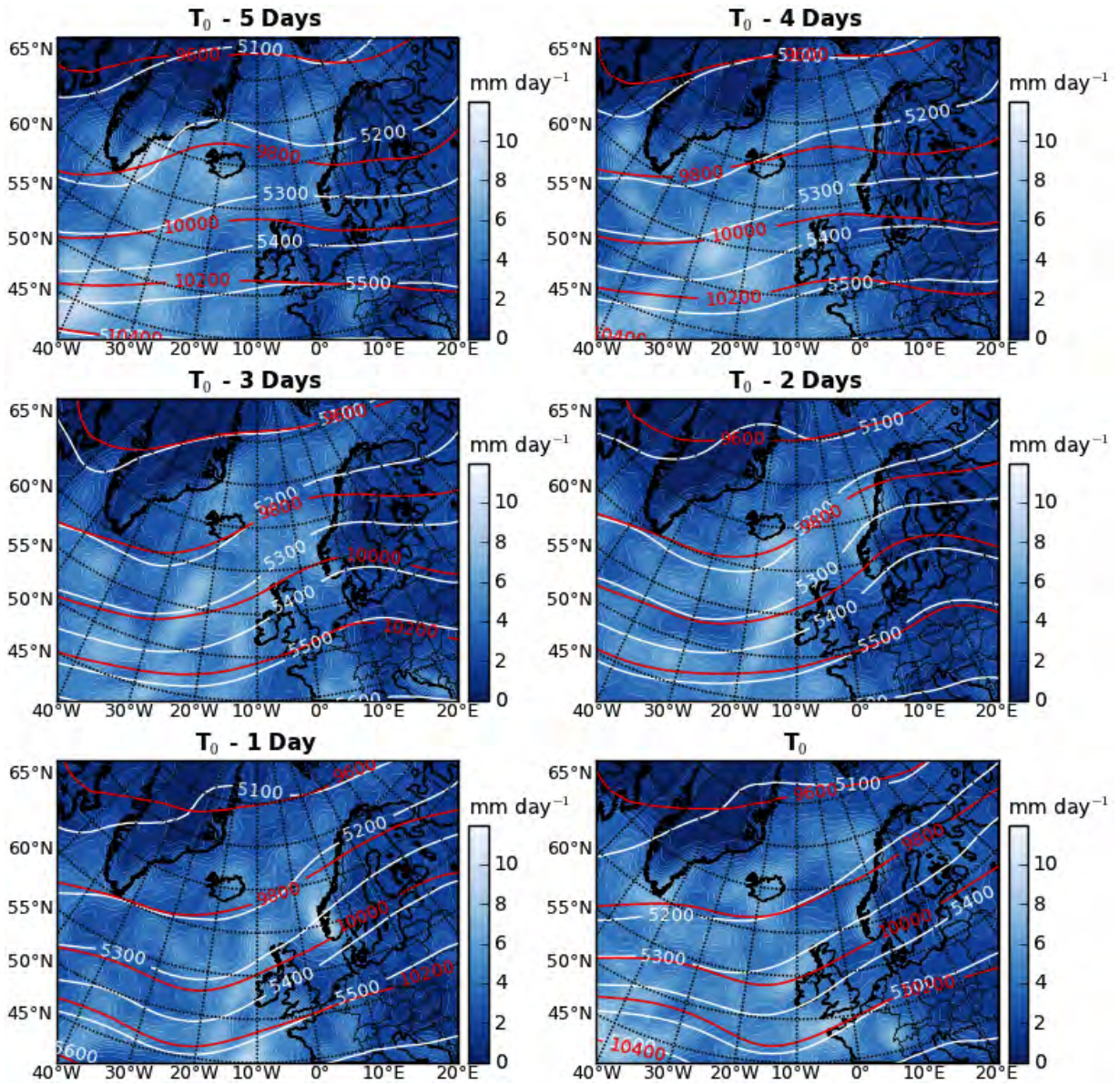


Figure 30. Ensemble mean evolution towards the start of major avalanche activity in Northern Iceland on day  $T_0$ : 500 hPa geopotential height (white contour lines), 250 hPa geopotential height (red contour lines), and total daily precipitation (coloured contours).

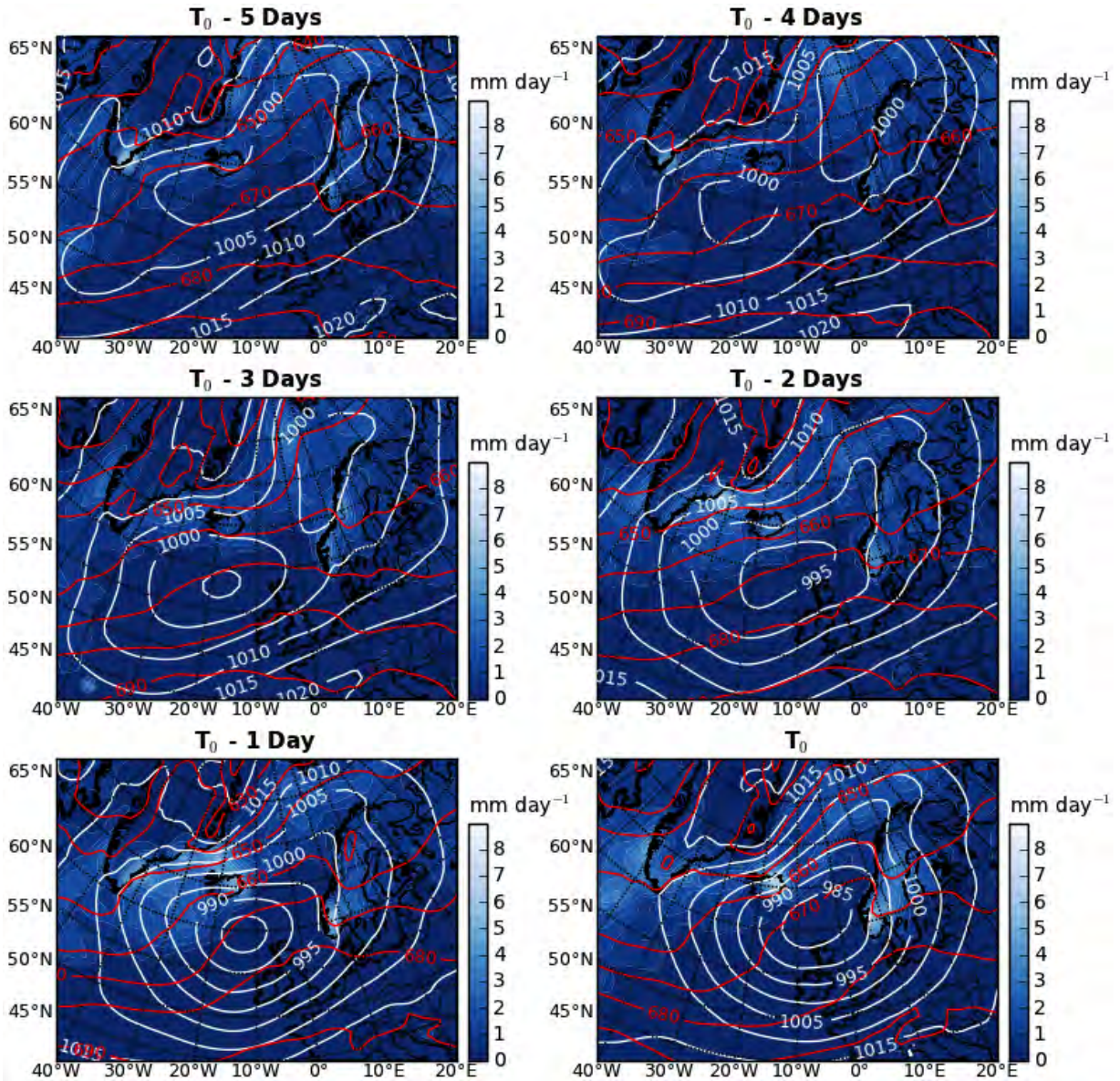


Figure 31. Ensemble mean evolution towards the start of major avalanche activity in Eastern Iceland on day  $T_0$ : mean sea level pressure (white contour lines), 925 – 850 hPa layer thickness (red contour lines), and daily snowfall (coloured contours).

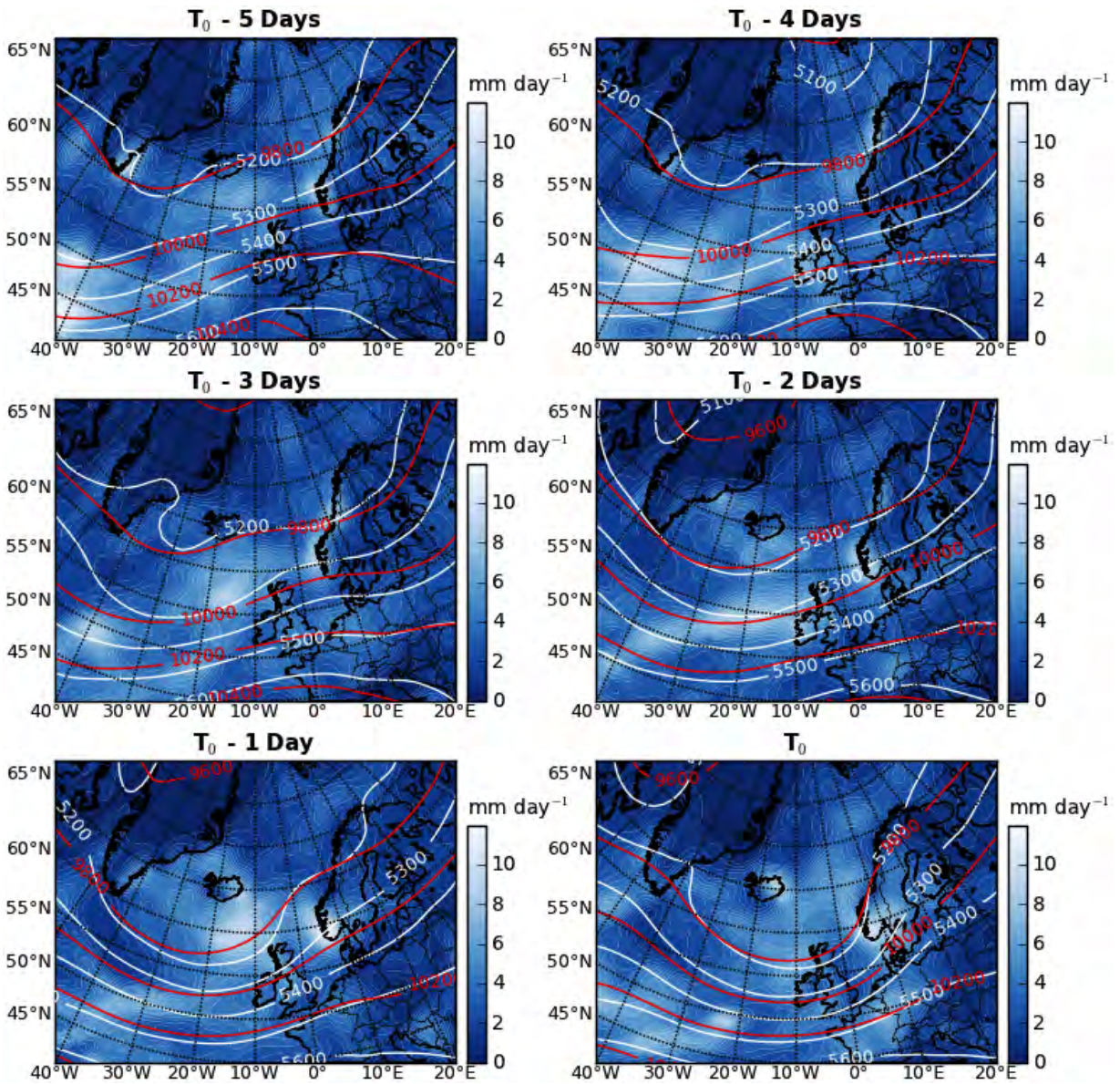


Figure 32. Ensemble mean evolution towards the start of major avalanche activity in Eastern Iceland on day  $T_0$ : 500 hPa geopotential height (white contour lines), 250 hPa geopotential height (red contour lines), and total daily precipitation (coloured contours).

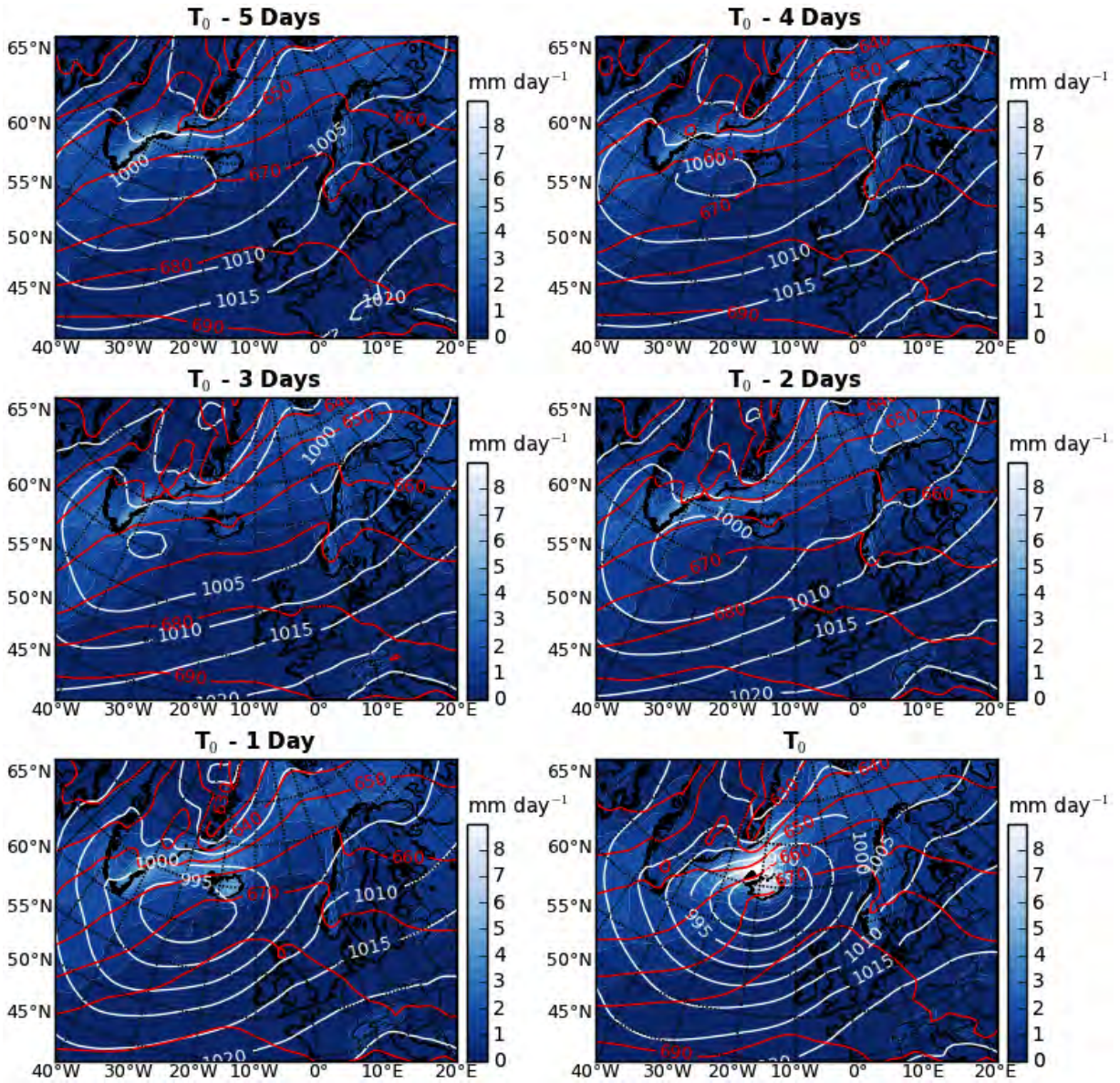


Figure 33. Ensemble mean evolution towards the start of severe snowstorm conditions in the Westfjords on day  $T_0$ : mean sea level pressure (white contour lines), 925 – 850 hPa layer thickness (red contour lines), and daily snowfall (coloured contours).

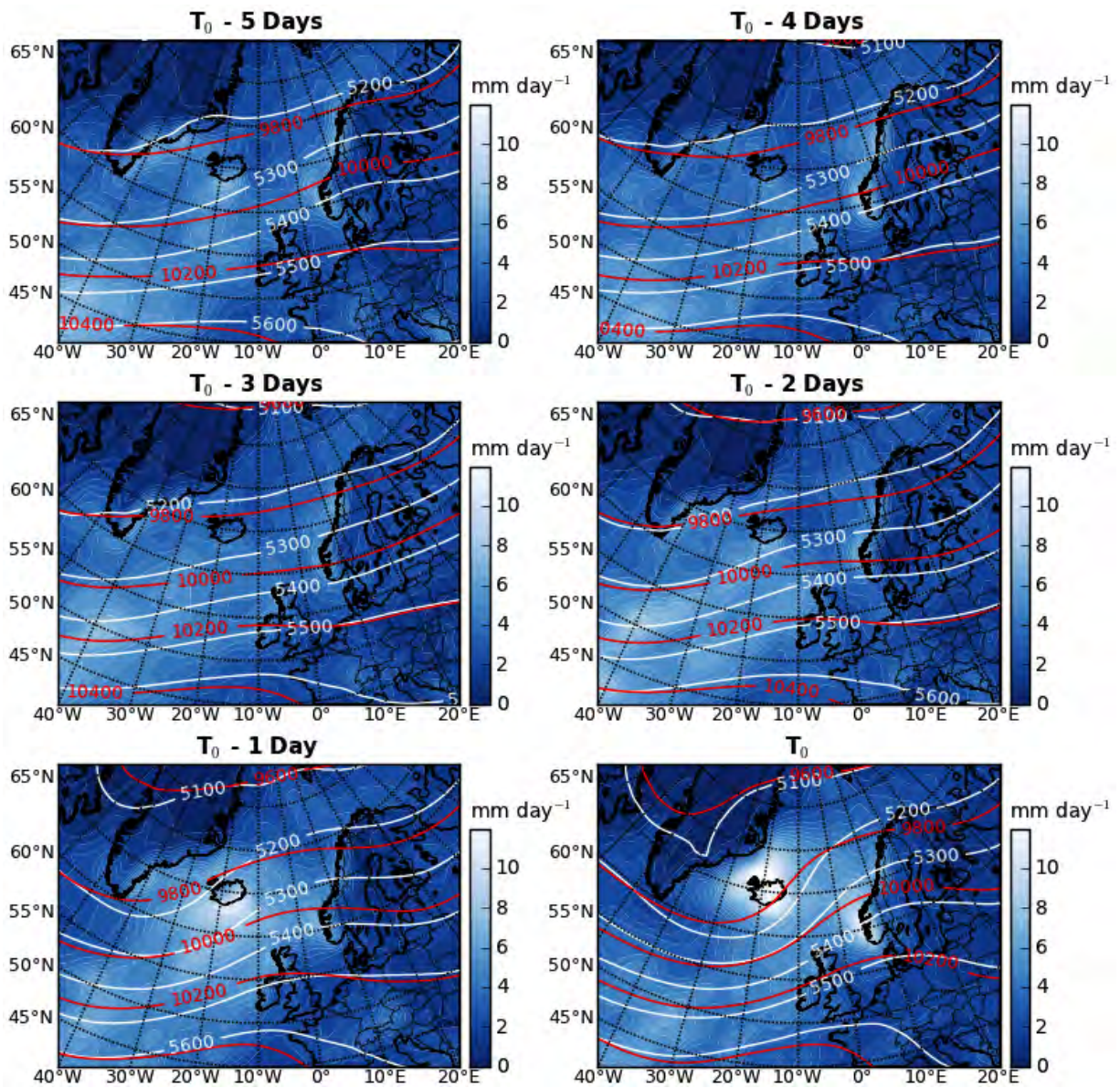


Figure 34. Ensemble mean evolution towards the start of severe snowstorm conditions in the Westfjords on day  $T_0$ : 500 hPa geopotential height (white contour lines), 250 hPa geopotential height (red contour lines), and total daily precipitation (coloured contours).

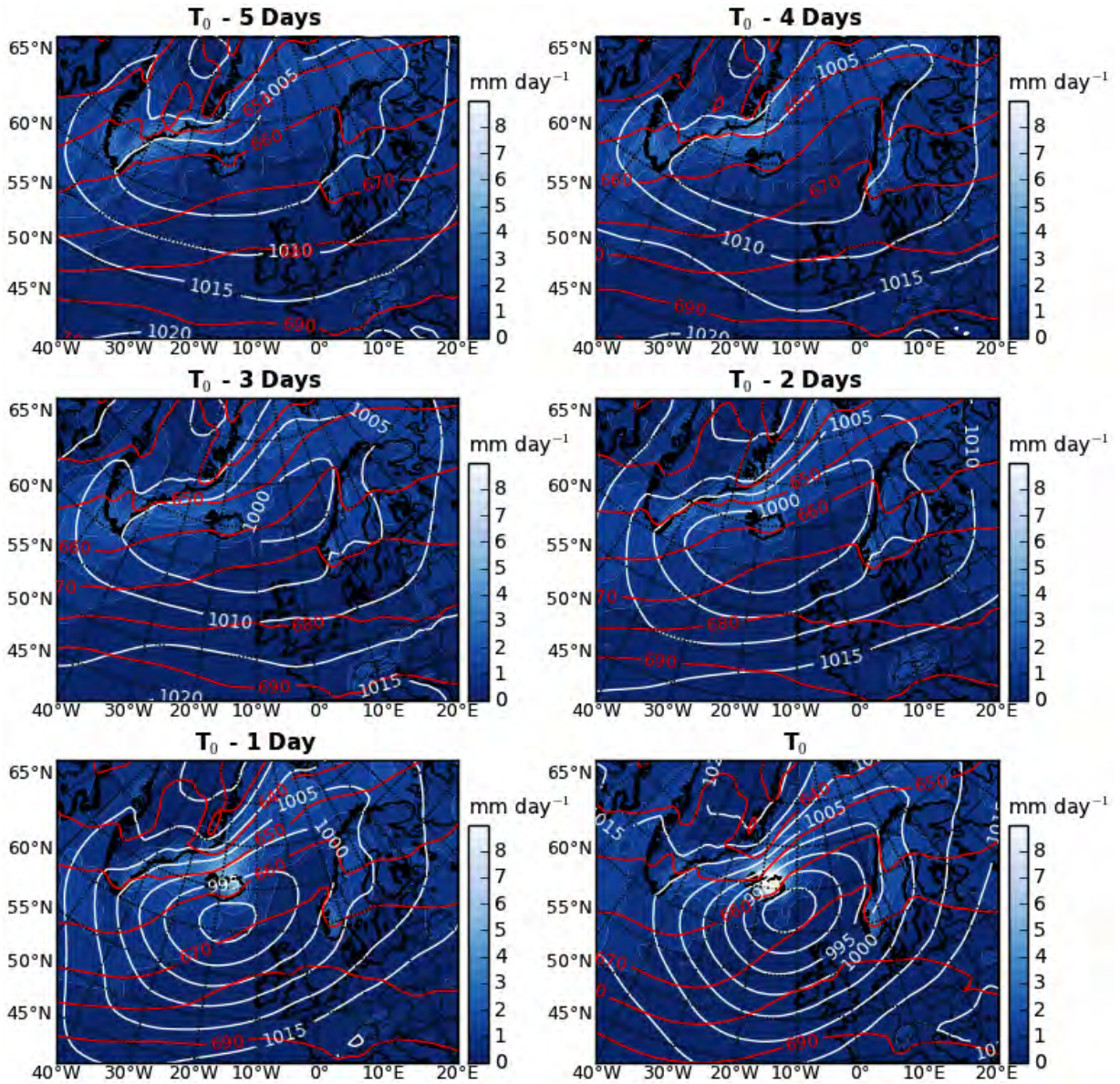


Figure 35. Ensemble mean evolution towards the start of severe snowstorm conditions in Northern Iceland on day  $T_0$ : mean sea level pressure (white contour lines), 925 – 850 hPa layer thickness (red contour lines), and daily snowfall (coloured contours).



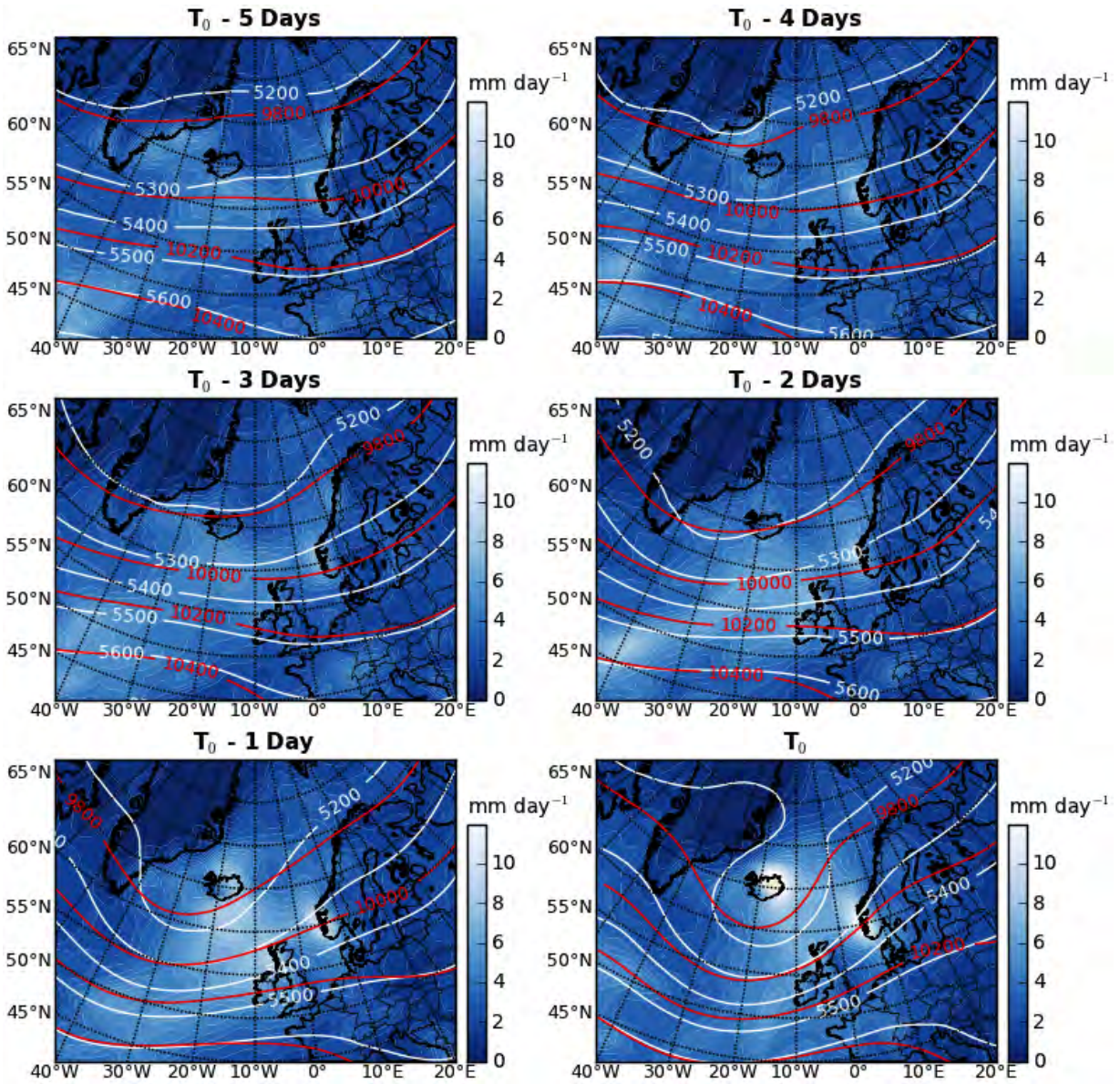


Figure 36. Ensemble mean evolution towards the start of severe snowstorm conditions in Northern Iceland on day  $T_0$ : 500 hPa geopotential height (white contour lines), 250 hPa geopotential height (red contour lines), and total daily precipitation (coloured contours).

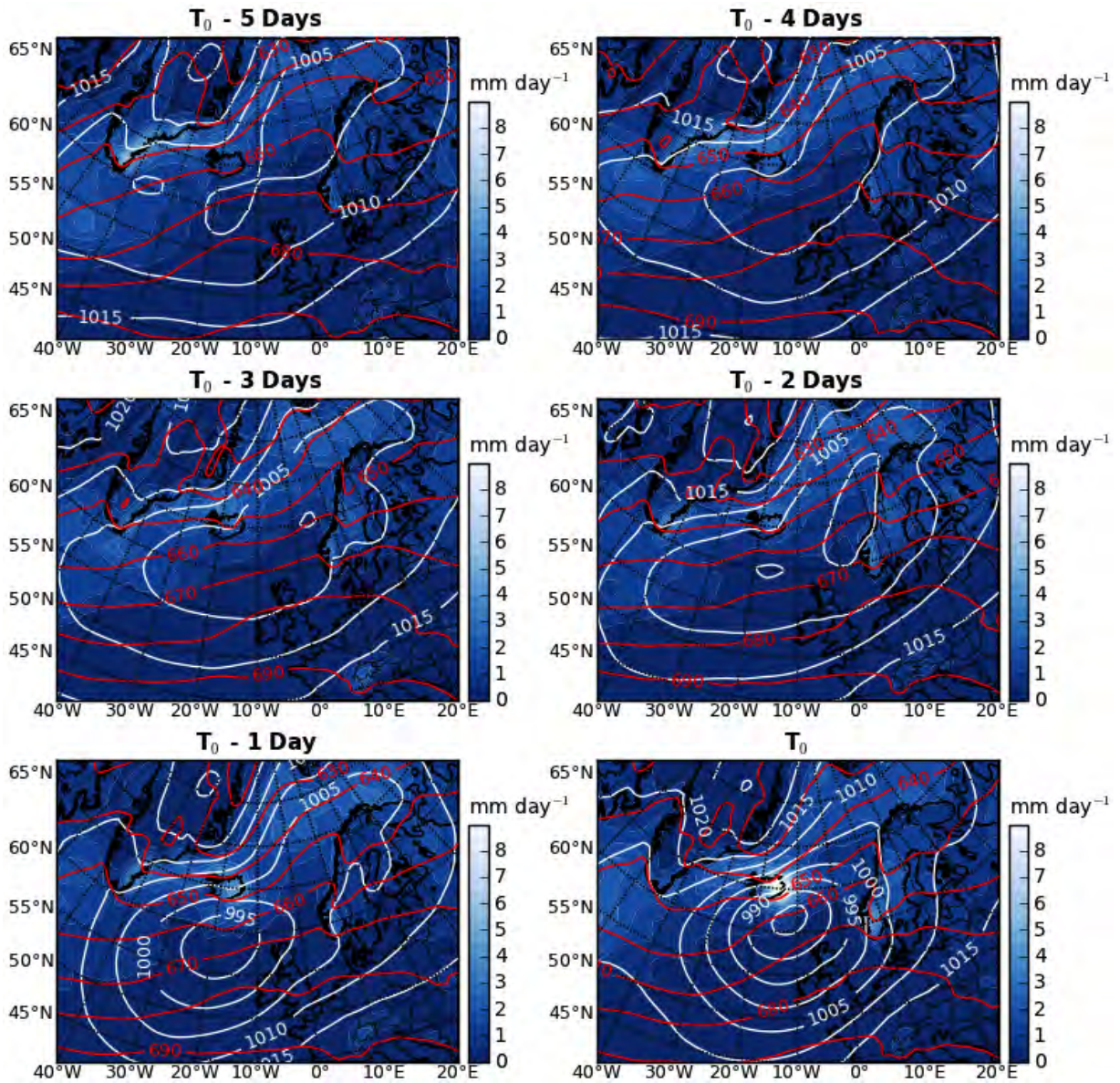


Figure 37. Ensemble mean evolution towards the start of severe snowstorm conditions in Eastern Iceland on day  $T_0$ : mean sea level pressure (white contour lines), 925 – 850 hPa layer thickness (red contour lines), and daily snowfall (coloured contours).

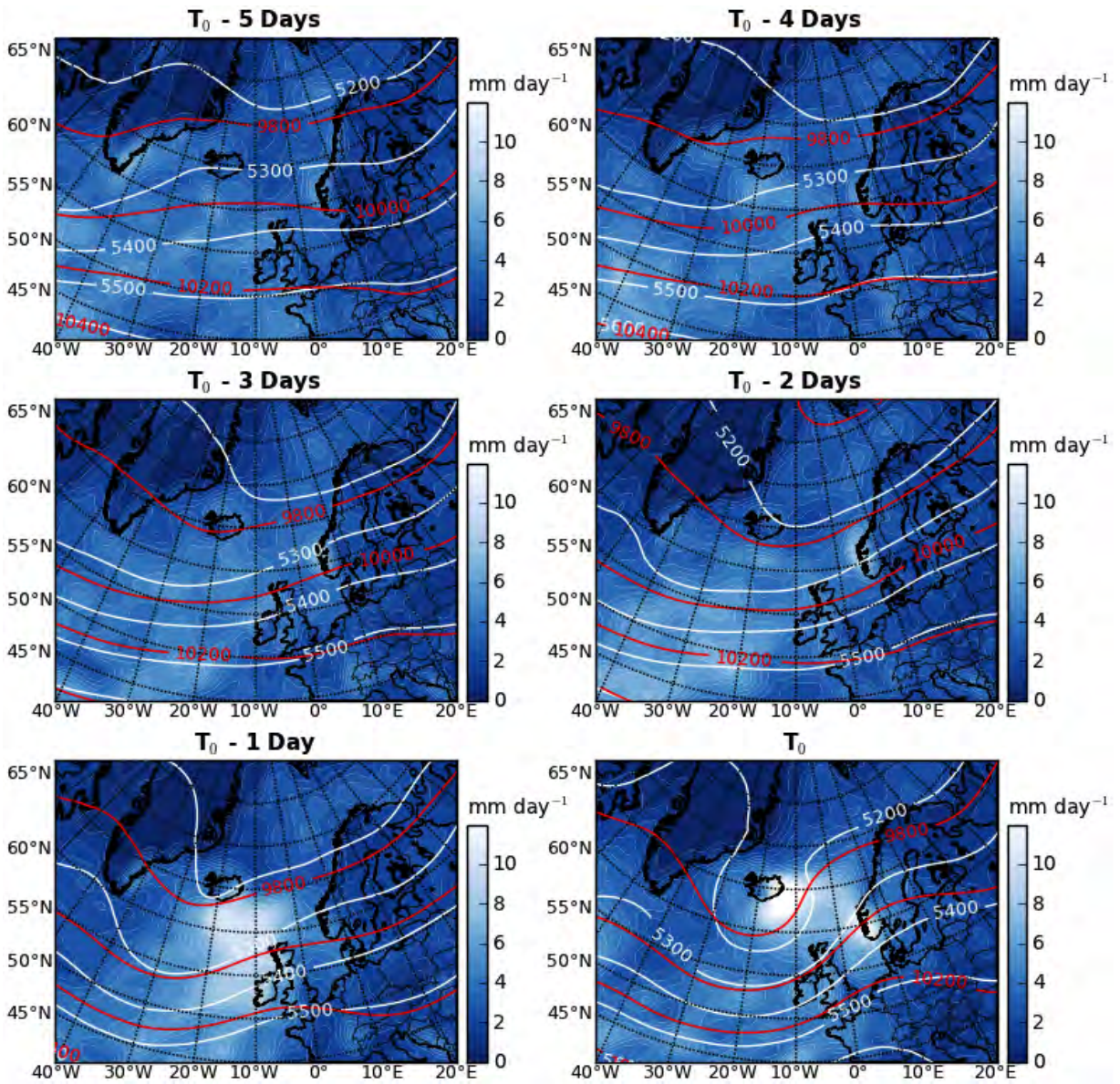


Figure 38. Ensemble mean evolution towards the start of severe snowstorm conditions in Eastern Iceland on day  $T_0$ : 500 hPa geopotential height (white contour lines), 250 hPa geopotential height (red contour lines), and total daily precipitation (coloured contours).

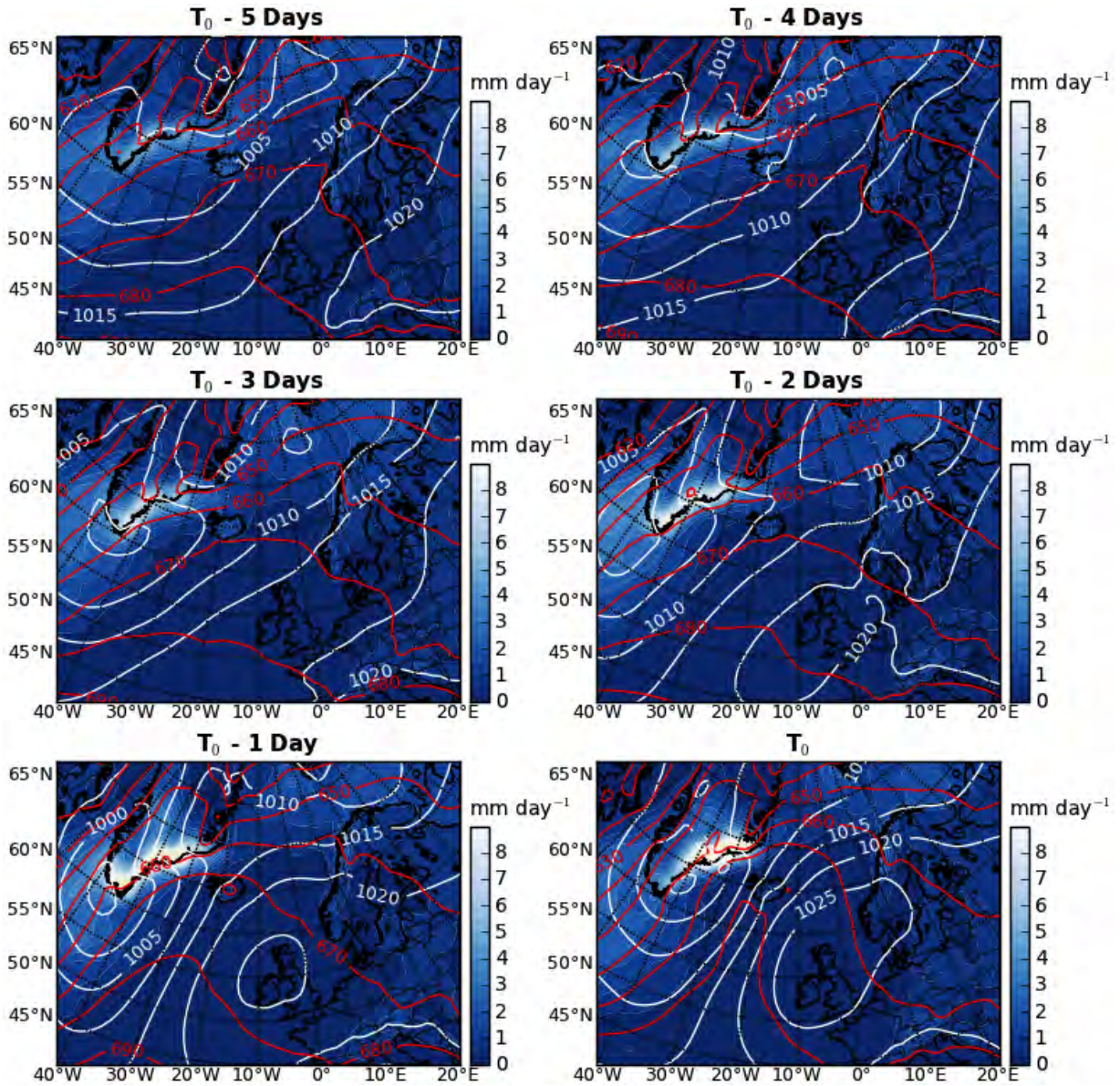


Figure 39. Ensemble mean evolution towards the start of strong wind events in the West-fjords on day  $T_0$ : mean sea level pressure (white contour lines), 925 – 850 hPa layer thickness (red contour lines), and daily snowfall (coloured contours).

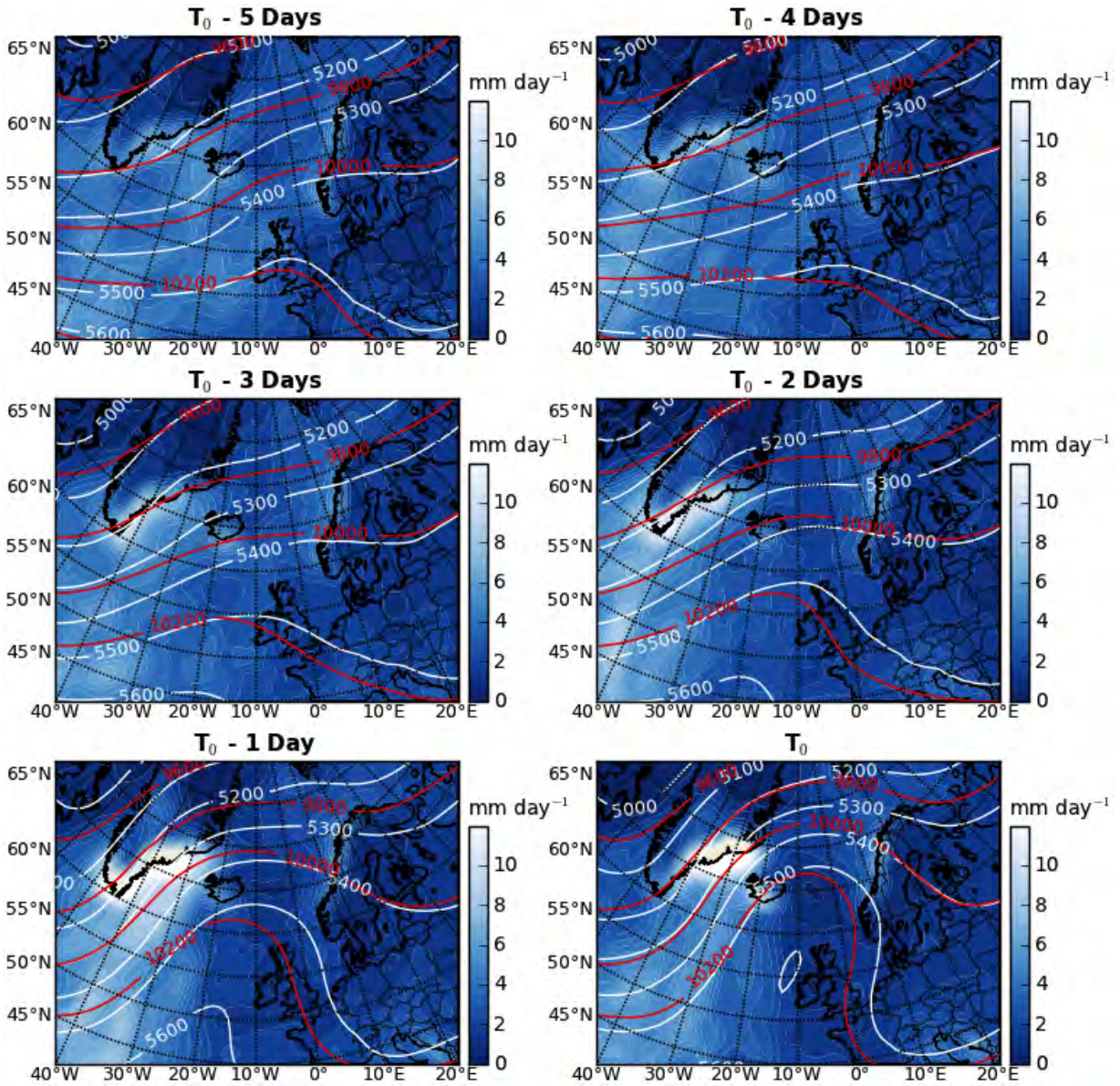


Figure 40. Ensemble mean evolution towards the start of strong wind events in the West-fjords on day  $T_0$ : 500 hPa geopotential height (white contour lines), 250 hPa geopotential height (red contour lines), and total daily precipitation (coloured contours).

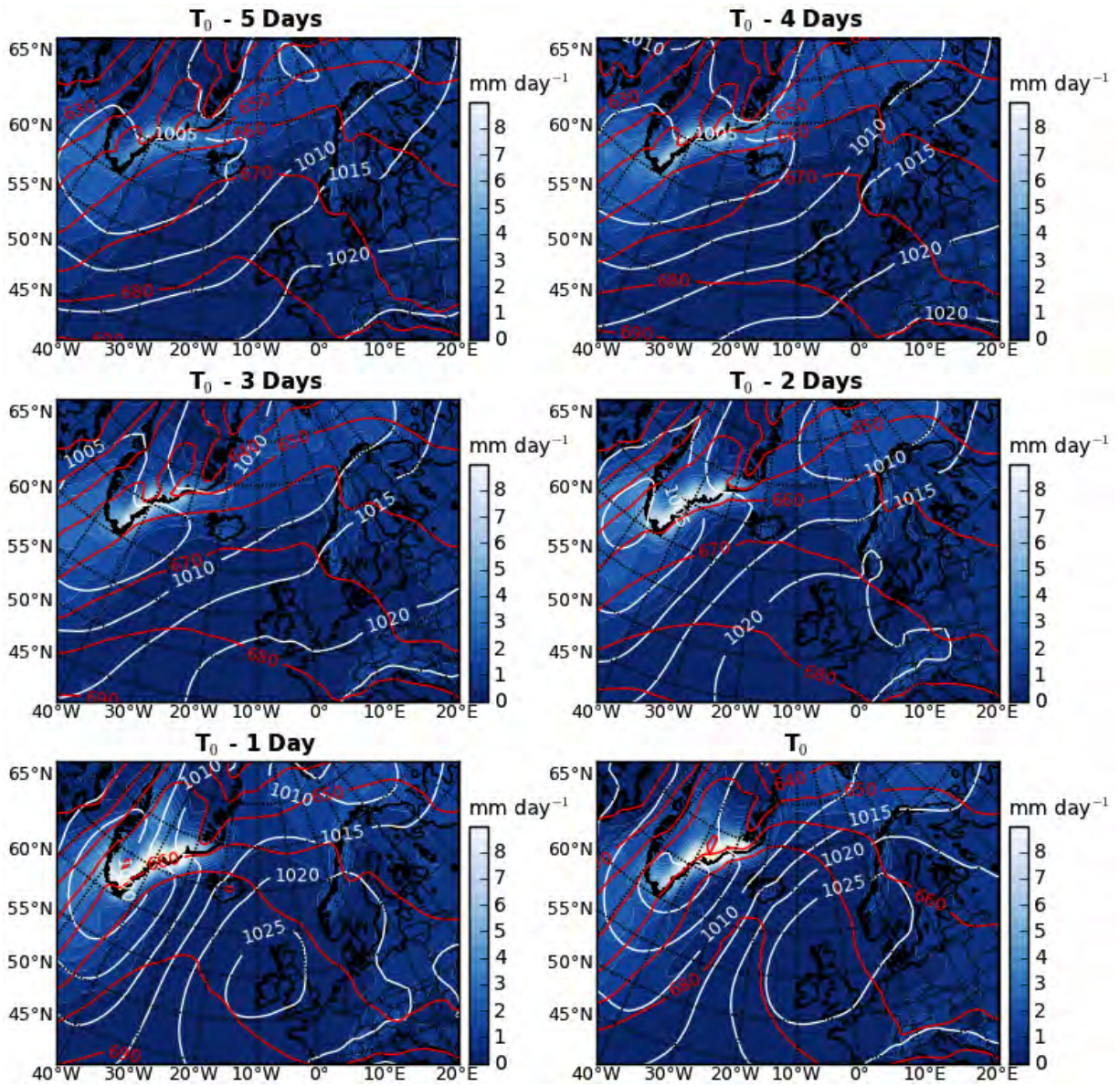


Figure 41. Ensemble mean evolution towards the start of strong wind events in Northern Iceland on day  $T_0$ : mean sea level pressure (white contour lines), 925 – 850 hPa layer thickness (red contour lines), and daily snowfall (coloured contours).

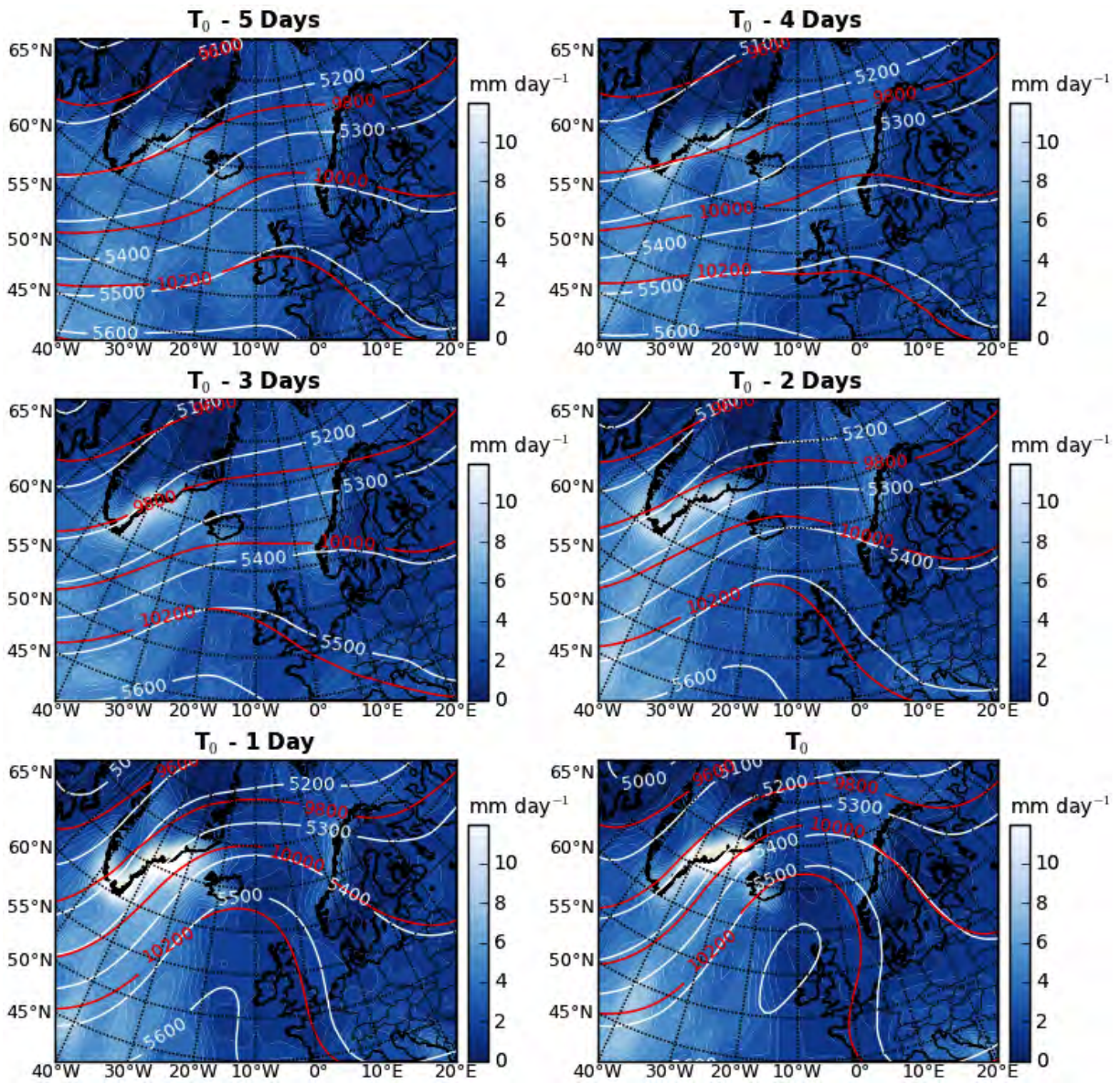


Figure 42. Ensemble mean evolution towards the start of strong wind events in Northern Iceland on day  $T_0$ : 500 hPa geopotential height (white contour lines), 250 hPa geopotential height (red contour lines), and total daily precipitation (coloured contours).

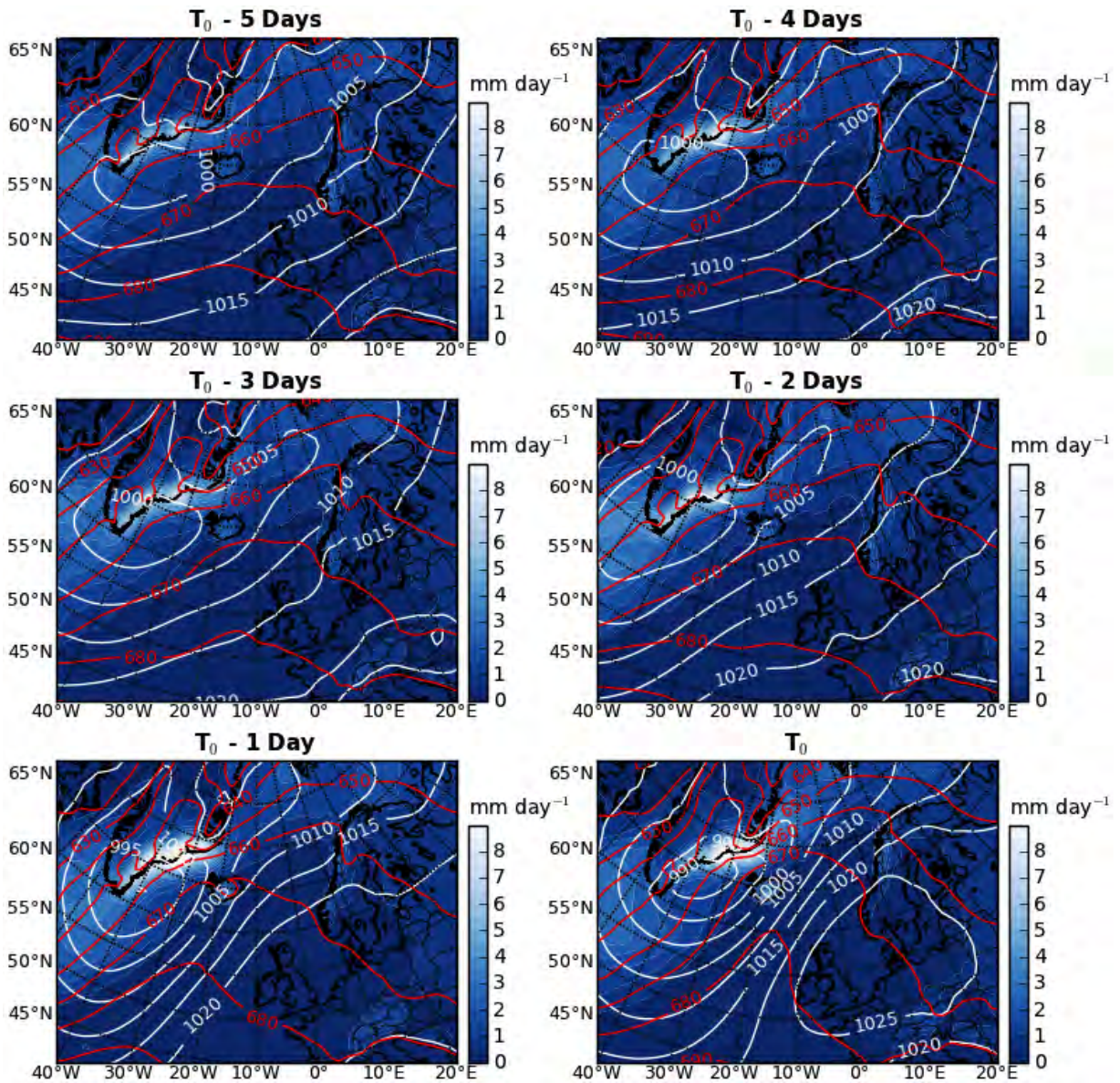


Figure 43. Ensemble mean evolution towards the start of strong wind events in Eastern Iceland on day  $T_0$ : mean sea level pressure (white contour lines), 925 – 850 hPa layer thickness (red contour lines), and daily snowfall (coloured contours).



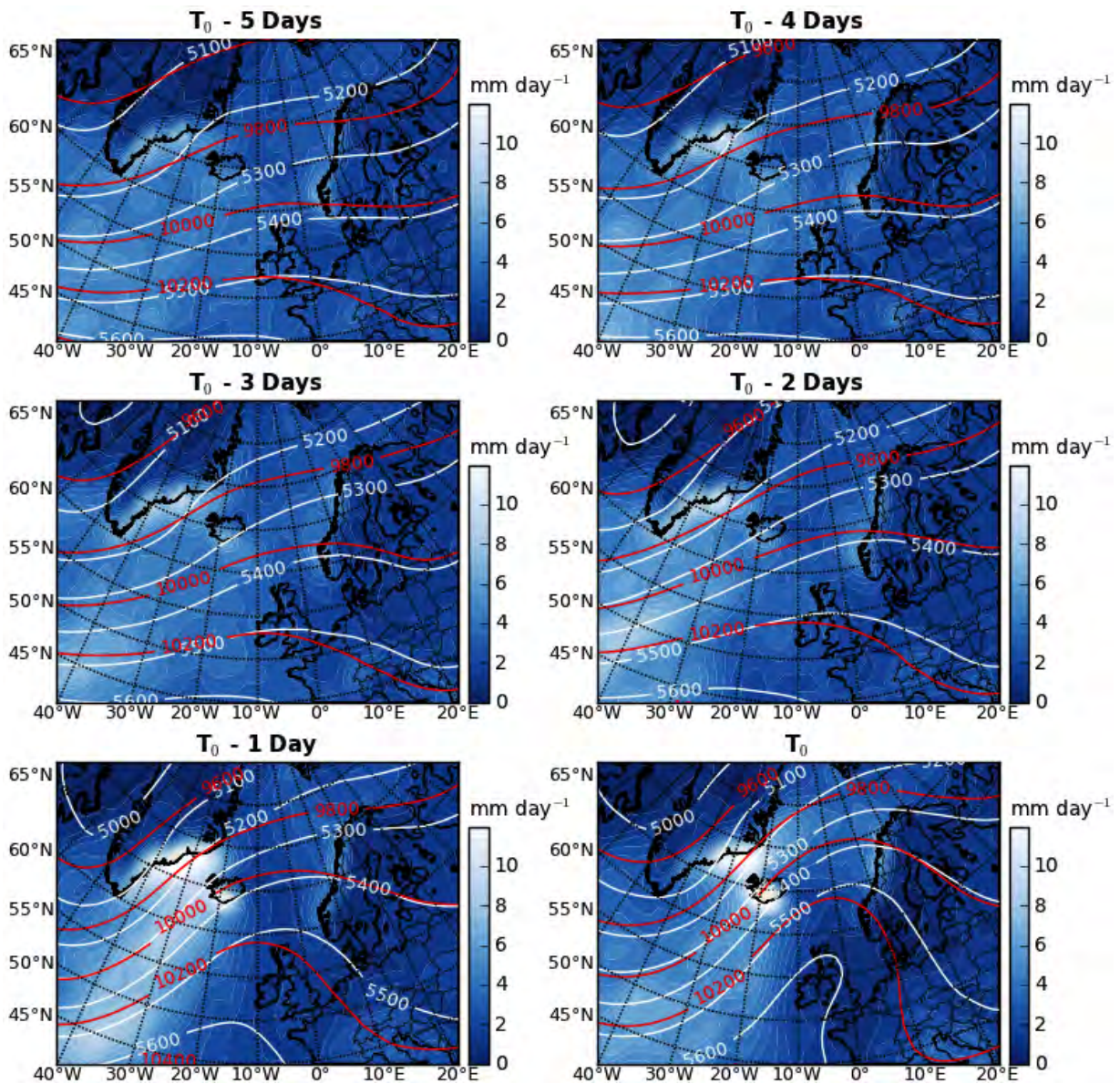


Figure 44. Ensemble mean evolution towards the start of strong wind events in Eastern Iceland on day  $T_0$ : 500 hPa geopotential height (white contour lines), 250 hPa geopotential height (red contour lines), and total daily precipitation (coloured contours).

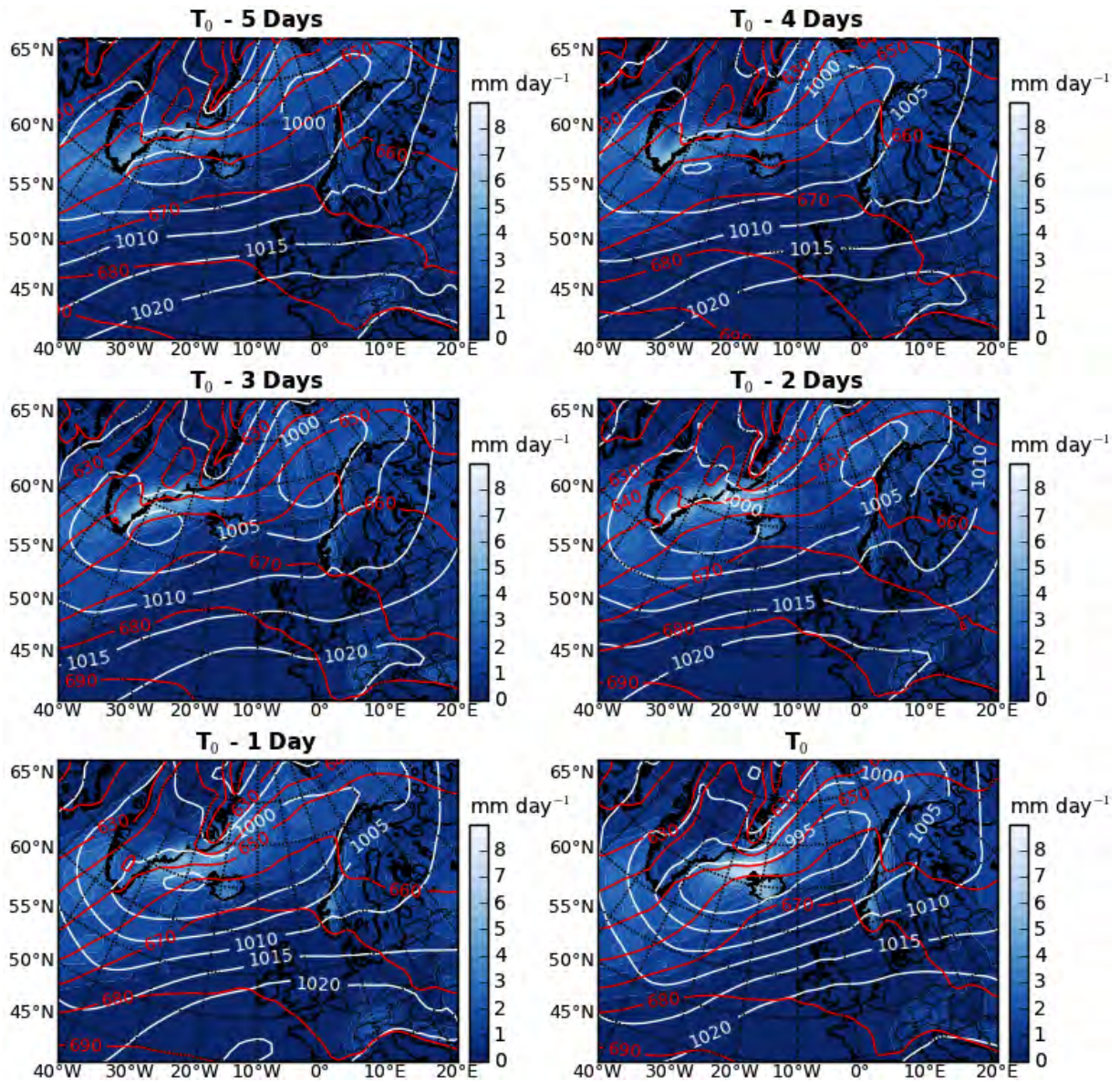


Figure 45. Ensemble mean evolution towards the start of heavy snowfall events in the Westfjords on day  $T_0$ : mean sea level pressure (white contour lines), 925 – 850 hPa layer thickness (red contour lines), and daily snowfall (coloured contours).

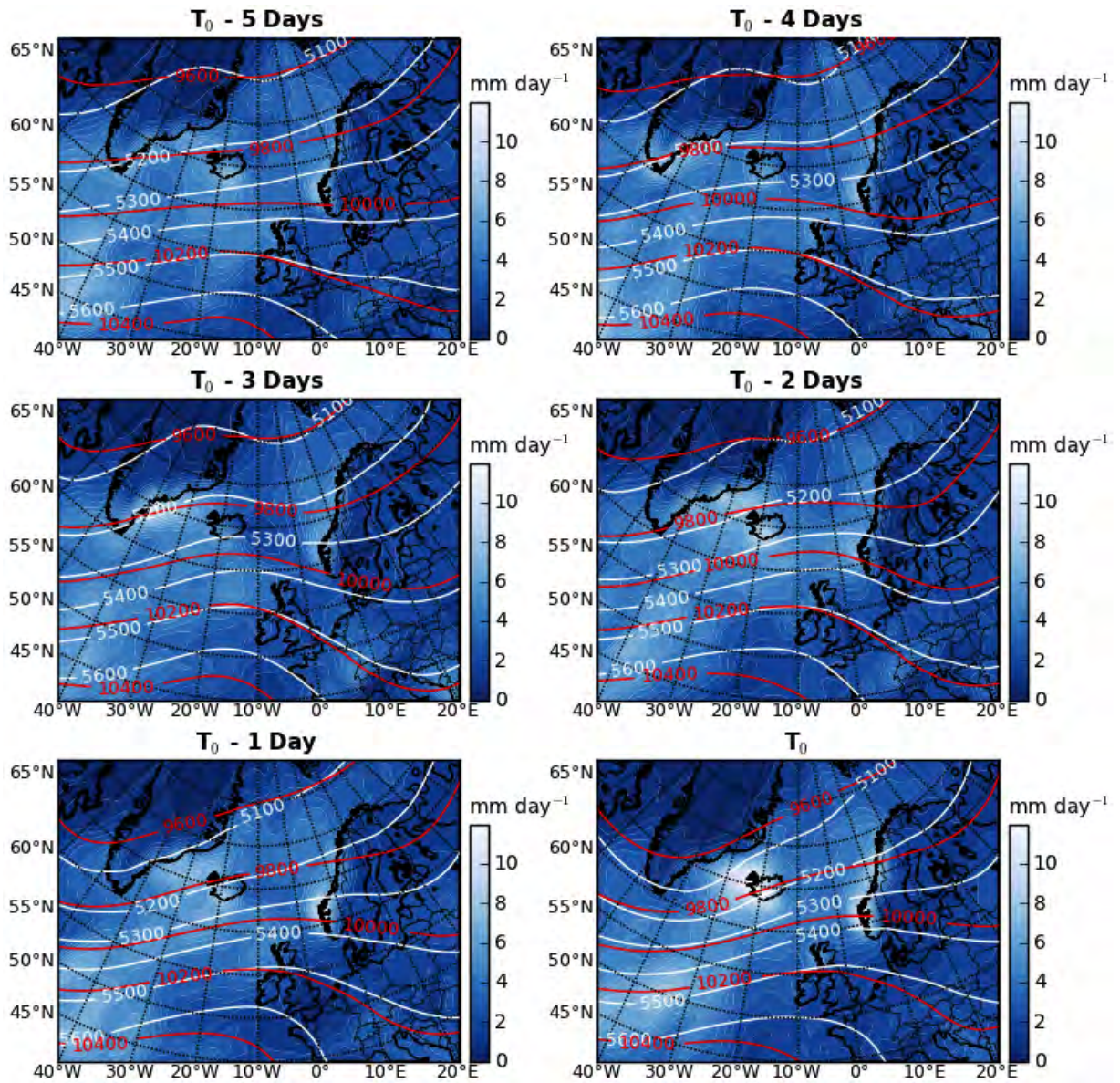


Figure 46. Ensemble mean evolution towards the start of heavy snowfall events in the West-fjords on day  $T_0$ : 500 hPa geopotential height (white contour lines), 250 hPa geopotential height (red contour lines), and total daily precipitation (coloured contours).

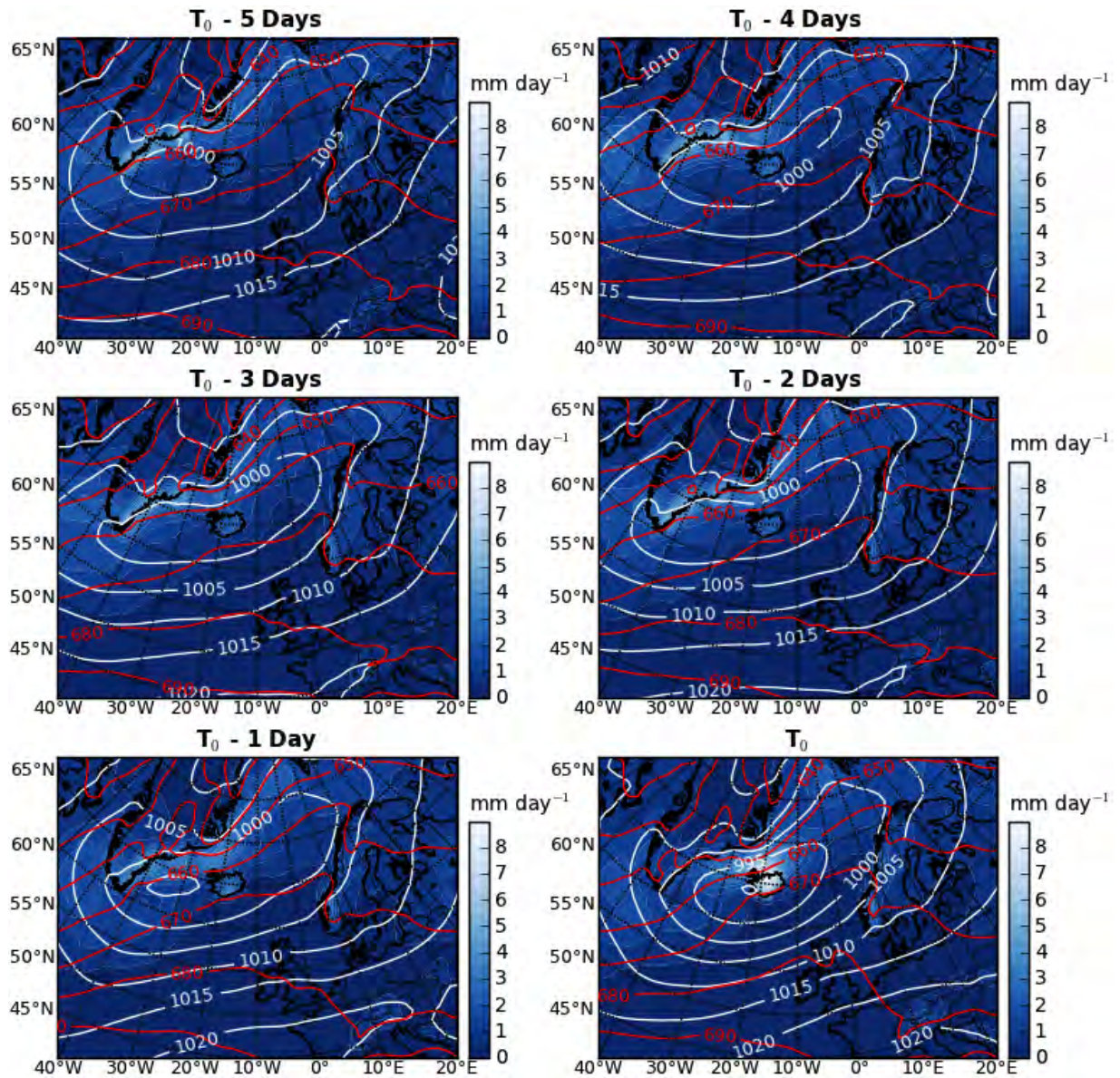


Figure 47. Ensemble mean evolution towards the start of heavy snowfall events in Northern Iceland on day  $T_0$ : mean sea level pressure (white contour lines), 925 – 850 hPa layer thickness (red contour lines), and daily snowfall (coloured contours).

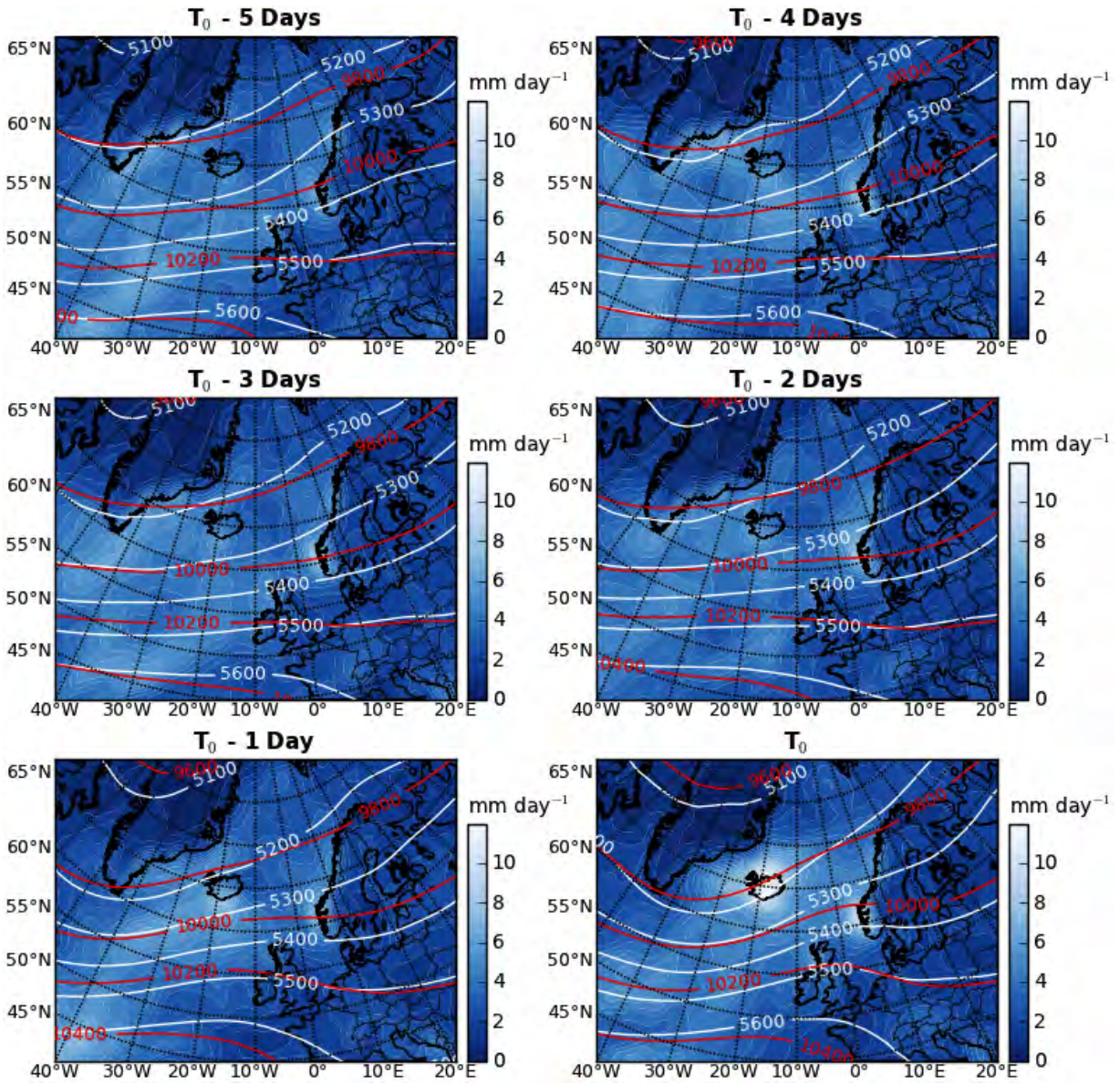


Figure 48. Ensemble mean evolution towards the start of heavy snowfall events in Northern Iceland on day  $T_0$ : 500 hPa geopotential height (white contour lines), 250 hPa geopotential height (red contour lines), and total daily precipitation (coloured contours).

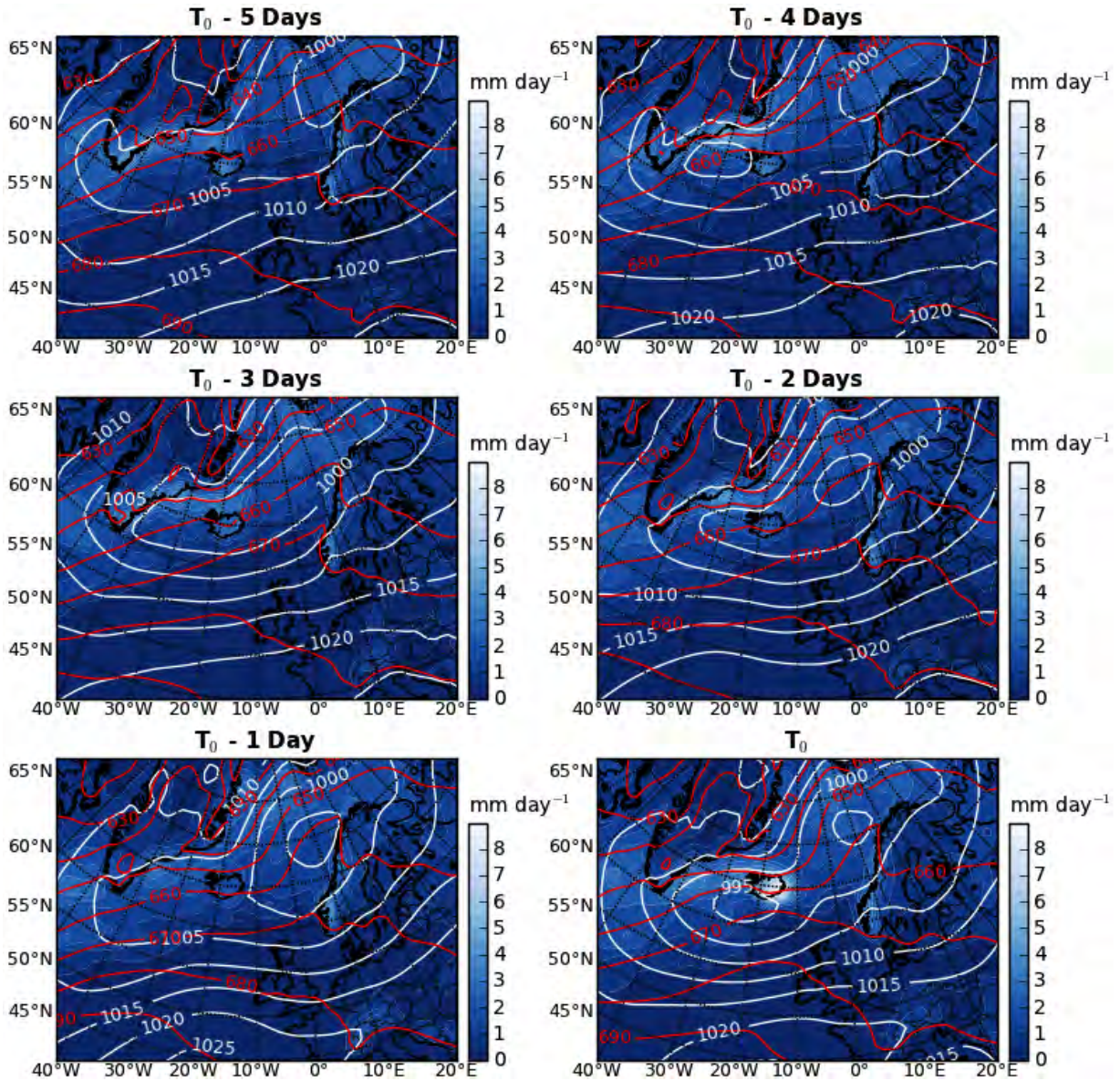


Figure 49. Ensemble mean evolution towards the start of heavy snowfall events in Eastern Iceland on day  $T_0$ : mean sea level pressure (white contour lines), 925 – 850 hPa layer thickness (red contour lines), and daily snowfall (coloured contours).

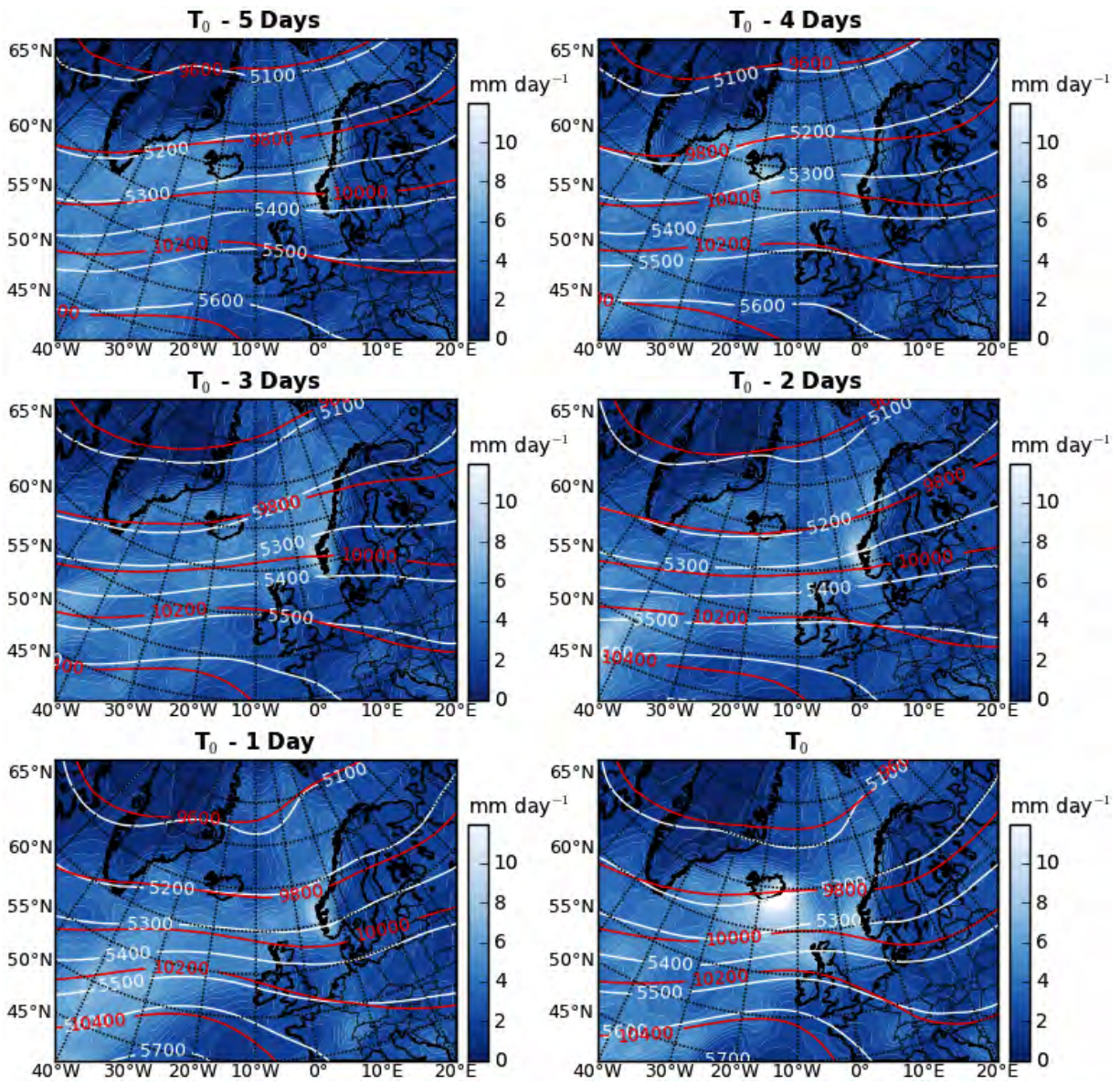


Figure 50. Ensemble mean evolution towards the start of heavy snowfall events in Eastern Iceland on day  $T_0$ : 500 hPa geopotential height (white contour lines), 250 hPa geopotential height (red contour lines), and total daily precipitation (coloured contours).

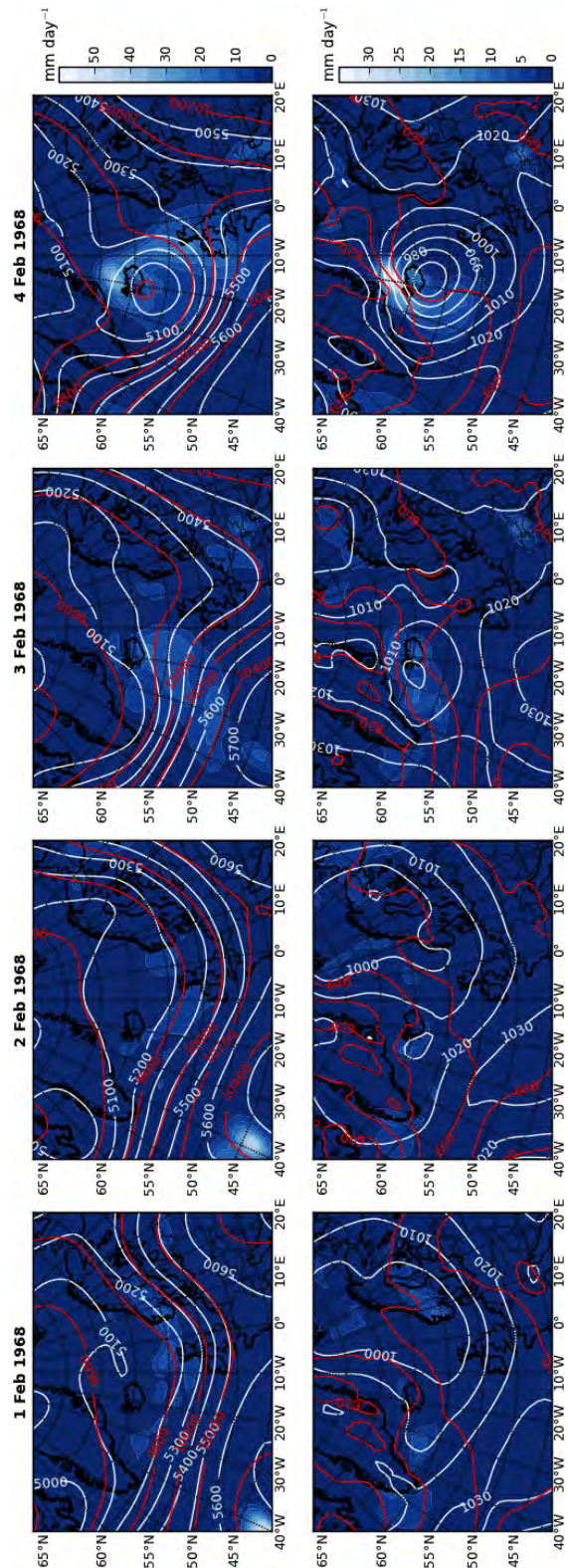


Figure 51. Atmospheric evolution leading up to the avalanche cycle starting on 4 Feb 1968. Top row: Daily fields of 500 hPa geopotential height (white contour lines), 250 hPa geopotential height (red contour lines), and total daily precipitation (coloured contours). Bottom row: Daily fields of mean sea level pressure (white contour lines), 925 – 850 hPa layer thickness (red contour lines), and daily snowfall (coloured contours).



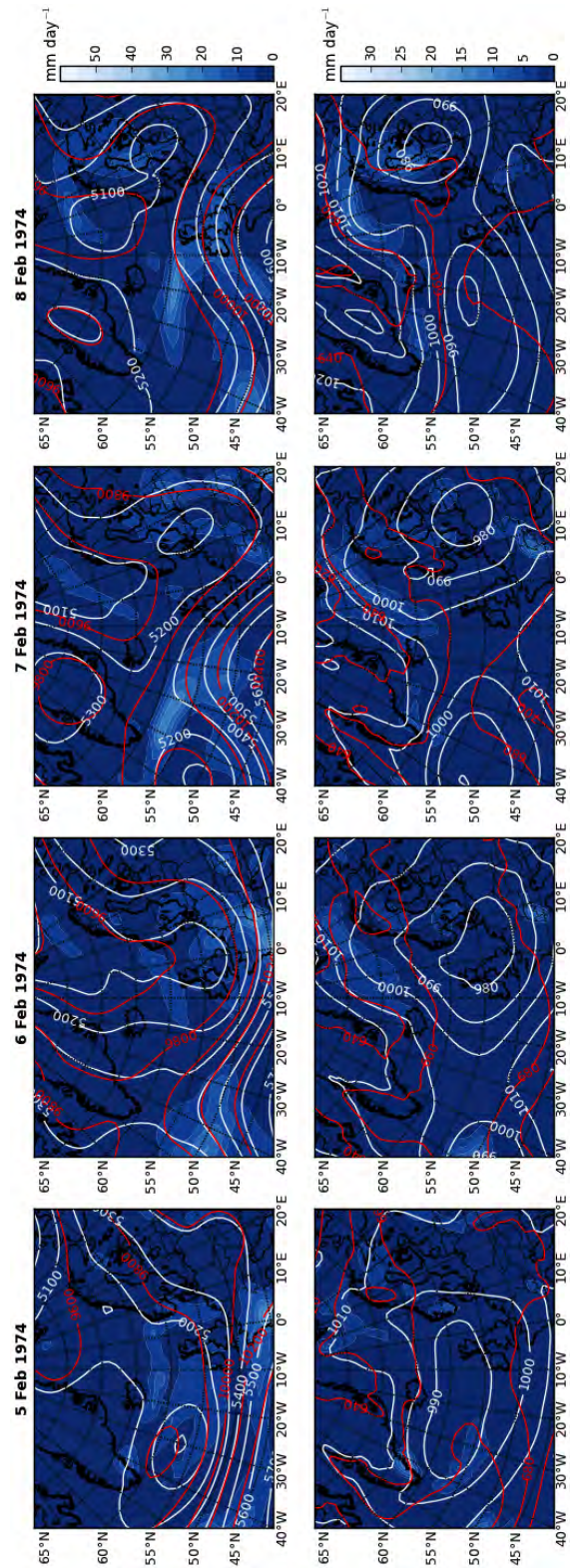


Figure 52. Atmospheric evolution leading up to the avalanche cycle starting on 8 Feb 1974. Top row: Daily fields of 500 hPa geopotential height (white contour lines), 250 hPa geopotential height (red contour lines), and total daily precipitation (coloured contours). Bottom row: Daily fields of mean sea level pressure (white contour lines), 925 – 850 hPa layer thickness (red contour lines), and daily snowfall (coloured contours).

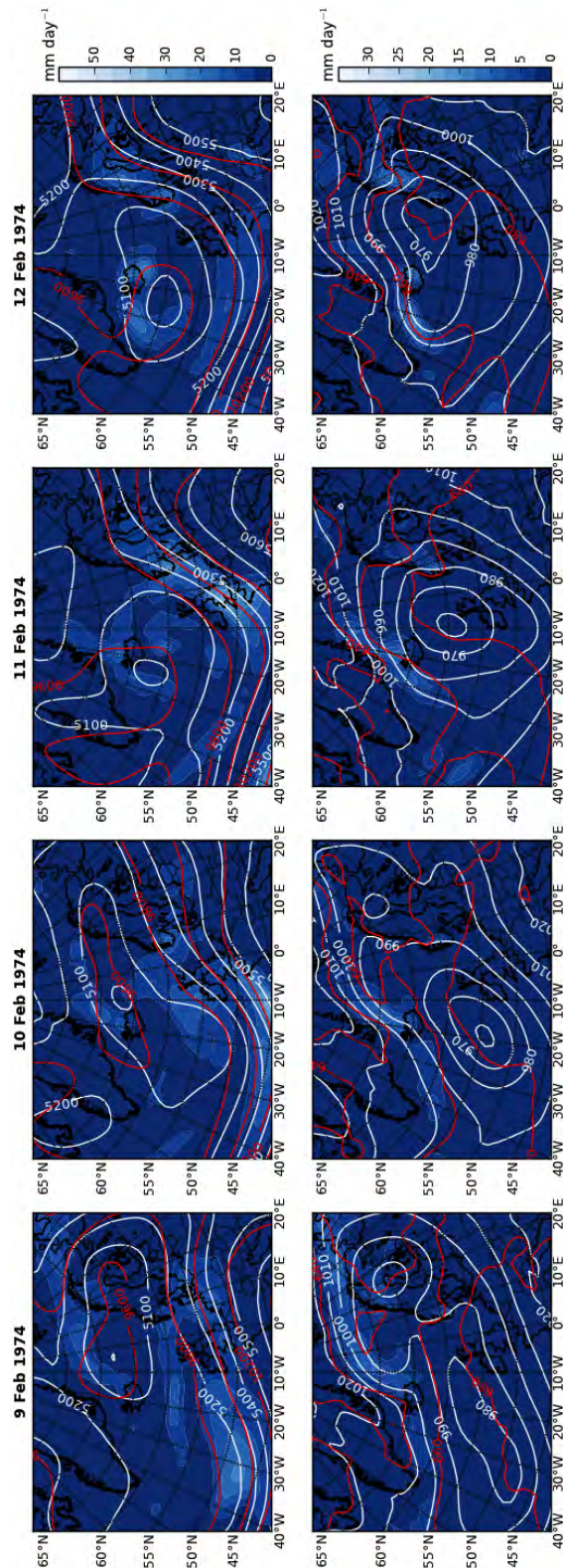


Figure 53. Atmospheric evolution during the avalanche cycle starting on 8 Feb 1974. Top row: Daily fields of 500 hPa geopotential height (white contour lines), 250 hPa geopotential height (red contour lines), and total daily precipitation (coloured contours). Bottom row: Daily fields of mean sea level pressure (white contour lines), 925 – 850 hPa layer thickness (red contour lines), and daily snowfall (coloured contours).

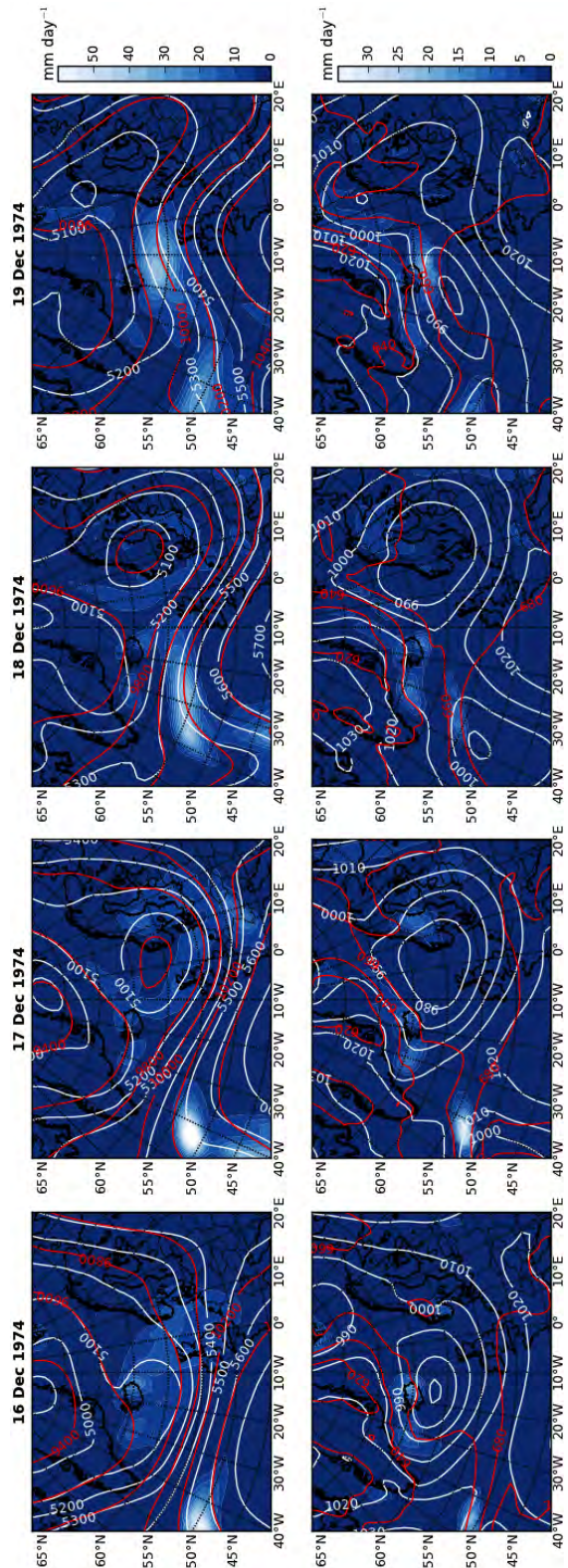


Figure 54. Atmospheric evolution leading up to the avalanche cycle starting on 19 Dec 1974. Top row: Daily fields of 500 hPa geopotential height (white contour lines), 250 hPa geopotential height (red contour lines), and total daily precipitation (coloured contours). Bottom row: Daily fields of mean sea level pressure (white contour lines), 925 – 850 hPa layer thickness (red contour lines), and daily snowfall (coloured contours).

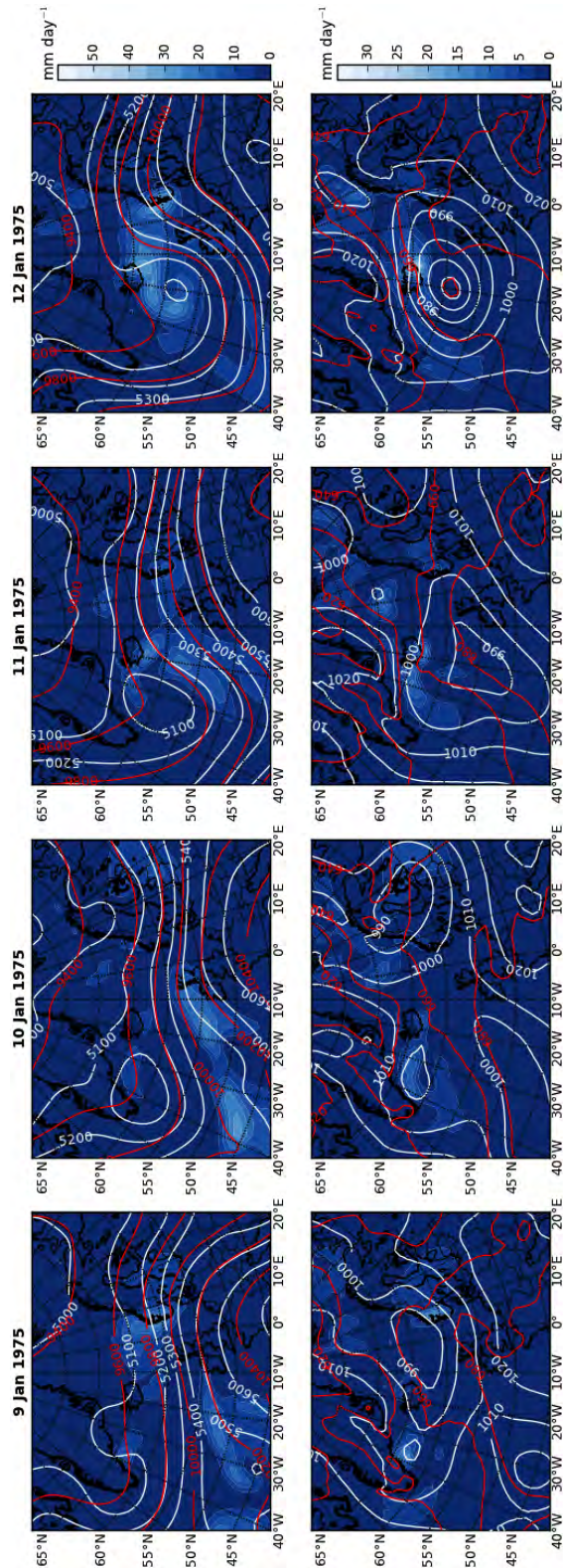


Figure 55. Atmospheric evolution leading up to the avalanche cycle starting on 12 Jan 1975. Top row: Daily fields of 500 hPa geopotential height (white contour lines), 250 hPa geopotential height (red contour lines), and total daily precipitation (coloured contours). Bottom row: Daily fields of mean sea level pressure (white contour lines), 925 – 850 hPa layer thickness (red contour lines), and daily snowfall (coloured contours).

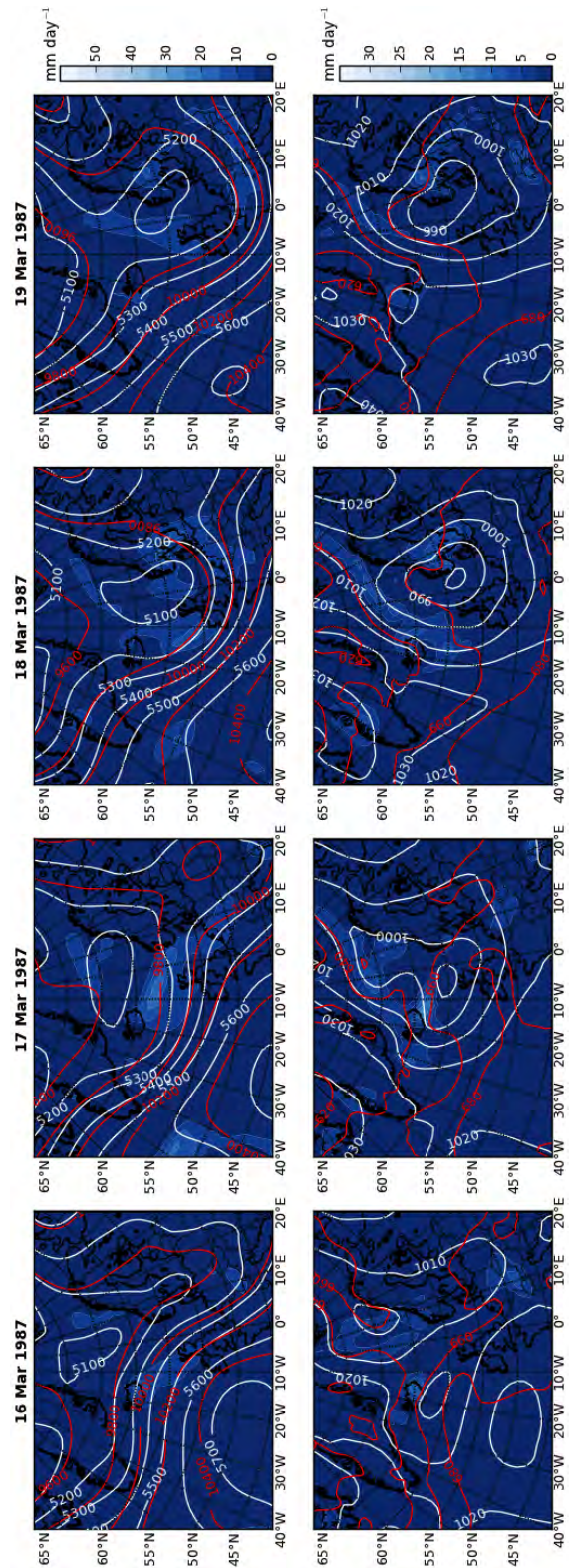


Figure 56. Atmospheric evolution leading up to the avalanche cycle starting on 19 Mar 1987. Top row: Daily fields of 500 hPa geopotential height (white contour lines), 250 hPa geopotential height (red contour lines), and total daily precipitation (coloured contours). Bottom row: Daily fields of mean sea level pressure (white contour lines), 925 – 850 hPa layer thickness (red contour lines), and daily snowfall (coloured contours).

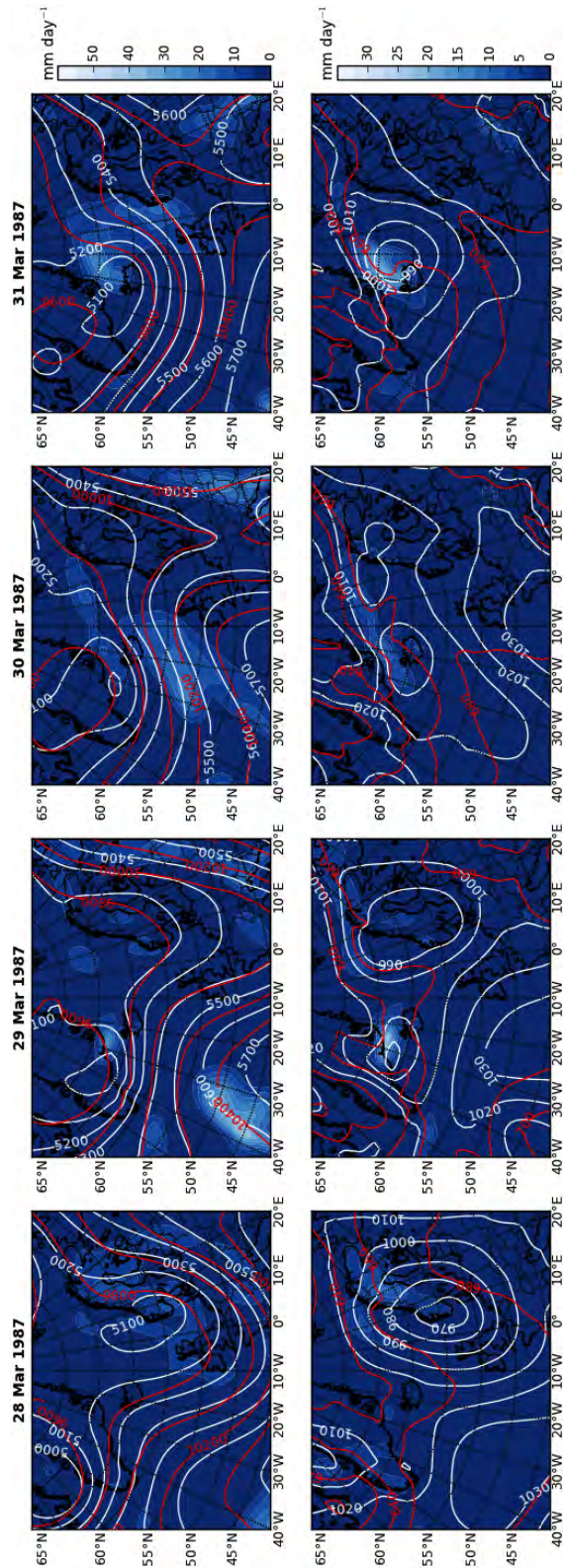


Figure 57. Atmospheric evolution leading up to the avalanche cycle starting on 31 Mar 1987. Top row: Daily fields of 500 hPa geopotential height (white contour lines), 250 hPa geopotential height (red contour lines), and total daily precipitation (coloured contours). Bottom row: Daily fields of mean sea level pressure (white contour lines), 925 – 850 hPa layer thickness (red contour lines), and daily snowfall (coloured contours).

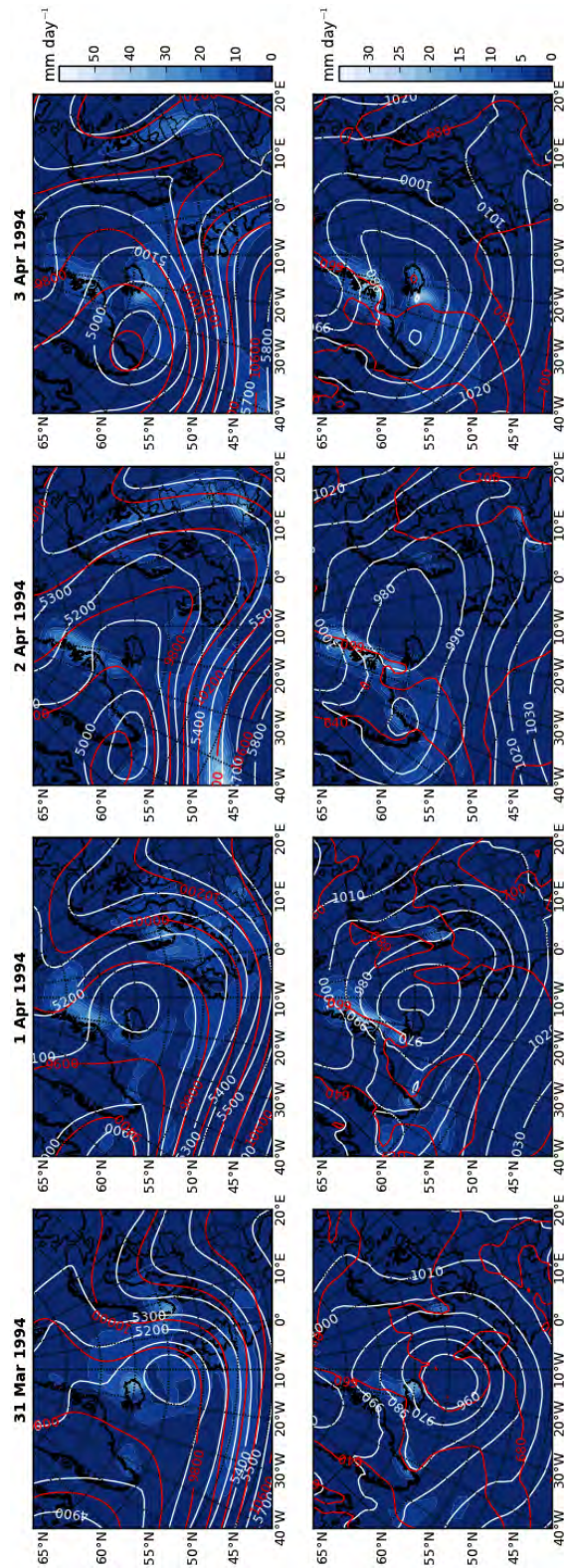


Figure 58. Atmospheric evolution leading up to the avalanche cycle starting on 3 Apr 1994. Top row: Daily fields of 500 hPa geopotential height (white contour lines), 250 hPa geopotential height (red contour lines), and total daily precipitation (coloured contours). Bottom row: Daily fields of mean sea level pressure (white contour lines), 925 – 850 hPa layer thickness (red contour lines), and daily snowfall (coloured contours).

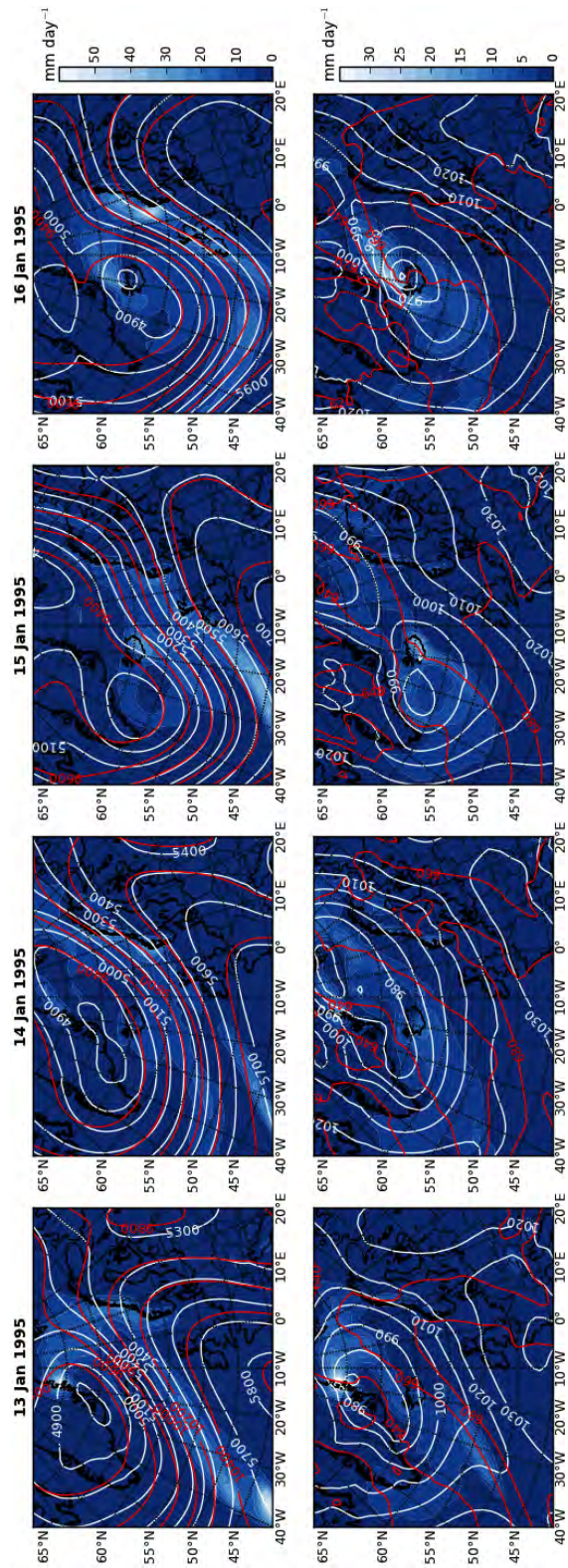


Figure 59. Atmospheric evolution leading up to the avalanche cycle starting on 16 Jan 1995. Top row: Daily fields of 500 hPa geopotential height (white contour lines), 250 hPa geopotential height (red contour lines), and total daily precipitation (coloured contours). Bottom row: Daily fields of mean sea level pressure (white contour lines), 925 – 850 hPa layer thickness (red contour lines), and daily snowfall (coloured contours).



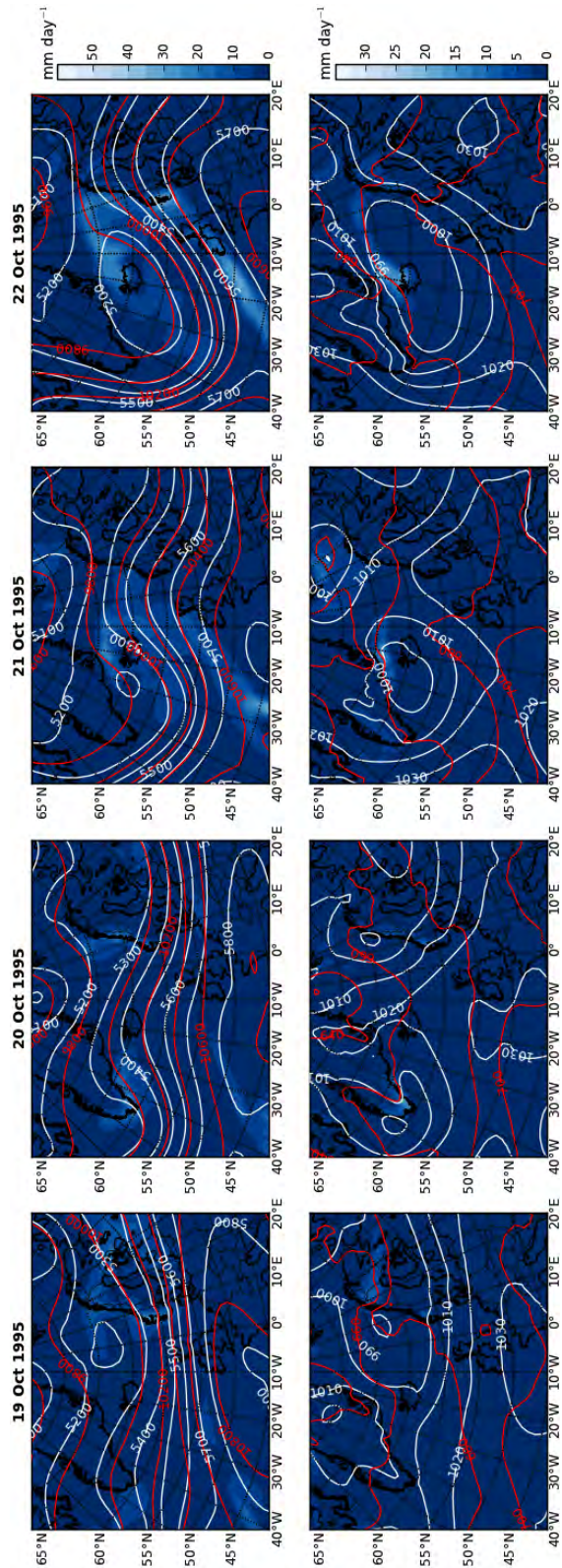


Figure 60. Atmospheric evolution prior to the avalanche cycle starting on 23 Oct 1995. Top row: Daily fields of 500 hPa geopotential height (white contour lines), 250 hPa geopotential height (red contour lines), and total daily precipitation (coloured contours). Bottom row: Daily fields of mean sea level pressure (white contour lines), 925 – 850 hPa layer thickness (red contour lines), and daily snowfall (coloured contours).

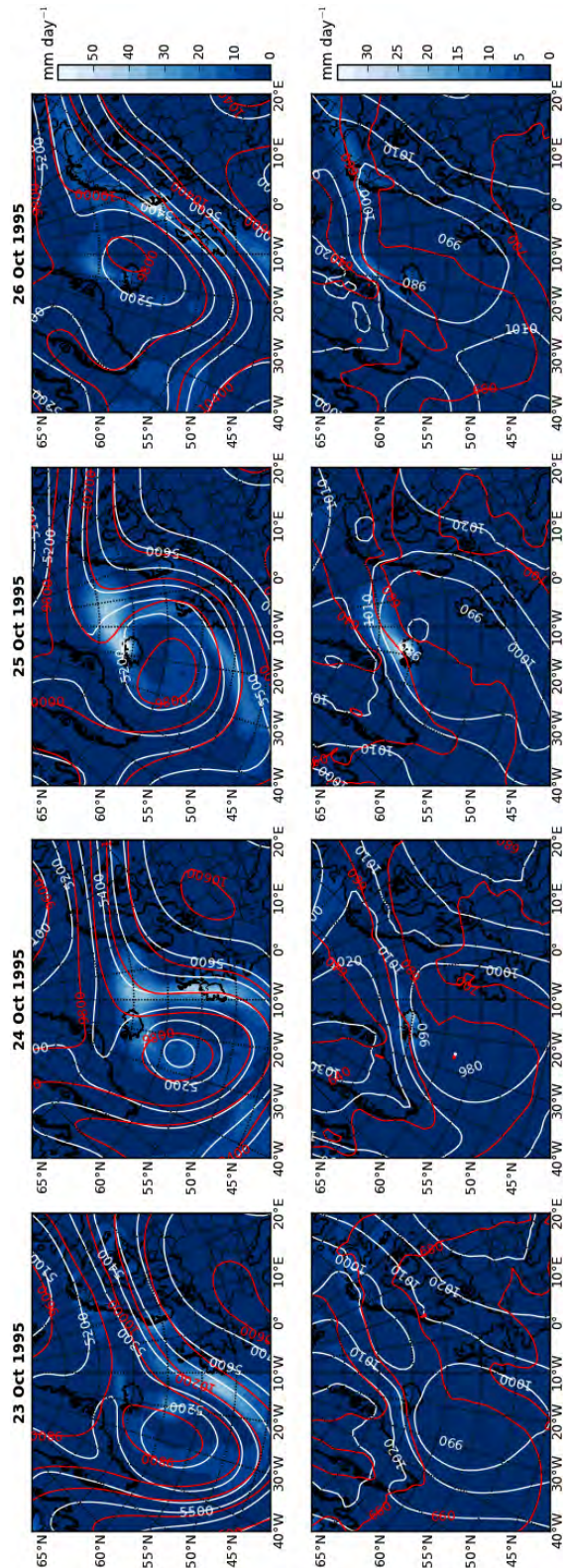


Figure 61. Atmospheric evolution during the avalanche cycle starting on 23 Oct 1995. Top row: Daily fields of 500 hPa geopotential height (white contour lines), 250 hPa geopotential height (red contour lines), and total daily precipitation (coloured contours). Bottom row: Daily fields of mean sea level pressure (white contour lines), 925 – 850 hPa layer thickness (red contour lines), and daily snowfall (coloured contours).

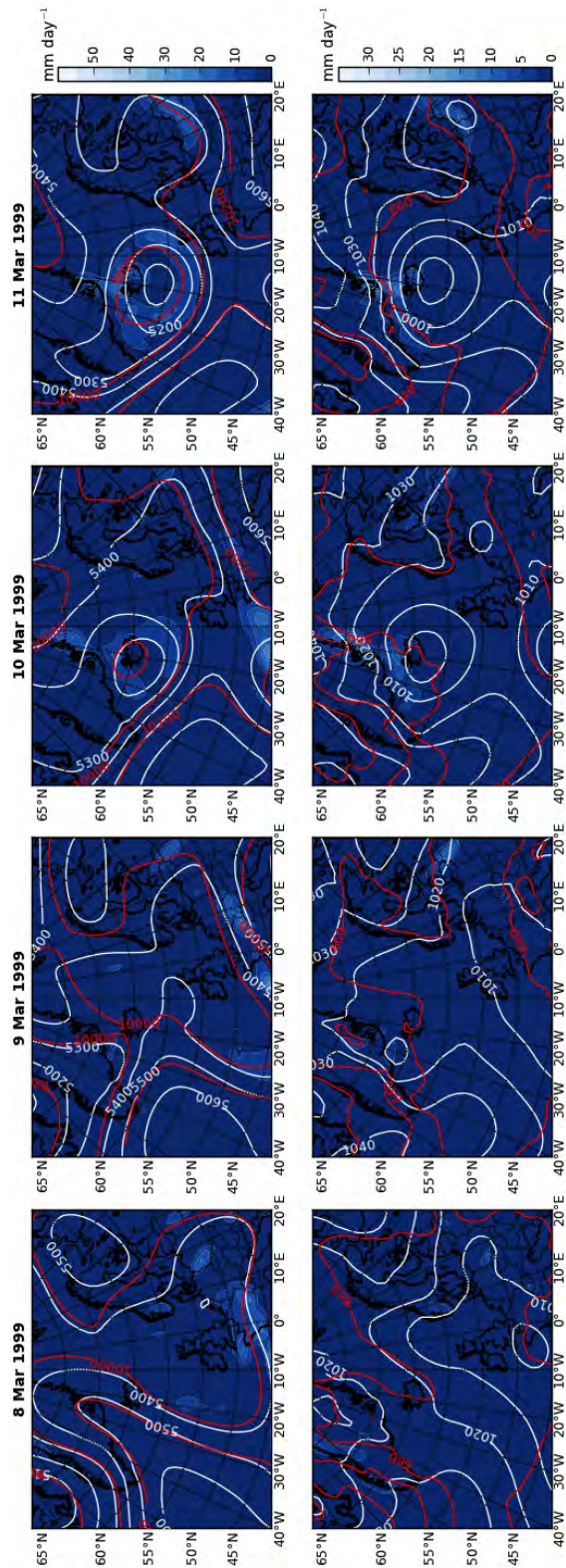


Figure 62. Atmospheric evolution leading up to the avalanche cycle starting on 11 Mar 1999. Top row: Daily fields of 500 hPa geopotential height (white contour lines), 250 hPa geopotential height (red contour lines), and total daily precipitation (coloured contours). Bottom row: Daily fields of mean sea level pressure (white contour lines), 925 – 850 hPa layer thickness (red contour lines), and daily snowfall (coloured contours).